

EVALUATION OF POLYPYRROLE-POLYETHYLENIMINE
(PPY-PEI) CONDUCTING POLYMERS AS ADSORBENTS
FOR THE REMOVAL OF METHYL ORANGE AND
CRYSTAL VIOLET FROM POLLUTED SOLUTIONS

NORHABIBAH BINTI MOHAMAD

FACULTY OF SCIENCE
UNIVERSITI MALAYA
KUALA LUMPUR

2023

**EVALUATION OF POLYPYRROLE-
POLYETHYLENIMINE (PPY-PEI) CONDUCTING
POLYMERS AS ADSORBENTS FOR THE REMOVAL
OF METHYL ORANGE AND CRYSTAL VIOLET
FROM POLLUTED SOLUTIONS**

NORHABIBAH BINTI MOHAMAD

**THESIS SUBMITTED IN FULFILMENT OF THE
REQUIREMENTS FOR THE DEGREE OF DOCTOR OF
PHILOSOPHY**

**DEPARTMENT OF CHEMISTRY
UNIVERSITI MALAYA
KUALA LUMPUR**

2023

UNIVERSITI MALAYA
ORIGINAL LITERARY WORK DECLARATION

Name of Candidate: **NORHABIBAH BINTI MOHAMAD**

Matric No: **17043036**

Name of Degree: **DOCTOR OF PHILOSOPHY**

Title of Thesis: **EVALUTAION OF POLYPYRROLE-
POLYETHYLENIMINE (PPy-PEI) CONDUCTING POLYMERS AS
ADSORBENTS FOR THE REMOVAL OF METHYL ORANGE AND
CRYSTAL VIOLET FROM POLLUTED SOLUTIONS**

Field of Study: **PHYSICAL CHEMISTRY**

I do solemnly and sincerely declare that:

- (1) I am the sole author/writer of this Work;
- (2) This Work is original;
- (3) Any use of any work in which copyright exists was done by way of fair dealing and for permitted purposes and any excerpt or extract from, or reference to or reproduction of any copyright work has been disclosed expressly and sufficiently and the title of the Work and its authorship have been acknowledged in this Work;
- (4) I do not have any actual knowledge nor do I ought reasonably to know that the making of this work constitutes an infringement of any copyright work;
- (5) I hereby assign all and every rights in the copyright to this Work to the Universiti Malaya ("UM"), who henceforth shall be owner of the copyright in this Work and that any reproduction or use in any form or by any means whatsoever is prohibited without the written consent of UM having been first had and obtained;
- (6) I am fully aware that if in the course of making this Work I have infringed any copyright whether intentionally or otherwise, I may be subject to legal action or any other action as may be determined by UM.

Candidate's Signature

Date: 21.08.2023

Subscribed and solemnly declared before,

Witness's Signature

Date: 21.08.2023

Name:

Designation:

ABSTRACT

Various conducting polymers have emerged as a new adsorbent for the removal of dyes from an aqueous environment. This research study focused on suitable polymeric adsorbents to remove dyes from aqueous solution at a very low cost, ease of preparation, and higher removal efficiency. Novel conducting polymer-based adsorbents, polypyrrole (PPy) and polypyrrole-polyethylenimine (PPy-PEI) have successfully been prepared as new adsorbents and utilized in the adsorption of dyes such as methyl orange (MO) and crystal violet (CV) dyes from aqueous environment. The adsorption characteristics of the prepared polymer-based adsorbents were characterized by the Brunauer-Emmet-Teller (BET) surface analyzer in order to measure the surface area measurements, Fourier transform infrared (FTIR) to identify the functional groups of the prepared adsorbents, X-ray diffraction pattern (XRD) to investigate the crystalline structure and field emission scanning electron microscopy (FESEM) to study the surface morphology of the adsorbents. The highest BET surface area of the PPy-PEI composite (1:1) was found to be $11.85 \text{ m}^2/\text{g}$, which is much greater than that of the pristine PPy (1:1) of $8.54 \text{ m}^2/\text{g}$. The performance of PPy-based adsorbents towards the adsorption of MO and CV dyes were investigated by the batch method. PPy-based adsorbents were prepared via chemical oxidative polymerization in the presence of $\text{FeCl}_3 \cdot 6\text{H}_2\text{O}$, anhydrous FeCl_3 , and $(\text{NH}_4)_2\text{S}_2\text{O}_8$ as oxidants, respectively. Different adsorption parameters such as contact time, adsorbent dose, initial dye concentration and solution pH on the adsorption efficiency of dye removal were explored. The maximum adsorption efficiency of both MO and CV dyes were exhibited using 1:1 mole ratio of monomer to oxidant. The findings confirmed higher dye removal potential in the presence of anhydrous FeCl_3 and ammonium persulfate as the oxidant for the MO and CV dye, respectively. The PPy-PEI composite adsorbent has exhibited high adsorption efficiency compared to the pristine

PPy adsorbent for the removal of MO and CV dye from aqueous solution. The present work reveals that the incorporation of PEI with Py monomer as a new conducting polymer composite improved the adsorption efficiency of the anionic MO and the cationic CV dyes in aqueous solution. Removal performance was obtained to be 79.1 % and 98.8 % for 100 ppm MO dye by pristine PPy and PPy-PEI composite adsorbents, respectively, at the optimum conditions; pH 3, adsorbent dosage of 0.1 g and with a contact time of 120 minutes. On the other hand, the removal performance for 100 ppm CV dye by pristine PPy and PPy-PEI composite adsorbents was to be 45.0 % and 70.9 %, respectively, at optimum conditions; pH 11, adsorbent dosage of 0.3 g and contact time of 180 minutes. It was observed that the PPy-based adsorbents presented high adsorption performance toward MO than CV dye. Adsorption kinetics was best described by the pseudo-second-order rate model for both dyes. The isotherm study manifested that the Langmuir model was best fitted to the equilibrium data of MO and CV dyes with the maximum monolayer sorption capacity of 232.56 and 142.86 mg/g, respectively at 27 °C. A regeneration study showed that PPy-PEI could be reused efficaciously for up to three consecutive adsorption-desorption cycles. The combined benefits of facile synthesis and good adsorption potential towards cationic and anionic dyes along with ease of preparation make PPy-PEI a novel adsorbent.

Keywords: Polymer Composite, Dye Adsorption, Polypyrrole, Polyethylenimine, Regeneration

ABSTRAK

Pelbagai polimer pengalir telah muncul sebagai penjerap baharu untuk menyingkirkan pewarna daripada persekitaran akueus. Kajian penyelidikan ini memberi tumpuan kepada penjerap polimer yang sesuai untuk mengeluarkan pewarna daripada larutan akueus pada kos yang sangat rendah, kemudahan penyediaan dan kecekapan penyingkiran yang lebih tinggi. Penjerap novel yang berasaskan polimer, polypyrrole (PPy) dan polypyrrole-polietileneimine (PPy-PEI) telah berjaya disediakan sebagai penjerap baharu dan digunakan dalam penjerapan pewarna seperti pewarna metil jingga (MO) dan ungu kristal (CV) daripada akueus persekitaran. Ciri-ciri penjerapan bahan penjerap berasaskan polimer yang disediakan telah diciri oleh penganalisis permukaan Brunauer-Emmet-Teller (BET) untuk mengukur ukuran luas permukaan, Fourier transform infrared (FTIR) untuk mengenal pasti fungsi kumpulan penjerap yang disediakan, diffractometer sinar-X (XRD) untuk menyiasat struktur kristal dan mikroskop elektron pengimbasan pemancaran (FESEM) untuk mengkaji morfologi permukaan penjerap. Luas permukaan BET tertinggi bagi komposit PPy-PEI (1:1) didapati 11.85 m²/g, yang jauh lebih besar daripada PPy tulen (1:1) iaitu 8.54 m²/g. Prestasi penjerap berasaskan PPy terhadap penjerapan pewarna MO dan CV telah disiasat dengan kaedah kelompok. Penjerap berasaskan PPy telah disediakan melalui pempolimeran kimia oksidatif dengan kehadiran FeCl₃.6H₂O, FeCl₃ kontang, dan (NH₄)₂S₂O₈ sebagai oksidan. Parameter penjerapan yang berbeza seperti masa tindak balas, dos penjerap, kepekatan pewarna dan larutan pH pada kecekapan penjerapan penyingkiran pewarna telah diterokai. Kecekapan penjerapan maksimum kedua-dua pewarna MO dan CV menunjukkan pada nisbah 1:1 mol monomer kepada oksidan. Penemuan mengesahkan potensi penyingkiran pewarna yang lebih tinggi dengan kehadiran FeCl₃ kontang dan ammonium persulfat sebagai oksidan untuk pewarna MO dan CV berbanding dengan yang lain. Penjerap komposit PPy-PEI telah menunjukkan kecekapan penjerapan yang

tinggi berbanding dengan penjerap PPy tulen untuk penyingkiran pewarna MO dan CV daripada larutan akueus. Kerja-kerja ini menunjukkan bahawa penggabungan PEI dengan monomer Py sebagai komposit polimer pengalir baharu meningkatkan kecekapan penjerapan anionik MO dan pewarna CV kationik dalam larutan akueus. Prestasi penyingkiran didapati 79.1 % dan 98.8 % untuk pewarna MO 100 ppm oleh penjerap PPy tulen dan penjerap PPy-PEI, masing-masing pada keadaan optimum; pH 3, dos penjerap 0.1 g dan dengan masa tindak balas 120 minit. Sebaliknya, prestasi penyingkiran untuk pewarna CV 100 ppm oleh penjerap PPy tulen dan penjerap PPy-PEI adalah masing-masing 45.0 % dan 70.9 %, pada keadaan optimum; pH 11, dos penjerap 0.3 g dan masa tindak balas 180 minit. Diperhatikan bahawa penjerap berasaskan PPy menunjukkan prestasi penjerapan yang tinggi terhadap MO berbanding pewarna CV. Kinetik penjerapan paling baik diterangkan oleh model kadar pseudo-second-order untuk kedua-dua pewarna. Kajian isoterma menunjukkan bahawa model Langmuir paling sesuai untuk data keseimbangan pewarna MO dan CV dengan kapasiti serapan monolayer maksimum 232.56 dan 142.86 mg/g, masing-masing pada 27 °C. Kajian penjanaan semula menunjukkan bahawa PPy-PEI boleh digunakan semula dengan berkesan sehingga tiga kitaran penjerapan-penyahjerapan berturut-turut. Manfaat gabungan sintesis mudah dan potensi penjerapan yang baik terhadap pewarna kationik dan anionik bersama-sama dengan kemudahan penyediaan menjadikan PPy-PEI sebagai penjerap baru.

Kata Kunci: Komposit Polimer, Penjerapan Pewarna, Polipirol, Polietilenaimina, Penjanaan Semula

ACKNOWLEDGEMENTS

All praises belong to the Almighty Allah.

First and foremost, I would like to express my sincere gratitude to my supervisors, Associate Professor Dr. H. N. M. Ekramul Mahmud and Dr. Noordini Mohamad Salleh, for their invaluable advice, continuous support, and patience throughout the period of the research work and in the completion of this thesis. Furthermore, their immense knowledge and plentiful experience have encouraged me in all of my research study and daily life. My gratitude also goes to my previous co-supervisor, Professor Dr. Rosiyah Yahya, for the care, kind advice, and courage you instilled in me, in particular.

I would like to acknowledge and thank all staff in the Chemistry Department for their assistance and support, especially during my time using analytical instruments here. Their assistance is greatly valued.

I would also like to thank all my colleagues and friends for their help, encouragement, and valuable collaboration throughout the study: Nurul Fathullah, Sakinah, Mogana, Nur Fariyah, Fatin Nur Liyana, Wan Nurul Aimi, Salwa, Noman, and Nur Linahafizza.

I owe my other half, Ahmad Baihaqi, for his continuous care, support, inspiration, and patience throughout the study. During a difficult period in my studies, I am deeply grateful and blessed for the special patience, uniqueness, and amazingness of a husband like him. Along with him, I am incredibly fortunate to have my two little, adored children, Aisyah and Nuh, who have been so understanding and patient with me throughout my challenging study period.

Finally, I would like to express my utmost gratitude to my beloved parents and parents-in-law for their love, prayers, and blessings. This column cannot be sufficient to express my gratitude to all my family members for their encouragement and patience during the study.

TABLE OF CONTENTS

ABSTRACT	iii
ABSTRAK	v
ACKNOWLEDGEMENTS.....	vii
TABLE OF CONTENTS.....	viii
LIST OF FIGURES	xiii
LIST OF TABLES	xv
LIST OF SYMBOLS AND ABBREVIATIONS	xvi
LIST OF APPENDICES.....	xviii
CHAPTER 1: INTRODUCTION.....	1
1.1 Overview	1
1.2 Dye effluents.....	2
1.3 Health risks of dye effluents.....	4
1.4 Efforts towards dyes treatment	4
1.5 Adsorption	6
1.6 Classification of adsorption.....	6
1.7 Polymer-based adsorbent.....	7
1.8 Conducting polymer-based adsorbent	8
1.9 Problem statement	9
1.10 Scope of research.....	10
1.11 Research objectives	11
CHAPTER 2: LITERATURE REVIEW.....	12
2.1 Dye pollution	12
2.2 Specific effects and properties of organic dyes	13

2.2.1	Anionic methyl orange (MO) dye	14
2.2.1	Cationic crystal violet (CV) dye.....	14
2.3	Dyes treatment techniques.....	15
2.4	Factors affecting adsorption of dye	17
2.4.1	Effect of solution pH	17
2.4.2	Effect of initial dye concentration	18
2.4.3	Effect of adsorbent dosage	19
2.4.4	Effect of temperature	20
2.4.5	Effect of contact time	21
2.4.6	Effect of surface area.....	22
2.5	Adsorbent materials.....	23
2.5.1	Polymer composite adsorbents.....	25
2.5.2	Conducting polymer-based composites.....	27
2.5.2.1	Review of adsorption of MO and CV dyes by polypyrrole-based composite adsorbents	28
2.5.3	Polyethylenimine-based (PEI) adsorbents.....	34
2.5.3.1	Review of adsorption of MO and CV dyes by polyethylenimine adsorbents.....	35
2.6	Regeneration and reusability of spent-adsorbent.....	41
2.7	Adsorption isotherms.....	42
2.7.1	Langmuir isotherm model	43
2.7.2	Freundlich isotherm model.....	44
2.8	Adsorption kinetic models.....	44
2.8.1	Pseudo-first-order kinetic model	45
2.8.2	Pseudo-second-order kinetic model	45
2.9	Adsorbent characterization methods.....	46

2.9.1	Fourier Transform Infra-Red Spectrometer (FTIR)	46
2.9.2	Field Emission Scanning Electron Microscopy (FESEM)	47
2.9.3	X-ray Diffraction (XRD)	48
2.9.4	Brunner-emmett-teller (BET)	48
CHAPTER 3: RESEARCH METHODOLOGY.....		50
3.1	Chemicals and materials	50
3.2	Methods	50
3.3	Synthesis of polypyrrole-based adsorbents	51
3.3.1	Synthesis of polypyrrole.....	51
3.3.2	Synthesis of PPy-PEI composite adsorbents	52
3.4	Batch adsorption experiments.....	53
3.5	Ultra-violet spectrophotometer	54
3.6	Regeneration experiments	55
3.7	Characterization.....	55
3.7.1	Fourier Transform Infra-Red Spectrometer (FTIR)	55
3.7.2	Field Emission Scanning Electron Microscopy (FESEM).....	56
3.7.3	X-ray Diffraction (XRD).....	56
3.7.4	Brunner-emmett-teller (BET).....	56
CHAPTER 4: RESULTS AND DISCUSSION.....		57
4.1	Characterization of adsorbents	57
4.1.1	BET surface area	57
4.1.2	FESEM analysis	59
4.1.2.1	Pristine PPy adsorbent.....	59
4.1.2.2	PPy-PEI composite adsorbent	63
4.1.3	X-ray diffraction (XRD) analysis.....	68

4.1.3	FTIR analysis.....	71
4.1.4.1	Pristine PPy adsorbent.....	71
4.1.4.2	PPy-PEI composite adsorbent	76
4.2	Adsorption studies	81
4.2.1	Effect of pyrrole to oxidant mole ratios	81
4.2.2	Effect of different oxidants.....	85
4.2.3	Effect of modified adsorbent (PPy-PEI composites).....	86
4.2.4	Effect of solution pH	86
4.2.4.1	Pristine PPy adsorbent.....	86
4.2.4.2	PPy-PEI composite adsorbent	87
4.2.5	Effect of adsorbent dosage	89
4.2.5.1	Pristine PPy adsorbent.....	89
4.2.5.2	PPy-PEI composite adsorbent	90
4.2.6	Effect of contact time	92
4.2.6.1	Pristine PPy adsorbent.....	92
4.2.6.2	PPy-PEI composite adsorbent	93
4.2.7	Effect of initial dye concentration	95
4.2.7.1	Pristine PPy adsorbent.....	95
4.2.7.2	PPy-PEI composite adsorbent	96
4.2.8	Adsorption kinetic models.....	97
4.2.9	Adsorption isotherm models.....	101
4.3	Regeneration and repeatability studies	107
CHAPTER 5: CONCLUSIONS.....		109
5.1	Conclusion.....	109
5.1	Suggestions for future works	111

REFERENCES.....	112
LIST OF PUBLICATIONS AND PAPERS PRESENTED	125
APPENDICES	126

Universiti Malaya

LIST OF FIGURES

Figure 1.1: The percentage of dyes in various types of industry	2
Figure 1.2: Structure of polypyrrole	9
Figure 1.3: Branched of polyethyleneimine.....	10
Figure 2.1: Structure of dyes (a) Methyl orange (b) Crystal violet.....	13
Figure 2.2: Schematic diagram of adsorption process	16
Figure 3.1: Chemical polymerization of pyrrole monomer to form polypyrrole.....	52
Figure 3.2: Synthesis design of PPy-PEI composite.....	53
Figure 4.1: FESEM image of PPy before adsorption with different magnifications ((a) x 5.00 k; (b) x 30.0 k; (c) x 70.0 k)	60
Figure 4.2: FESEM image of PPy before adsorption with internal particle diameter measurement; magnification x 130 k).....	61
Figure 4.3: FESEM image of PPy after adsorption with different magnifications ((a) x 5.00 k; (b) x 30.0 k; (c) x 70.0 k)	62
Figure 4.4: FESEM image of PPy after adsorption with internal particle diameter measurement; magnification x 70 k).....	63
Figure 4.5: FESEM image of PPy-PEI before adsorption with different magnifications ((a) x 5.00 k; (b) x 30.0 k; (c) x 70.0 k)	64
Figure 4.6: FESEM image of PPy-PEI before adsorption with internal particle diameter measurement; magnification x 130 k).....	65
Figure 4.7: FESEM image of PPy-PEI after adsorption with different magnifications ((a) x 5.00 k; (b) x 30.0 k; (c) x 70.0 k)	67
Figure 4.8: FESEM image of PPy-PEI after adsorption with internal particle diameter measurement; magnification x 130 k).....	68
Figure 4.9: XRD diffractograms for PPy-PEI before and after MO dye adsorption	70
Figure 4.10: XRD diffractograms for PPy-PEI before and after CV dye adsorption	70
Figure 4.11: FTIR spectrum of MO dye	71
Figure 4.12: FTIR analysis for PPy before and after MO dye adsorption	72

Figure 4.13: FTIR spectrum of CV dye	74
Figure 4.14: FTIR analysis for PPy before and after CV dye adsorption.....	75
Figure 4.15: FTIR analysis for PPy-PEI before and after MO dye adsorption.....	77
Figure 4.16: FTIR analysis for PPy-PEI before and after CV dye adsorption.....	79
Figure 4.17: Effect of monomer to oxidant ratios by pristine PPy adsorbent on adsorption of (a) MO and (b) CV.....	83
Figure 4.18: Effect of monomer to oxidant ratios by PPy-PEI composite adsorbent on adsorption of (a) MO and (b) CV.....	84
Figure 4.19: Effect of initial solution pH by pristine PPy and PPy-PEI composite adsorbents on adsorption of (a) MO and (b) CV.....	89
Figure 4.20: Effect of adsorbent dosage by pristine PPy and PPy-PEI composite adsorbents on adsorption of (a) MO and (b) CV.....	92
Figure 4.21: Effect of contact time by pristine PPy and PPy-PEI composite adsorbents on adsorption of (a) MO and (b) CV.....	95
Figure 4.22: Effect of initial dye concentration by pristine PPy and PPy-PEI composite adsorbents on adsorption of (a) MO and (b) CV.....	97
Figure 4.23: Pseudo-first-order kinetic model for the adsorption of (a) MO and (b) CV	100
Figure 4.24: Pseudo-second-order kinetic model for the adsorption of (a) MO and (b) CV	101
Figure 4.25: Langmuir isotherm model for the adsorption of (a) MO and (b) CV	105
Figure 4.26: Freundlich isotherm model for the adsorption of (a) MO and (b) CV	106
Figure 4.27: Reusability of PPy-PEI adsorbent for MO adsorption	108
Figure 4.28: Reusability of PPy-PEI adsorbent for CV adsorption	108

LIST OF TABLES

Table 1.1: List type of dyes used in textile industries.....	3
Table 1.2: Advantages and drawbacks of commonly used methods for removal of pollutants from wastewaters Table 1.1: List type of dyes used in textile industries.....	5
Table 1.3: Properties of physisorption and chemisorption	7
Table 2.1: Comparison of the adsorption capacities of dyes for different adsorbents....	24
Table 2.2: Comparison of the adsorption capacities of MO and CV dyes reported in the literature for different polymer-based composite adsorbents.....	26
Table 2.3: Common types of conducting polymers and its structure.....	27
Table 3.1: The physical properties of the investigated dyes	50
Table 4.1: Characteristics of polypyrrole and composite, surface area measurements and pore volume distribution	58
Table 4.2: Chemical bonding for PPy adsorbent before and after adsorption of MO dye	73
Table 4.3: Chemical bonding for PPy adsorbent before and after adsorption of CV dye	76
Table 4.4: Chemical bonding for PPy-PEI adsorbent before and after adsorption of MO dye.....	78
Table 4.5: Chemical bonding for PPy-PEI adsorbent before and after adsorption of CV dye.....	80
Table 4.6: Adsorption kinetic model parameters for MO dye adsorption	98
Table 4.7: Adsorption kinetic model parameters for CV dye adsorption	99
Table 4.8: Adsorption isotherm model parameters for MO dye adsorption	103
Table 4.9: Adsorption isotherm model parameters for CV dye adsorption	104

LIST OF SYMBOLS AND ABBREVIATIONS

APS	:	Ammonium peroxodisulphate
ATR	:	Attenuated Total Reflectance
b	:	Langmuir equilibrium constant (L/mg)
BET	:	Brunner-Emmett-Teller
°C	:	Degree Celsius
C_e	:	Equilibrium concentration of dye (mg/L)
C_i	:	Initial dye concentration (mg/L)
C_f	:	Final dye concentration (mg/L)
cm	:	Centimeter
CV	:	Crystal Violet
FeCl ₃	:	Ferric chloride anhydrous
FESEM	:	Field emission scanning electron microscopy
FTIR	:	Fourier transform infrared
g	:	Gram
h	:	Hour
HCl	:	Hydrochloric
K_1	:	Pseudo-first-order rate constant (min ⁻¹)
K_2	:	Pseudo-second-order rate constant of adsorption (g/mg min)
K_F	:	Freundlich coefficients
L	:	Liter
mg	:	Milligram
MO	:	Methyl Orange
NaOH	:	Sodium hydroxide
nm	:	Nanometer

PEI	:	Polyethyleneimine
PPy	:	Polypyrrole
Q_e	:	Equilibrium adsorption capacity (mg/g)
Q_t	:	Solid-phase concentration at time t (mg/g)
Q_m	:	Maximum monolayer adsorption capacity (mg/g)
R^2	:	Correlation coefficients
R_L	:	Separation factor
t	:	Time
XRD	:	X-ray diffraction

LIST OF APPENDICES

Appendix A: Synthesis of polypyrrole.....	126
Appendix B: Synthesis of PPy-PEI composite	127
Appendix C: Preparation of stock solution	128
Appendix D: Standard calibration curve for methyl orange dye	129
Appendix E: Standard calibration curve for crystal violet dye	130

Universiti Malaya

CHAPTER 1: INTRODUCTION

1.1 Overview

Water, which covers approximately 70% of the earth, is the key to sustaining life. Water is the most essential element for life and forms about 65% of human body constituents. Thus, the availability of clean and safe water is of supreme priority to human beings. However, water resources are not only the basis of living creatures but also an indispensable precious resource for industrial and agricultural production (Wu *et al.*, 2021). In this regard, water plays a key role in supporting life from living cells to the whole ecosystem. However, the water environment has been seriously damaged in the past few decades with the rapid development of human society. Regrettably, the environment is increasingly threatened by large amounts of toxic industrial effluents being discharged into natural water bodies without proper treatment (Das *et al.*, 2017).

Industrial wastewater contains a variety of pollutants, including azo dyes, heavy metal ions, antibiotics, endocrine disruptors, and pesticides. It is well known that the textile industries, pulp mills, and dyestuff manufacturing discharge highly colored wastewater which has provoked serious environmental concerns all over the world (Rahchamani *et al.*, 2011). Figure 1.1 shows the textile industries are the largest consumers of dyes. The textile industry (54%) releases the highest amount of dye effluent, contributing to more than half of the existing dye effluents seen in the environment around the world (Katheresan *et al.*, 2018).

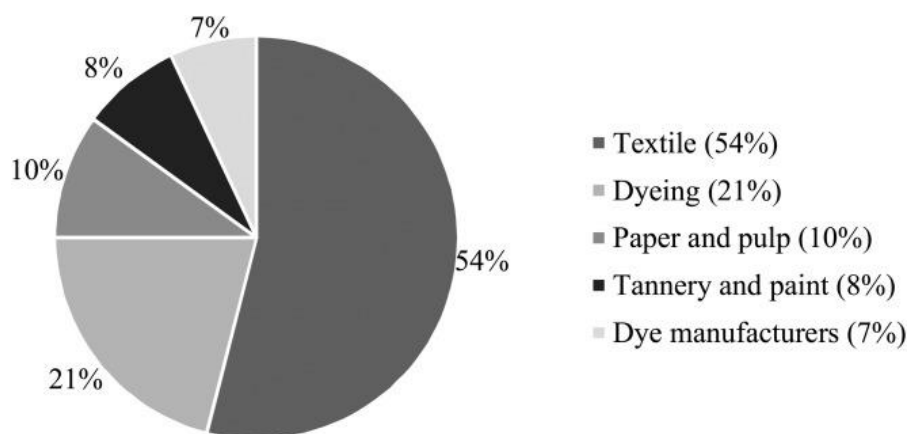


Figure 1.1: The percentage of dyes in various types of industry.

1.2 Dyes effluents

Dyes are defined as attractively coloured compounds which outcast other compounds because of the presence of auxochrome and chromophore groups (Ayad *et al.*, 2018). Dyes industries that cover the production of rubber, printing, cosmetic products, and clothes are the biggest scale of dyes consumers. Dyes themselves can be categorized as a synthetic dye and natural dyes. Natural dyes are simply obtained by extracting them from natural resources, animals, or plants. Natural dyes are very minimally used due to their extraction amount which is little and they can't meet the demand of the market industry. However, it is vice versa for the obtaining of synthetic dyes whereby it is processed rapidly using chemicals to meet the requirements of booming industries. Synthetics are widely used in textiles, leather, paper, cosmetics, photoelectron chemical cells, and other similar industries to colour their products. Based on the chemical structures and applied methods, synthetic dyes are classified as basic dyes, acid dyes, reactive dyes, direct dyes, azo dyes, mordant dyes, vat dyes, disperse dyes and sulfur dyes (Bhaumik *et al.*, 2016). Table 1.1 shows the various types of dyes used in various textile industries (Christie, 2007; Yadav *et al.*, 2014).

Table 1.1: List type of dyes used in textile industries.

Dye Types	Description	Fiber types	Chemical structure	Type of Pollutant generated
Acid	water -soluble anionic compounds	wool, silk and animal hair	azo, anthraquinone, triphenylmethane, nitro and nitroso	colour, organic acid and unfixed dyes
Basic	water -soluble, applied in weakly acidic dye baths; very bright dyes	fur, leather, silk and cotton	triarylmethane, azene, xanthenes, thiazine, polymethene, acridine	colour, unfixed dyes
Direct	water -soluble, anionic compounds; can be applied directly to cellulosic without mordant' s (or metal s like chromium and copper)	natural fibers, rayon, nylon, paper and leather	diazo, triazo, polyazo, thiazole, phthalocyanine	colour, salt, unfix dyes, cationic and surfactants
Disperse	water -insoluble	nylon and polyester	simple azo, anthraquinone, and nitroarylamine	colour, organic acid, phosphate and lubricants
Reactive	water -soluble, anionic compounds; largest dye class	cotton, rayon, silk, linen, wool and nylon	azo, anthraquinone, phthalocyanine, stilbene	colour, alkali, oxidizing agent, reducing agent
Sulphur	Organic compounds Containing sulfur or sodium sulfide	cotton and rayon	sulphur dyes	colour, alkali, oxidizing agent reducing agent
Vat	water -insoluble; oldest dyes; more chemically	cotton, rayon and silk	anthraquinone, polycyclic, quinine, indigo	colour, alkali, oxidizing agent, reducing agent

1.3 Health risks of dye effluents

Approximately 10,000 commercial natural and synthetic dyes have been used for colouring applications. Most synthetic dyes are hazardous and their high stability makes them poorly biodegradable (Das *et al.*, 2017). Synthetic dyes are biologically non-degradable due to their aromatic structure and their synthetic origin (Salama, 2017). Azo dyes are the most widely used type of synthetic dyes in textile and garment applications. Azo colors are engineered natural colors which contain nitrogen (N) as the azo group with “-N=N-” as part of the molecular structure (Gupta *et al.*, 2009). About 10%-15% of these dyes are discharged into the environment without treatment and may seriously affect the health of the contact. Azo dyes can decompose and produce more than 20 kinds of carcinogenic aromatic amines under certain conditions. After being activated, it can change the DNA structure of the human body to cause lesions and induce cancer (Li *et al.*, 2018). Therefore, this type of dye must be detoxified before discharge.

1.4 Efforts towards dyes treatment

It is of concern that more than 10% of dyes used in the industry commonly find their way to effluents when they do not bind entirely to the targeted fibres, creating serious environmental pollution (Das *et al.*, 2017). Most textile industries do not really obey the proper and safe disposal of dyes but instead, choose the easy way out by flushing drums of unwanted and untreated dyes into streams of rivers. As a consequence, a number of global actions have been implemented to reduce or eliminate the contents of dyes released from various sources (Ansari *et al.*, 2011). There are numerous existing treatments for removing textile dyes from effluent streams like adsorption, photocatalytic degradation, electrochemical degradation, cation exchange membranes, and biological treatment among many others. However, most of these techniques have considerable disadvantages,

such as incomplete metal removal, expensive equipment and monitoring system, high reagent and energy requirements, or generation of toxic sludge or waste that requires proper disposal (Nolasco *et al.*, 2019). Furthermore, the treatment of azo dyes in wastewater is a great challenge because these dyes are believed to be electron-deficient xeno-biotic compounds with complex structures that make them resistant to degradation (Cheruiyot *et al.*, 2019). From Table 1.2, it could be observed each treatment has its advantages as well as disadvantages when being used to remove dyes from wastewater (Sivamani *et al.*, 2021).

Table 1.2: Advantages and drawbacks of commonly used methods for removal of pollutants from wastewaters.

Methods	Advantages	Disadvantages
Ozonation	Applied in gaseous state no alternative of volume	Short half-life of ozone (20mins)
Oxidative process (H ₂ O ₂)	Simplicity of application	(H ₂ O ₂) should be first activated
Fenton reagents	Effective decolourization of both soluble and insoluble Dyes	Big sludge production
Photocatalysis	No sludge production	Formation of by products
Adsorption	Low cost, high efficiency for removal of different types of dyes and metal ions	Some adsorbents have low surface area, possible side reactions loss of adsorbents, performance dependents on wastewater characteristics
Ionic exchange	Regeneration, no adsorbent loss	Not effective all types of dyes
Electrochemical treatment	Degraded compounds are non-hazardous	High cost
Irradiation	Effective oxidation at lab scale	High cost, requires a lot of dissolved O ₂
Biological process	Environmentally friendly, public acceptance, economically Attractive	Slow process, needs adequate nutrients, narrow operating temperature range
Coagulation and precipitation	Effective for all dyes	High sludge production, high cost

1.5 Adsorption

At present, among the numerous techniques reported for the treatment of dye-containing wastewater, adsorption is a worldwide and acceptable technique, widely considered one of the most promising methods due to its simplicity, low cost, efficiency, reusable, eco-friendly, and rapid method for the treatment of industrial effluents carrying dyes, and it does not contribute to the production of any harmful secondary pollutants (Senguttuvan *et al.*, 2022). In the current study, adsorption by polymer-based materials has been investigated for the removal of dye ions from wastewater.

1.6 Classification of adsorption

Adsorption can be divided into two categories: physisorption and chemisorption, depending on how the adsorbate and adsorbent interact. Weak forces between the species are what cause the physisorption interaction, which is generally non-specific. The adsorbed molecule is free to move about the surface throughout this phase since it is not attached to a specific location on the solid surface (Naushad *et al.*, 2013).

Vander Waals, dispersion, and hydrogen bonding are three examples of physical interactions between species that are based on electrostatic forces. On the other hand, chemisorption includes the adsorbate being chemically altered as chemical bonds are formed. Though chemisorption is also based on electrostatic forces, these forces play a significant role in this process. Covalent or ionic bonds between atoms, with shorter bond lengths and greater bond energies, are what attract the adsorbent and adsorbate in chemisorption. The differences between chemisorption and physisorption are given in Table 1.3 (Naushad *et al.*, 2013).

Table 1.3: Properties of physisorption and chemisorption.

Chemisorption	Physisorption
Monolayer adsorption	Multilayer adsorption
High degree of specificity. Depends on the number of active sites	Low degree of specificity
High values to enthalpy of chemisorption	Low values to enthalpy of chemisorption
Endothermic or Exothermic	Exothermic

1.7 Polymer-based adsorbent

In general, the process costs associated with such dye removal techniques depend mainly on the cost of the adsorbent and its regeneration (Li *et al.*, 2018). To date, biomaterials, modified clays, activated carbon materials, polymer composite, biochar, hydrogels, and zeolites have been applied as adsorbents to remove dyes (Li *et al.*, 2018; Salama, 2017). Some of the adsorbents are effective in removing dyes and various pollutants, but some are not. Although a variety of adsorbents have been used for the removal of dyes from water, synthetic and real industrial effluents, each of the adsorbents has its own disadvantages. Factors like adsorbent size, surface area and porous nature, rate of diffusion, and chemical and/or ionic interactions between pollutants and adsorbent highly alter the adsorption rate (Senguttuvan *et al.*, 2022). Hence, new effective adsorbents are needed which should be cost-effective, energy-efficient, design flexible, biodegradable, and available (Rahman and Akter, 2016), and there is a continued interest in searching for new adsorbents that can rapidly and effectively adsorb dyes from water, synthetic and real industrial effluents (Senguttuvan *et al.*, 2022).

1.8 Conducting polymer-based adsorbent

Several polymers are in use as adsorbents for the adsorption of dyes and heavy metal ions from wastewater. In the past decades, conducting polymer-based adsorbent have been an area of intense research and various types of research have been performed associated with the physics and chemistry of conducting polymers. This is due to their particular physicochemical properties, they are considered a new dimension in the environmental remediation of pollutants and besides and they are easy to separate from solution after use with a simple filtration method (Huang *et al.*, 2014). A wide range of possible applications has been proposed for conducting polymers such as rechargeable batteries, conductive paint, heavy metals separation, removal of dyes, optical devices, shielding, antistatic coating, sensors and biosensors, biomedical applications, and so on (Hasani *et al.*, 2013).

As one of the novels conducting polymers, polypyrrole (PPy) (Figure 1.2) has been widely studied as one of the most valuable materials for its high electrical conductivity, facile synthesis on a large scale, non-toxicity, long-term environment stability, excellent redox property and the existence of positively charged nitrogen atoms in the polymeric backbone (Xin *et al.*, 2015). Polyaniline, polypyrrole, polyacetylene, and polythiophene are the most common conducting polymers, but in terms of synthesis, doping, and dedoping process, polypyrrole is economical and eco-friendly over other conducting polymers (Bai *et al.*, 2015). However, different surface functional materials can be used with polypyrrole to form composite materials that can yield higher sorption efficiency for dye ions. In recent times, materials such as sawdust, natural and synthetic zeolite, cellulose, activated carbon, chitin, or graphene are the commonly used components with polypyrrole or other conducting polymers to remove various dyes from the aqueous environment (Huang *et al.*, 2014).

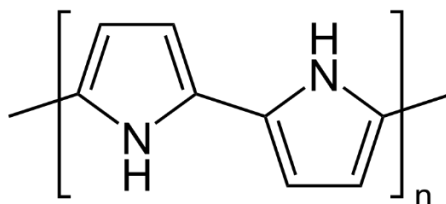


Figure 1.2: Structure of polypyrrole.

1.9 Problem statement

Despite the previous efforts, till now, the development of polypyrrole composite adsorbents that have a high surface area and rich surface functional groups, such that can result in higher sorption capacities are still much anticipated for dye ions removal and have not been fully investigated as potential adsorbents for organic dyes, especially MO and CV dyes. Hence, an alternative effort is to prepare low-cost, high-efficiency, and recyclable adsorbents by synthesizing PPy composites to enhance their adsorption properties. As it is seen from these promising applications, PPy conducting polymer has been made composites with polyethyleneimine (PEI) (Figure 1.3), a cationic polyelectrolyte containing branched chains in addition to primary, secondary, and tertiary amino groups, due to its high charge density and good biocompatibility (Xin *et al.*, 2015). PEI has a strong potential for the adsorption of methyl orange (MO) and crystal violet (CV) dyes from wastewater. PEI has more nitrogen-containing groups in the compounds that can be added to the pyrrole structure. To date, no effort has been made to evaluate the adsorption properties of these conducting polymer composites toward the removal of MO and CV dyes from wastewater. The combined effect of polypyrrole with polyethyleneimine will have a strong adsorption capacity for both dyes.

Therefore, a thorough study is imperative to investigate the adsorption properties of polypyrrole-polyethyleneimine (PPy-PEI) composites in removing dyes effectively from wastewater by using different oxidants at various process conditions. The goal is to

investigate the ideal parameters such as contact time, initial pH solution, mole ratio, adsorbent dosage, and initial dye concentration which will result in high removal of dye from wastewater. Hence, in this work, we wish to propose the synthesis of homogeneous structures of PPy-PEI at various conditions with the most cost-effective technique.

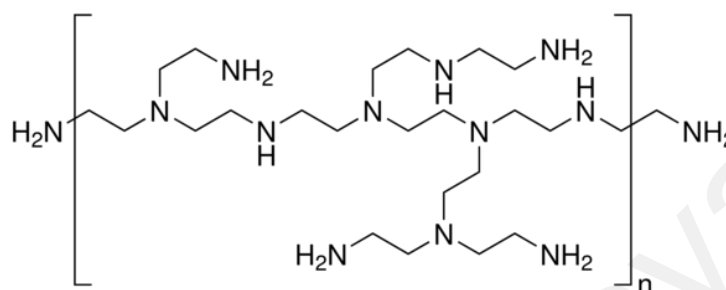


Figure 1.3: Branched of polyethyleneimine.

1.10 Scope of research

This research concerns the removal of MO and CV dyes from wastewater by adsorption method using PPy and PPy-PEI composite as adsorbents. The materials that will be used are Py monomer, PEI, and oxidants (ammonium persulfate, iron (III) chloride hexahydrate, and iron (III) chloride anhydrous). The experiment will be performed at the following monomer-to-oxidant ratios of 1:0.5, 1:1, 1:2, and 1:3 respectively, at room temperature. Different initial dyes concentration to be used are from 25 ppm to 300 ppm with the contact time at 30 min to 300 min, adsorbent dosage varying from 0.05 g to 0.4 g, and solution pH will be carried out between the range of 1 to 13. The structure and morphology of the prepared polymer composite will be characterized by analytical techniques such as attenuated total reflectance Fourier transform infrared (FTIR), Brunner-Emmett-Teller (BET), X-ray diffraction pattern (XRD), and field emission scanning electron microscopy (FESEM).

1.11 Research objectives

This study embarks on the following objectives:

1. To synthesize polypyrrole and polypyrrole-polyethyleneimine composites using various oxidants such as ferric chloride anhydrous, ferric chloride hexahydrate, and ammonium persulfate, respectively, for the adsorption of dyes from wastewater.
2. To characterize the prepared polymer-based adsorbents by BET, FESEM, FTIR, and XRD.
3. To study the effects of various parameters such as mole ratio, contact time, adsorbent dose, solution pH, and the initial dye concentration on the adsorption efficiency of methyl orange and crystal violet dyes.
4. To study the adsorption isotherm and kinetics of methyl orange and crystal violet dyes.
5. To evaluate the regeneration of adsorbents and repeatability studies.

CHAPTER 2: LITERATURE REVIEW

2.1 Dye pollution

In general, dyes are dissolved in wastewater as particulates and emulsified phases. Different dyes have different constituents; hence it is a tough challenge to treat them satisfactorily. It can be said that the denser the effluents contained in wastewater due to dyes, the harder it is to segregate them (Alghamdi *et al.*, 2019). The decomposition of these compounds is controversial due to their aromatic structure and molecular size which led to their good stability and solubility (Shanehsaz *et al.*, 2015). Dyes are known as toxic organic materials of low biodegradability and play the main role in some environmental problem as aesthetic pollution, eutrophication, and perturbations of the aquatic system. Additionally, the presence of dyes as pollutants in the water resources can reduce the water quality and be responsible for mutagenic and carcinogenic effects which may infect the human and the surrounding wildlife (Mohamed *et al.*, 2018).

Dye pollution is a global issue owing to the hazardous nature of dyes. It is considerably visible in the environment, as dyes are commonly highly water-soluble and not readily degradable under natural conditions, resulting in a relatively long-time residence in the environment (Alghamdi *et al.*, 2019). The dyes in waters even at low concentrations may be toxic to aquatic life and may cause health problems to human beings, such as kidney disease, damage to the nervous system, genetic mutation, and cancer (Zhang *et al.*, 2019). Furthermore, the existence of dyes in water bodies decreases the depth of light penetration, inhibits the growth of biota, and imparts toxicity to aquatic life. Hence, the water contaminated by dye at even a concentration of 1.0 mg/L would cause a change in color and make it improper for human usage. Consequently, removing dyes from wastewater before discharging them into rivers and natural streams is one of the serious environmental concerns (Shanehsaz *et al.*, 2015).

2.2 Specific effects and properties of organic dyes

Organic dyes, especially azo dyes, are commonly employed to color products such as textiles, pulp and paper, dyestuffs, and plastics, which leads to the discharge of large volumes of colored wastewater into the environment. Azo dyes are the most widely used type of synthetic dyes in textile and garment applications (Li *et al.*, 2018). The most common type of textile dyestuff being used, constituting about half of the annual production is azo dyes, with Methyl Orange (MO) and Crystal Violet (CV) (Figure 2.1) considered as the model water-soluble azo dyes as they are widely used in various industrial fields (Nolasco *et al.*, 2019; Cheruiyot *et al.*, 2019). These dyes are resistant to the natural environment even through long-term exposure to sunlight, water, and other harsh conditions, and without proper treatment, these dyes remain in the environment for a long period of time (Nolasco *et al.*, 2019). Since this study focuses on MO and CV dyes, hence, their specific properties and health effects are considered important to be investigated.

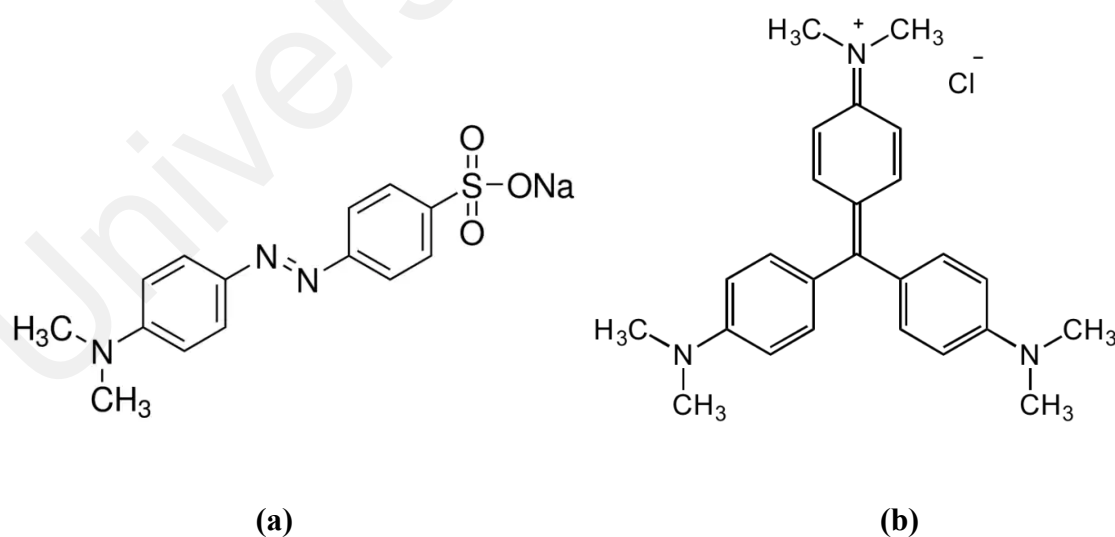


Figure 2.1: Structure of dyes (a) Methyl orange (b) Crystal violet

2.2.1 Anionic methyl orange (MO) dye

MO is an anionic, water-soluble azo dye, which can function as a weak acid having an approximate pH of 6.5 when dissolved in water. Besides its use for industrial colouring, it also serves as a pH indicator in various laboratories, with a red to yellow colour-change range of 3.1–4.4. MO is a sulfonated azo dye, and the functional groups that are responsible for their bright colour in water make them difficult to remediate through conventional methods. Dyes bearing aromatic amines in their chemical structures are carcinogenic due to the production of benzidine compounds via biotransformation (Alghamdi *et al.*, 2019). Because of its high chromaticity, complex organic components, stable chemical quality, and difficulty in microbial degradation, MO-containing wastewater becomes more difficult to treat (Xin *et al.*, 2015). Therefore, MO from industrial effluents must be significantly removed from wastewater before discharge (Nolasco *et al.*, 2019).

2.2.2 Cationic crystal violet (CV) dye

Meanwhile, CV also known as gentian violet is a synthetic cationic dye belonging to the triphenylmethane group (Alghamdi *et al.*, 2021), known to be carcinogenic, mutagenic and still extensively used in commercial textile operations, biological staining and as a dermatological agent (Cheruiyot *et al.*, 2019), similar to MO dye. Compared with anionic dyes, cationic dyes are more toxic to mammalian cells due to their ability to interact with negatively charged cell membrane surfaces, which enables them to penetrate into cells and concentrate in the cytoplasm (Alghamdi *et al.*, 2021). The dye can be absorbed in harmful amounts through the skin and cause skin irritation and digestive tract irritation. Exposure to the dye may induce moderate eye irritation and painful sensitization to light. In extreme cases, it may lead to respiratory complications, kidney failure and permanent blindness (Cheruiyot *et al.*, 2019).

These harmful effects necessitate efficient strategies for the removal of CV (and similar toxic dyes) from water bodies.

2.3 Dyes treatment techniques

Some physical and chemical methods have been introduced to remove the dyes from aquatic bodies. These include photocatalytic oxidation, membrane separation, flocculation, irradiation, ozonation, etc (Shanehsaz *et al.*, 2015). However, most of these techniques have considerable disadvantages, such as incomplete metal removal, expensive equipment and monitoring system, high reagent and energy requirements, or generation of toxic sludge or waste that requires proper disposal (Nolasco *et al.*, 2019). The advantages, as well as disadvantages while being used to remove dyes from wastewater by different dye treatment techniques, also have been summarized in Table 1.2 (Chapter 1). At present, among the numerous techniques reported for the treatment of dye-containing wastewater, adsorption is considered one of the most promising methods due to its simplicity, effectiveness, and low cost (Li *et al.*, 2018), and hence, the present study concerns the use of adsorption technique to remove MO and CV dyes from aqueous environment.

Over the last few years, a sizeable research investigation has been undertaken by various researchers for wastewater treatment using the adsorption process. The adsorption process is utilized as a stage of an integrated chemical-physical-biological process for the treatment of wastewater. Adsorption can be divided into two types which are chemical sorption and physical sorption. Chemical sorption (chemisorption), is defined by the formation of strong chemical associations between molecules or ions of adsorbate, which is generally due to the exchange of electrons where the process is irreversible. Physical sorption (physisorption) involves the weak Van der Waals intraparticle bonds between

adsorbate and adsorbent and thus physisorption generally is reversible in most cases (Seow *et al.*, 2016).

Figure 2.2 shows the schematic diagram of the adsorption process (Soliman and Moustafa (2020)). Adsorbate is the substance where it experiences adsorption whereas adsorbent is the substance that adsorbs the adsorbate. The adsorption process does not really require expensive starting materials as they can be obtained from existing low-cost adsorbents. Also, the adsorption process needs to be accompanied by varying parameters like contact time, dye concentration, mole ratio, and so on (Xin *et al.*, 2015).

The adsorption process of dye molecules consists of four consecutive steps. The first step is the diffusion of dye molecules through the bulk of the solution. In the second step, the dye molecules will diffuse through a diffusional boundary layer (film diffusion). The third step is followed by the diffusion of dye molecules from the surface into the interior of the adsorbent materials. The last stage is where the dye molecules will attach to the surface of the materials through molecular interactions (Seow *et al.*, 2016).

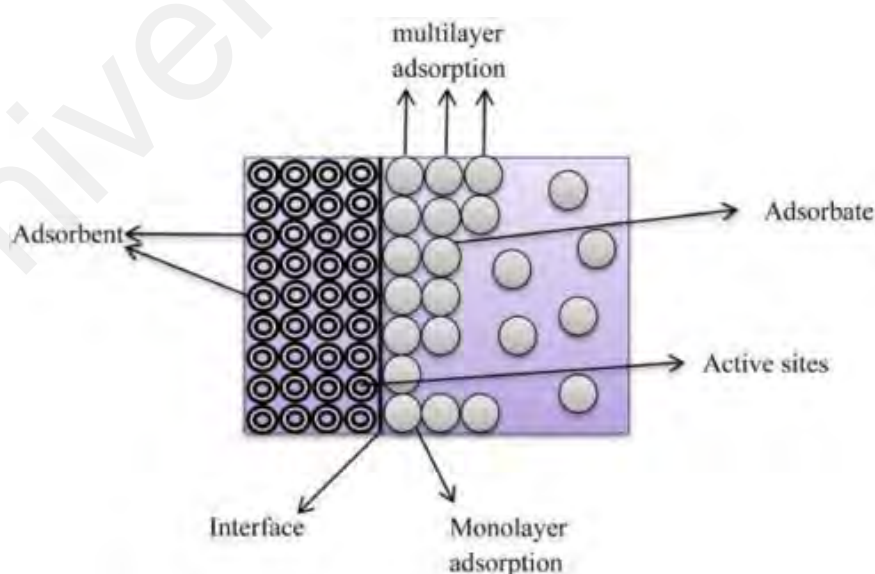


Figure 2.2: Schematic diagram of adsorption process.

Adsorption is well known for its effectiveness and reasonable economic value for the removal of various solutes when compared to other high-ended techniques. This explains the ease of handling and design, adsorbate-specificity, and effective treatment with negligible waste generation. Also, the adsorption method has better secondary levels whereby it has the capability of reusing its adsorbent, ease of regeneration and low-cost operation (Mohamed *et al.*, 2018). With all these being said, and many other advantages that the adsorption process possesses, this specific technique is one of the leading approaches in the removal of dyes from wastewater.

2.4 Factors affecting adsorption of dye

There are many factors that affect the number of adsorbed dyes and the efficiency of dye removals such as solution pH, initial dye concentration, adsorbent dosage, temperature, contact time and surface area and pore size of the adsorbent. For a practical application, optimization of these factors is very important from the economic and environmental points of view.

2.4.1 Effect of solution pH

The initial pH is a critical factor in controlling the adsorption capacity and surficial chemical functional groups of the used adsorbents and catalysts. It can cause protonation and/or deprotonation for the exposed functional groups which in turn give the catalyst a negative or positive charge. As a result, the rate of adsorption will vary with the pH of the medium used (Mohamed *et al.*, 2018).

For an adsorbate having a neutral pH, the adsorption efficiency would be high as more adsorbate solutes will be piled up together on the sorbent surface. However, the variable in this mechanism highly depends on the physic-chemical properties of sorbent with the pH solution. In addition, a property related to the solution of pH is the point zero

charge (pH_{pzc}) which owns the adsorbent surface. This point zero charge exhibits reading zero when a solid is submerged in an electrolyte. This shows the ability of adsorption and the type of active surface. It is known that H^+/OH^- are potential-determining ions whereby a value of pH_{pzc} can be used to determine adsorption systems only (Seow *et al.*, 2016).

When the solution is acidic (low pH), the positive charge on the solution interface will increase and the adsorbent surface will appear positively charged, which results in an increase in anionic dye adsorption and a decrease in cationic dye adsorption. Thus, anionic dye adsorption is favored at low pH ($\text{pH} < \text{pH}_{\text{pzc}}$). In contrast, when the solution is too alkalized (high pH), the positive charge on the solution interface will decrease and the adsorbent surface will appear negatively charged, which results an in increase in cationic dye adsorption and a decrease in anionic dye adsorption. Thus, cationic dye adsorption is favored at high pH ($\text{pH} > \text{pH}_{\text{pzc}}$) (Noreen *et al.*, 2020).

Mohamed *et al.*, (2018) studied the effect of solution pH on the adsorption of safranin dye from water using polypyrrole nanofiber/Zn-Fe layered double hydroxide (PPy NF/Zn-Fe LDH). The removal percentage of the studied safranin dye exhibits a gradual increase in the value with increasing the pH value from pH 2 to pH 8 achieving the best results at neutral to alkaline conditions at pH from 7 to 8. The results obtained showed that the adsorption of cationic safranin dye was more favored in an alkaline medium.

2.4.2 Effect of initial dye concentration

The initial concentration of the adsorbate is an important factor that determines the amount of adsorbate ion that is adsorbed on the adsorbent surface. The connection exists when the interaction of adsorbent-adsorbate is strong in which the amount of adsorbate that could be adsorbed in bulk versus the sorption capacity of an adsorbent (Zhou *et al.*, 2017). The sorption capacity of an adsorbent will increase linearly with the increasing

amount of initial concentration as a higher driving force exists to win over the resistance of mass transfer of the adsorbent and the solution itself. However, the higher the initial concentration, the lower the adsorption rate because there is a high number of ions per unit mass of adsorbents with a specific amount of adsorbent dosage being a constant here, which is attributed to the saturation of the sorbent surface (Bhatti *et al.*, 2020).

Xin *et al.*, 2015 studied the effect of initial dye concentration on the MO adsorption of the PPy nanofibers by varying the initial MO concentrations from 30 to 200 mg/L. From the results, it could be easily observed that the equilibrium adsorption capacities of MO at different concentrations presented an increasing trend (from 29.01 to 169.55 mg/g) since the initial MO concentration gradient could provide a driving force to overcome the mass transfer resistance of the dye. But the removal efficiency of MO by PPy nanofibers exhibited a trend of increasing at low concentrations and then decreasing at high concentrations. It could be accounted for that the certain amount of PPy nanofibers had limited adsorption capacity.

2.4.3 Effect of adsorbent dosage

The amount of adsorbent is an important factor to determine adsorption capacity according to specified operating conditions. In an era where industries need the saving of amount of adsorbent being used, it is best that the smaller the amount of adsorbent used, the better the adsorption capacity it must be at the industrial scale. Generally, the dye efficiency increases with an increasing the adsorbent dosage due to the number of sorption sites at the surface of the adsorbent will increase as increasing adsorbent doses. As a result, the efficiency of dye removal from wastewater will increase. Furthermore, increasing the adsorbent dosage will provide more surface area and more binding sites for the adsorption process (Seow *et al.*, 2016).

A study on the effect of adsorbent dosage on the removal of synthetic textile dye, reactive blue 19 (Shanehsaz *et al.*, 2015) was individually carried out by adding different amounts of magnetic nanoparticles (MNPs) from 5 to 40 mg into 25 mL of dye solution (50 mg/L, pH 3.0, room temperature) with a contact time of 10 min. It was found that an increase in the amount of adsorbent up to 20 mg increased the removal efficiency. However, it was found that at higher amounts, no considerable changes in removal efficiency were observed. It could be attributed to the unavailability of the binding sites during the adsorption process as all the binding sites have been occupied, thus the adsorbent surface is saturated.

2.4.4 Effect of temperature

Temperature is a vital factor in textile wastewater treatment because it affects the solubility, mobility, and chemical properties of dyes and the interaction between dyes and adsorbents (Senguttuvan *et al.*, 2022). If the adsorption is an endothermic process, the adsorption capacity will increase with increasing temperature due to the increase in the number of active sites and the mobility of the dye molecules at higher temperature. On the other hand, when the adsorption capacity decreases with an increase in temperature, the adsorption process is exothermic, due to a higher temperature may decrease the adsorptive forces between the dye molecules and the active sites on the adsorbent surface (Zhou *et al.*, 2017).

Senguttuvan *et al.*, (2022) investigated the adsorption of Reactive blue (RB) and Reactive red (RR) dyes onto PPy/Ze nanocomposite at different temperatures (30 °C, 40 °C, 50 °C and 60 °C). Both RB and RR adsorption rate increased according to increasing temperature and reached a maximum of 50 °C. However, the adsorption rates of RB and RR decreased at 60 °C. The author concluded that the increased adsorption rate of 50 °C could be due to decreased solubility and increased mobility of dyes. Zhang *et al.*, (2019)

studied the effect of temperature (25 °C, 35 °C, 45 °C) on the adsorption of Eosin Y, methyl orange and brilliant green. From the results, the adsorption capacity of the three dyes increases marginally with the increasing temperature, which indicated that the adsorption was an endothermic process.

2.4.5 Effect of contact time

A certain technology that has been introduced should have contact time as a preference factor for adsorption time to take place. The optimum equilibrium in which adsorption time is short and effective is achieved when the technology to separate adsorbate from its solutions is suitable and economically viable appraised (Saharan *et al.*, 2019). Achieving a good contact time however depends on the strength of the interaction of adsorbent-adsorbate, the number of available sites on the adsorbent surface; inter solute diffusion of adsorbate onto the opening pores of adsorbent, and so on. An optimum contact time needed for the set-up of dynamic equilibrium of adsorbate-adsorbent interaction is purely determined by a thorough and good contact time. During this duration, the contact time will project the rate of adsorption with respect to time (Kim *et al.*, 2014).

The effect of contact time on the adsorption of MO and Cr (VI) over polypyrrole@magnetic chitosan nanocomposite was performed by at different reaction times ranging from 0 to 300 min (Alsaiani *et al.*, 2021). During the initial stage, there was rapid adsorption efficiency of MO and Cr (VI). The synergistic effects between adsorbate and adsorbent in the aqueous solution were responsible for a clear high adsorption efficiency. In the case of the present adsorbent, saturation was achieved after 40 min due to the interaction between adsorbent surface sites and the adsorbate ions. This stage is the saturation phase in which all possible adsorption sites are saturated with the pollutants. After the saturation phase, there was no substantial change. Thus, the

adsorption of MO and Cr (VI) over the nano adsorbent polypyrrole@magnetic chitosan was related to the physicochemical interactions between the adsorbate and adsorbent in water. Particle diffusion and mass transfer indicate that this system was chemically rate controlled. Zhang *et al.*, (2019) also reported that the amounts of adsorbed Eosin Y, methyl orange and brilliant green onto Fe₃O₄/PPy increased rapidly in the first 10 min, afterward the adsorption rate slowed down with the progress of adsorption, and finally, the adsorption attained equilibrium in 20–30 min. At the initial stage, a large number of active sites on the Fe₃O₄/PPy are vacant, which is beneficial for dyes to be adsorbed by Fe₃O₄/PPy. After that, these surface sites are gradually occupied, so the adsorption rate gradually decreases until the adsorption equilibrium is established.

2.4.6 Effect of surface area

Since adsorption is a surface phenomenon, the study of the surface characteristics of a preferred sorbent is very essential. The surface area of an adsorbent depends on the average particle size of the materials, which largely affects the adsorption process. Generally, an excellent sorbent for sorption must have a larger surface area, thus more sorption sites are available or higher pore volume to accommodate the adsorbate. The surface area is obtained from the nitrogen adsorption test at the temperature at which nitrogen changes from liquid to gas (Mohamed *et al.*, 2018).

Senguttuvan *et al.*, (2022) studied the effect of the surface area of PPy/Ze nanocomposite on the adsorption of reactive dyes using a Micromeritics Accelerated Surface Area and Porosimetry 2020 analyzer. The results showed the Brunauer-Emmett-Teller (BET) surface area of zeolite, PPy and PPy/Ze nanocomposite were 242.17 m²/g, 12.13 m²/g and 214.87 m²/g, respectively. Thus, the composite exhibited a higher surface area than its individual components of PPy. The authors confirmed a good surface area

of PPy/Ze nanocomposite provides high adsorption capacity on reactive dyes from wastewater.

2.5 Adsorbent materials

The adsorbent is one of the key factors during the course of adsorption, determining the effectiveness of adsorption processes, so it has become an important research direction to find a suitable adsorbent for the removal of dyes (Xin *et al.*, 2015). The adsorbents used for wastewater treatment come from various sources, they are either from natural origins or as a result of industrial production and/or due to the activation process of some materials. To date, waste red mud, coconut husks, bagasse fly ash, waste materials, biomaterials, modified clays, activated carbon materials, biochar, hydrogels, zeolites and novel polymer have been applied as adsorbents for the removal of various dyes (Rahchamani *et al.*, 2011; Li *et al.*, 2018; Salama, 2017). However, cost is an essential factor for comparison and selection of the suitable adsorbents. An adsorbent can be measured as a cheap materials if it requires the modest processing and available abundantly in nature.

Since this study focuses on the removal of MO and CV dyes from aqueous environment, thus Table 2.1 presents a comprehensive summary of the various types of adsorbents such as commercial activated carbon, metal oxide-based, carbon-based, and metal–organic framework adsorbents used in MO and CV dyes remediation of contaminated water that has been conducted by other researchers (Dutta *et al.*, 2021). These various adsorbents have been shown to be efficient in the removal of dye pollutants from wastewater. Thus, it is anticipated that dye removal by adsorption can provide a feasible solution for the treatment of dye from aqueous environment

Table 2.1: Comparison of the adsorption capacities of dyes for different adsorbents.

Classes of adsorbents	Adsorbent	Dyes	Adsorption capacity/removal efficiency	
			(mg/g)	(%)
Activated carbon	Mesoporous carbon material	MO	294.1	
	Apricot stones	MO	32.25	
	Commercial activated carbon	MO	35.43	
Non-conventional adsorbents	Coal fly ash	CV		> 90
	Acid-treated Palygorskite	CV	223.43	
		MO	276.11	
	Flower-like LDH	MO	500.6	
	Hollow LDH nanowires	MO	210	
	Neem sawdust	CV	2.197	
Hybrid nanomaterial	Ni/porous carbon-CNT	MO	271	
	Calcium alginate/ multi-walled carbon nanotubes	MO	12.5	
	Finger-citron-residue-based activated carbon	MO	934.58	
	MgAl-layered double hydroxide supported MOF	MO	600	99
Metal oxide-based hybrid	Magnetic graphene oxide modified by chloride imidazole ionic liquid	CV	69.44	
	Fe ₃ O ₄ /GO	MO	714.3	
	Fe–Mn–Zr metal oxide	MO	196.07	
	Al cation-doped MgFe ₂ O ₄	MO	274.6	
	Magnetic Fe ₃ O ₄ @UiO-66	MO	244	
	MgFe ₂ O ₄	MO	181.34	
	Sulfonic acid-modified polyacrylamide magnetic composite	CV	2106.37	
Metal–organic frameworks	Porous MOF material-based on chromium-benzene dicarboxylate	MO	194	
	Zirconium-based MOFs	CV	63.38	

2.5.1 Polymer composite adsorbents

At present year different cost-effective, commercially available adsorbents have been used for the removal of dyes from aqueous environments. However, adsorption efficiency with cost-effective, energy-efficient, design flexible, available and high adsorption efficiency are highly demanded. Nowadays, the development of new adsorbents having such properties has generated great interest in wastewater treatment. Several polymers with different functional groups have attracted great interest due to their high adsorption capacities, especially regeneration abilities and reuse for continuous processes (Rahchamani *et al.*, 2011).

Generally, polymer composite adsorbents have more improved physicochemical properties for adsorption over pure polymers owing to the synergistic effect of individual components. The conditions of interaction and chemistry of the polymer intended to be used with the guest-host material are very important to yield homogeneous dispersion. Polymeric adsorbents are preferred to conventional adsorbents due to the simplicity in their processing, the possibility to shape them into other forms such as membranes and beads, and their relatively easy regeneration. Polymeric adsorbents could either be natural or synthetic (Chen *et al.*, 2019).

The search for more efficient and cost-effective adsorbents has led scientists to develop an array of composite adsorbents for the removal of various pollutants from the environment. Composite adsorbents are a distinct category of adsorbents that comprise two or more materials or categories of other adsorbents. The characteristics of the individual adsorbent are usually distinct from the properties of the composite material formed by them. Such materials usually have better adsorption properties than the individual compound used to make up the composite (Dutta *et al.*, 2021). Table 2.2

presents some recent various polymer-based composites that have been used in the removal of MO dye from aqueous environment.

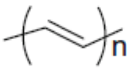
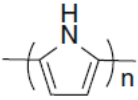
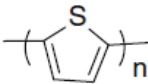
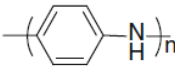
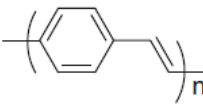
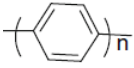
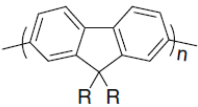
Table 2.2: Comparison of the adsorption capacities of MO and CV dyes reported in the literature for different polymer-based composite adsorbents.

Dye	Adsorbent	Removal efficiency (%)	q _{max} (mg/g)	Ref.
MO	Polyaniline/AC	70.0	285.0	[Hassan <i>et al.</i> , 2019]
	ZnO/polyaniline	99.1	240.8	[Deb <i>et al.</i> , 2019]
	Fe ₃ O ₄ /poly(stylenesulfonate)/ZIF-67	92.0	738.0	[Yang <i>et al.</i> , 2018]
	Chitosan/PVA/TiO ₂	-	425.0	[Habiba <i>et al.</i> , 2017]
	AC/polytetrafluoroethylene	-	176.0	[Xiao <i>et al.</i> , 2018]
	Co ₃ O ₄ nanocube/polyaniline	94.0	107.0	[Shahabuddin <i>et al.</i> , 2016]
	Polyaniline/glass plates	100.0	93.0	[Haitham <i>et al.</i> , 2019]
	LDH/Fe ₃ O ₄ /polyvinyl alcohol	97.0	19.5	[Mallakpour <i>et al.</i> , 2019]
	Fe ₂ O ₃ /polypeptidylated hemoglobin	-	15.2	[Essandoh <i>et al.</i> , 2021]
	Cellulose acetate/polyurethane	25.5	0.185	[Iqhrammullah <i>et al.</i> , 2020]
	Chitosan/polyaniline/copper(II) oxide	98.9	-	[Rathore <i>et al.</i> , 2019]
CV	Magnetic Nanostructures Based on Poly(Benzofuran-co-Arylacetic Acid) Functionalized with Folic Acid (MNP@PAAA-FA)	92.7	25.1	[Ganea <i>et al.</i> , 2021]
	ZIF-67-PAA	-	1606.0	[Liu <i>et al.</i> , 2021]
	Polydopamine/montmorillonite	-	112.4	[Qi <i>et al.</i> , 2021]
	Poly(acrylamide)-kaolin (PAAm-K) hydrogel	96.0	13.4	[Shirsath <i>et al.</i> , 2015]
	Polyurethane foam/rubber granulate	-	20.9	[Sulyman <i>et al.</i> , 2021]
	Polyaniline/Tectona grandis sawdust	-	263.2	[Mashkoor <i>et al.</i> , 2019]
	Poly(3-nitrothiophen)/AgTiO ₂	-	43.1	[Alqarni, 2022]

2.5.2 Conducting polymer-based composites

In recent years, conducting polymers has been the subject of particular interest to chemists and physicists. Generally, conducting polymers are made up of Carbon, Hydrogen and a few heteroatoms such as Nitrogen and Sulphur. They are conjugated polymers with π -electron in the polymer backbone and also exhibit the unique properties of conventional polymers, such as ease of synthesis and flexibility in processing, mainly by dispersion (Xin *et al.*, 2015). Conjugated polymers become conducting polymers after doping. Table 2.3 shows the main chain structures of representative conducting polymers, including polyacetylene (PA), polypyrrole (PPy), polyaniline (PAn or PANi), polythiophene (PT or PTh), poly(p-phenylene vinylene) (PPV), poly(p-phenylene) (PPP), and polyfluorene (PF) (Momina and Ahmad, 2021).

Table 2.3: Common types of conducting polymers and its structure.

Name	Structure
Polyacetylene (PA)	
Polypyrrole (PPy)	
Polythiophene (PTh)	
Polyaniline (PAn)	
Poly(p-phenylene vinylene)	
Poly(p-phenylene)(PPP)	
Polyfluorene (PF)	

In this study, PPy has been selected as a promising conducting polymer-based adsorbent because of its non-toxic nature, environmental stability, low cost and simple preparation. Because of the existing positively charged nitrogen atoms in the PPy matrix, PPy possessed the adsorption ability through ion exchange or electrostatic interaction. Moreover, PPy can undergo protonation or deprotonation processes when it is treated with acid or alkali solution, resulting in the change of its surface charges, followed by the doping or dedoping of counter ions. Owing to the reversible transformation capability, PPy would have excellent regeneration ability, but this was rarely reported. Nevertheless, pristine PPy showed poor adsorption capacity. Some publications have reported that the composites formed through PPy polymerizing on the surface of substrate materials can provide improved adsorption capacity, as compared with pristine PPy (Li *et al.*, 2013). The most commonly researched adsorption of MO and CV dyes using PPy-based composite adsorbent have been studied and are briefly reviewed in the following sections.

2.5.2.1 Review of adsorption of MO and CV dyes by polypyrrole-based composite adsorbents

Xin *et al.*, (2015) studied the potential of the PPy nanofibers as dye adsorbent for the removal of a typical anionic MO dye from aqueous solution. The PPy nanofibers were synthesized by an oxidative template assembly route in the presence of hexadecyl trimethyl ammonium bromide (CTAB) and ammonium persulphate (APS). The as-synthesized PPy nanofibers were characterized by SEM, TEM, FTIR, XRD, and N₂ sorption. Besides, the study further investigated the effects of contact time, initial MO concentration, temperature, and initial solution pH on the adsorption process. From SEM images, the as-synthesized PPy was shown flexible and owned homogenous fibrous morphology with an average diameter of 60-80 nm, TEM images revealed that the solid PPy nanofibers had rough surface, XRD showed the as-synthesized PPy nanofibers were

amorphous with a broad peak at about 26° , and from BET method, it showed the specific surface area of the PPy nanofibers was calculated to be $86 \text{ m}^2/\text{g}$. From the results obtained, the PPy nanofibers showed excellent adsorption capacity of 169.55 mg/g for MO with optimum condition at 120 min equilibrium time, 150 mg/L of MO initial concentration, temperature 298 K, and pH range from 7-10. The adsorption of MO followed the pseudo-second-order kinetic model with correlation coefficients R^2 (0.9999) and the thermodynamic studies indicated the adsorption process was endothermic and spontaneous in nature. Regeneration of the adsorbent was carried out using 0.2 M sodium hydroxide solution (base treatment) and revealed that up to 79.42% of the reuse of MO even after three cycles. The adsorbent was reported to possess good adsorption capacity and stability and the adsorbent could be used many times.

Zhang *et al.*, (2019) reported the adsorption of Eosin Y, MO and brilliant green dyes from aqueous solution using ferroferric oxide/polypyrrole ($\text{Fe}_3\text{O}_4/\text{PPy}$) magnetic composite by an in-situ polymerization method, in the presence of ferric chloride hexahydrate, polyvinylpyrrolidone and γ -Aminopropyltriethoxysilane (KH-550). XRD, FTIR, TGA, and SEM were conducted to analyse the structure and morphology of $\text{Fe}_3\text{O}_4/\text{PPy}$. The influence factors including adsorption time, solution temperature and initial dye concentration were also investigated. From XRD patterns, a broad peak was observed at $2\theta = 26^\circ$, which corresponds to the characteristic reflection of amorphous PPy and the peak intensities of $\text{Fe}_3\text{O}_4/\text{PPy}$ composites decrease, which was associated with the amorphous PPy coated onto Fe_3O_4 . SEM images exhibited uniform spheres with the size about 100–150 nm for pure Fe_3O_4 and the $\text{Fe}_3\text{O}_4/\text{PPy}$ shows similar spherical morphology but larger size in comparison with pure Fe_3O_4 . The equilibrium contact time exhibited for Eosin Y, methyl orange and brilliant green on $\text{Fe}_3\text{O}_4/\text{PPy}$ were 20, 45 and 20 min, respectively, the adsorption capacity of three dyes increases marginally with the increasing temperature, and the equilibrium adsorption capacity of three dyes increases

with the increasing initial dye concentration. The experimental data were well fitted to the pseudo-second order and Langmuir isotherm model with maximum adsorption capacities of Eosin Y, methyl orange and brilliant green at 25 °C of 212.31, 149.48 and 263.85 mg/g, respectively. Thermodynamic studies reported that the adsorption process occurred spontaneously, in an endothermic and physisorption nature, and with increased disorder. From the study, the convenient magnetic separability of Fe₃O₄/PPy makes it a good candidate for practical application in the removal of organic dyes from polluted water.

Another study on the adsorption of azo dye MO from aqueous solutions was investigated by Alghamdi *et al.*, (2019), using alkali-activated polypyrrole-based graphene oxide (PACK). The pyrrole monomer was polymerized using ammonium persulfate as an oxidant and HCl as a dopant and the PPy was thoroughly mixed with KOH under the following condition: nitrogen atmosphere, heating ramp rate of 3 °C/min; activation time of 2 h, and activation temperature of 650 °C. The structural, thermal, and morphological properties of the PACK before and after MO adsorption were analysed by FTIR, SEM, CHN, EDX, TGA, and DSC methods. The experimental data showed the time-dependent adsorption behaviour was rapid in the initial period (5 min) and after that, the adsorption increased slowly, showing practically negligible increase after 195 min, assuming a physisorption mechanism, which may be controlled by the diffusion process. In the column operations, the equilibrium adsorption capacity, the saturation percentage, breakthrough point, and exhaustion times were found to be 57.21 mg/g, 87%, 90, and 290 min, respectively. The kinetic study revealed a preferably pseudo-second-order ($R^2 = 0.9996$) and the thermodynamic adsorption tests resulted in negative ΔG° , ΔH° , and ΔS° values, which decreased as the temperature and concentration increased, indicating the spontaneous and exothermic adsorption over 25–45 °C. The experimental data fitted in the order of Langmuir \approx Freundlich $>$ Temkin, with evidence of adsorption operating

well via the monolayer physical adsorption process, and maximum monolayer adsorption ranging from 520.8 to 497.5 mg/g. The regeneration process showed a 73% MO recovery during 80 min, with 66% desorbed in the first 20 min. Thus, the authors concluded that PACK is a highly effective adsorbent for the removal of dyes from wastewater.

A novel adsorbent of PPy@magnetic chitosan nanocomposite was synthesized for the removal of MO and Cr (VI) from water (Alsaiani *et al.*, 2021). This novel adsorbent contained magnetic Fe₃O₄ nanoparticles and several N-containing functional groups. The synthesized magnetic chitosan was modified using pyrrole monomers according the oxidative polymerization method in the presence of ammonium persulfate, ferrous sulfate heptahydrate, and ferric chloride hexahydrate. The nanocomposite studied was successfully characterized using different techniques including SEM, TEM, TGA XRD, and FTIR. The effect of contact time, pH, and co-existed ions on the adsorption of MO and Cr (VI) over the synthesized nanocomposite were studied. From the characterization images, it was observed that polypyrrole was successfully loaded over the magnetic chitosan, which clearly indicated the presence of coated Fe₃O₄ nanoparticles, which were mainly implanted between the chitosan and polypyrrole (in the interior of the formed PPy@magnetic chitosan nanocomposite), while in FTIR and XPS studies, approved the successful adsorption of both MO and Cr (VI) over the adsorbent surface in addition to the reduction of Cr (VI) to Cr (III). The authors reported maximal removal efficiencies of MO and Cr (VI) over this magnetic polymer nanocomposite reached 95 and 105 mg/g, respectively. The study of the contact time effect indicated that the saturation was achieved after 40 min due the interaction between adsorbent surface sites and the adsorbate ions and after the saturation phase, there was no substantial change observed. The pH effect study revealed that MO and Cr (VI) adsorption were more suitable in a neutral or an acidic medium at an optimal pH value between 2 and 4.5. It was reported that the pH increase led to a decrease in MO and Cr (VI) removal capacity due to the

strong electrostatic interaction between the adsorbent positive charge at low pH and pollutants negative charge. While, the study of the co-existing ions effect revealed that the most affected co-ion on adsorption efficiency was sulfate, while bicarbonate had the lowest effect. The adsorption isotherm best fitted with the Langmuir isotherm, suggested monolayer adsorption of MO and Cr (VI). The reusability study using 0.1 M NaOH as eluent also indicated an excellent reusability of the nanocomposite up to 5 successive cycles with a slight reduction in the removal efficiency toward MO and Cr (VI), which was attributed to the loss of functional group activity. As a conclusion, the authors concluded that ppy@magnetic chitosan nanocomposite was a promising adsorbent for removing MO and Cr (VI) from water.

Mashkoo *et al.*, (2020) explored the adsorption characteristic of polypyrrole decorated chitosan-based adsorbent (MChs/PPy) in the presence of ammonium persulfate, ferrous chloride dihydrated, and anhydrous ferric chloride for the elimination of cationic crystal violet and anionic methyl orange dye from wastewater. The TGA, SEM/EDAX, TEM, BET, FTIR, VSM, and XRD analyses were conducted to study the characteristics of MChs/PPy. The effect of MChs/PPy doses, adsorbate/adsorbent interaction time, solution pH, initial dye concentration, and temperature of the system on the adsorption of dyes were investigated via batch method. The study reported that the optimum pH for the adsorption of MO and CV dye was found to be 5 and 8, respectively. The adsorption process attains equilibrium after 150 and 120 min for CV and MO, respectively and the adsorption capacity raises with the rise in initial CV and MO concentration. It was clearly visible that the adsorption of MO was greater than that of CV dye. The isotherm study manifested that the Langmuir model was best fitted to the equilibrium data of CV and MO dyes with the maximum monolayer sorption capacity of 62.893 and 89.286 mg/g, respectively at 303 K. The kinetics study followed pseudo-second-order model for CV and pseudo-first-order model for MO removal with R^2 values

was found to be closer to 1. The percent desorption of CV and MO dye was about 62.36 and 69.02% up to three-cycles using ethanol and 0.1 M sodium hydroxide with the removal efficiency of 61.60 and 54.42%, respectively. From these results the authors confirmed that MChs/PPy was stable enough to be used repeatedly for the elimination of both CV and MO dye from aqueous solution.

Adsorption of cationic CV dye by polypyrrole composite also has been explored by other researchers. Alghamdi *et al.*, (2021) investigated the adsorptive performance of the polypyrrole-based KOH-activated carbon (PACK) in the removal of the basic dye CV using a batch adsorption system. Batch adsorption processes were performed to investigate the effects of contact time (0–120 min, and up to 24 h), initial CV concentration (50–500 mg/L), and temperature (25–45 °C). From the experimental results, the equilibrium time has reached after 60 min and it was observed that as the initial dye concentration increases, the adsorption capacity (q_e) increases while the efficiency (R_e) decreases. The adsorption kinetics study better fitted pseudo-second-order model ($R^2 \geq 0.9996$) and isotherm study was found to be best expressed by the Langmuir model with a maximum monolayer capacity, q_m , of 497.51 mg/g at 318 K. The thermodynamic studies indicated a spontaneous and endothermic adsorption system in which the spontaneity slightly increases with temperature and decreases with initial CV concentration. The results for regeneration generally indicate a total mass recovery of CV of about 72% after three cycles of the adsorption-desorption process using elution systems of 25% acetone and 75% of 0.25 NaOH. The results indicate the reusability of the adsorbent with possible regeneration enhancement; however, it necessitates further optimization of the regeneration conditions including solvents types, concentrations, solution pH, etc. Overall, the authors confirmed that the PACK was a promising adsorbent for the removal of CV and potentially other cationic dyes from industrial effluent.

Polypyrrole has emerged as a conducting polymer-based dye adsorbent. Many studies pristine polypyrrole has been known for its adsorption for dyes. However, in order to improve the adsorption efficiency for both cationic and anionic dyes, polyethyleneimine has been added to polypyrrole structure which appears to be very suitable for adsorption for both cationic and anionic dyes from aqueous solution due to large quantity of nitrogen atoms of amino groups in polypyrrole-polyethyleneimine structure. The synergistic effect of both the components in this newly reported polypyrrole-polyethyleneimine adsorbent has been realized with a high efficiency for both the cationic and anionic dyes in aqueous solution. The role of increasing the amine group on adsorption of different anionic and cationic dyes has been sought.

2.5.3 Polyethyleneimine-based (PEI) adsorbents

Polyethylenimine, a highly water-soluble polyamine, has gained considerable attention in the field of wastewater remediation owing to the high affinity of its high-density of amine groups on the molecular backbone towards hydrophilic pollutants. Several studies have reported that heavy metal ions can be easily adsorbed by these nitrogen containing moieties through chelation and anionic dyes could also be selectively attracted through electrostatic attraction (Chen *et al.*, 2019). In PEI, one end of the polymer chain contains methyl and the other end is made up of hydroxyl. PEI is a cationic water-soluble polyamine which could be divided into two types; linear and branched PEIs. Branched PEI (Figure 1.3) has a high concentration of polar groups containing nitrogen atoms. Nevertheless, PEI is soluble in water, hence a solid support is required for attachment of PEI to enable the adsorption property (Wong *et al.*, 2018).

Despite the advantages of PEI material, only few studies were reported on the application of such materials in adsorption of pollutants from wastewater, especially for CV removal from wastewater. However, the most commonly researched on the

adsorption of dyes using PEI-based composite adsorbent have been studied and are briefly reviewed in the following subtopic.

2.5.3.1 Review of adsorption of MO and CV dyes by polyethyleneimine adsorbents

Li *et al.*, (2018) reported the successful synthesis of a green and efficient bioadsorbent (PTP) of methyl orange (MO) through the cationic modification of persimmon tannin (PT) using polyethyleneimine (PEI) via glutaraldehyde crosslinking. The SEM, FTIR, BET, TGA, and Zeta potential measurements were conducted to study the physicochemical properties of the prepared bioadsorbent. Systematic batch adsorption experiments were carried out with pH, bioadsorbent dosage, initial MO concentration and contact time. The characterization results confirmed the successful synthesis of the PTP bioadsorbent. From the experimental results, it was confirmed that the adsorption of MO onto PTP was highly dependent on pH, bioadsorbent dosage, initial MO concentration, and temperature, with a maximum adsorption capacity of 225.74 mg/g at 323 K and pH 4 when the initial concentration of MO was 35 mg/L, the PTP bioadsorbent dosage was 15 mg, and an equilibrium time of 120 min was employed. Furthermore, the equilibrium data indicated that the Freundlich isotherm model was the best fit for this system, suggesting that the adsorption process followed the multi-site adsorption isotherm for heterogeneous surfaces. Moreover, kinetic regression analysis indicated that the adsorption processes followed the pseudo-second order model, indicated that the rate limiting step may involve a chemisorption-based mechanism. Thermodynamic data revealed that the adsorption of MO onto PTP was feasible, spontaneous and endothermic. The authors also reported a possible mechanism for the adsorption of MO on PTP where electrostatic interactions, hydrogen bonding, and $\pi - \pi$ interactions dominated the adsorption of MO onto PTP. The recyclability of PTP for MO and simulation wastewater containing inorganic compounds were evaluated and it was found that MO removal

efficiency compounds were evaluated and it was found that MO removal efficiency remained high (81.47%) after six cycles. This work concluded that PTP can be considered suitable for application as an efficient adsorbent for the removal of anionic dyes from wastewater.

A study on MO dye adsorption by polyethyleneimine-graphene oxide polymer nanocomposite beads was reported by Nolasco *et al.*, (2019). Nanocomposite beads containing 2% chitosan (CS), 2% polyethyleneimine (PEI), and 1,500 ppm graphene oxide (GO) were synthesized for the removal of MO from water. The CS-PEI-GO beads was characterized by FTIR and SEM and it showed favorable adsorbent properties as given by the presence of numerous surface functional groups and a porous structure. From the results obtained, FTIR and SEM analyses after adsorption confirmed the presence of MO on the surface of the beads and revealed an intact and also stable structure. Effects of different parameters such as pH which adjusted from 2.0 to 9.0, contact time with different time intervals from 0 to 24h, and initial concentration from 25 to 500 ppm, on the percentage removal of MO and adsorption capacity of the beads were investigated by performing batch adsorption experiments. The results showed the maximum removal of MO was achieved at pH 3 at 25 °C using 50 ppm MO concentration and 24 h contact time, and as overall, MO removal of more than 85% was achieved by the beads across a wide pH range. Kinetic studies followed a pseudo-second order kinetic equation (R^2 of 0.9999). Furthermore, adsorption equilibrium data for MO were best described by the Toth isotherm model ($R^2 = 0.9644$), suggesting multilayer adsorption on heterogeneous adsorption sites with a maximum adsorption capacity of 421.51 mg/g. The desorption and regeneration studies showed that the best desorption agent is NaOH with desorption efficiency reaching up to 76.77%. The author reported that MO is best desorbed from the beads in an alkaline environment as hydroxide ions compete with anionic MO by deprotonating the amine groups found in the beads. The regeneration studies were carried

out in four cycles of adsorption-desorption. The results showed a decrease in the adsorption capacity of the beads through repeated use, which may be due to occupied adsorption sites that hinder the uptake of new MO ions. Nevertheless, even after four cycles, the beads can still remove up to 9.16 mg of MO per g of beads. The authors concluded that the beads can be further explored through continuous column studies for industrial applications.

Another study revealed on dye removal by polyethyleneimine adsorbent was conducted by Huang *et al.*, (2019). The authors investigated the adsorption performance of polyethyleneimine modified magnetic core-shell $\text{Fe}_3\text{O}_4@\text{SiO}_2$ nanoparticles ($\text{Fe}_3\text{O}_4@\text{SiO}_2/\text{PEI}$) on the removal of the anionic dyes MO and congo red (CR) from aqueous solution. Various techniques such as TEM, TGA, FTIR, XRD, VSM and XPS were conducted to study the structure and properties of the adsorbent $\text{Fe}_3\text{O}_4@\text{SiO}_2/\text{PEI}$. The effect of contact time, solution pH, and temperature on the adsorption of MO and CR by $\text{Fe}_3\text{O}_4@\text{SiO}_2/\text{PEI}$ were studied. The results showed that the adsorption rate of anionic dyes MO and CR increased rapidly then decreased gradually as the pH increased. The adsorption capacity of $\text{Fe}_3\text{O}_4@\text{SiO}_2/\text{PEI}$ for MO was better than that for CR, and the maximum adsorption capacity for MO and CR was 231.0 mg/g at pH 4 and 134.6 mg/g at pH 6, respectively. The equilibrium adsorption capacities for MO and CR increased rapidly in the initial 40 min, and reached equilibrium in approximately 180 min. Both of the adsorption processes followed the pseudo-second-order kinetics model and better fitted with Freundlich isotherm model and the higher correlation coefficients were observed for the Freundlich isotherm model than that of the Langmuir isotherm model, indicating that both of the uptake of MO and CR on the sorbent are preferably followed the multilayer adsorption process. The removal mechanism of adsorption was mainly related to electrostatic attraction and the number of active sites occupied by anionic dyes. While for regeneration study, the results showed that the regenerated $\text{Fe}_3\text{O}_4@\text{SiO}_2/\text{PEI}$

exhibited an excellent regeneration for the adsorption of MO and CR, and the removal efficiency of $\text{Fe}_3\text{O}_4@\text{SiO}_2/\text{PEI}$ adsorbent decreased to approximately 75.4% and 74.5% even after the fourth reusability cycle, indicating that the $\text{Fe}_3\text{O}_4@\text{SiO}_2/\text{PEI}$ could be a potential and efficient adsorbent for the MO and CR removal due to the excellent multiple reusability performance.

Zhang *et al.*, (2022) studied the performance of a novel ultralight and porous cellulose nanofibers/polyethyleneimine (CNF/PEI) composite on anionic MO dye adsorption, with epichlorohydrin (ECH) serving as a crosslinker. Various characterization methods were studied such as FTIR, SEM, MTS, EA, and BET analysis. The effect of contact time, pH and adsorbent dosage were investigated on the performance of CNF/PEI composite for anionic dye removal. CNF/PEI composite with a weight ratio of 1: 0.5, 1:1, and 1:2 of CNF to PEI were investigated and the sample notation was defined as CPE-0.5, CPE-1, CPE-2, according to the CNF: PEI weight ratio at 1: 0.5, 1:1, and 1:2, respectively. The resultant CNF/PEI samples was reported to exhibit excellent adsorption performance for the anionic dyes and the adsorption capacity of CPE-2 toward MO was 1226 mg/g at pH 6 and 1745 mg/g at pH 2, with adsorbent dose of 0.5 mg at 300 mg/L dye concentration. In addition, the adsorption column packed with CPE-2 showed excellent dye removal ability and could purify around 4 L of dye contaminated water (10 mg/L) at a removal efficiency above 90%. It was also observed that after 12 h of time-dependent adsorption process, the MO solution became nearly transparent, indicated that MO dye was successfully adsorbed by the CNF/PEI adsorbent. The results showed that the adsorption performance fitted well with the pseudo-second-order kinetics and monolayer Langmuir adsorption process. The CPE-2 exhibited excellent recyclability (over 84% after 10 cycles). However, the study showed that CNF/PEI adsorbent was selective adsorptive towards cationic and anionic mixtures. The authors confirmed that

this paper presents a new strategy to prepare low-cost and highly efficient adsorbents to remove organic dyes from wastewater for potential practical applications.

In another study, Chen *et al.*, (2019) reported polyethyleneimine modified magnetic MWCNTs composite (denoted as MWCNTs@Fe₃O₄/PEI) was applied as an adsorbent for removing MO and Cr(VI) from aqueous solution. The physicochemical properties of the as-designed adsorbent were investigated using various analytical techniques, such as XRD, FTIR, SEM, TEM, VSM, and zeta potential. The adsorption kinetics, thermodynamics, isotherms, and effect of pH varying from 2 to 11, on the adsorption of each pollutant by the as-prepared adsorbent were also investigated in a batch experiment. All the characterization results confirming the successful adsorption of MO and Cr(VI) by MWCNTs@Fe₃O₄/PEI composite. It was found that the surface charge properties of the MWCNTs as well as its dispersion in aqueous solution were greatly changed after the introduction of PEI molecules. The removal of MO and Cr(VI) by the adsorbents was highly dependent on the solution pH values. At a pH below 6, the adsorption capacity of the MWCNTs@Fe₃O₄/PEI for MO declined sharply with the raising of pH values. Over a pH range of 6–9, the adsorption process was almost not affected by the solution pH. At pH above 9, the removal of MO on the MWCNTs@Fe₃O₄/PEI was significantly depressed. A relatively satisfactory removal efficiency of 96.1% for MO and 49.0% for Cr(VI) for a model textile effluent with 200 mg/L of MO or 50 mg/L of Cr(VI) (compared with a removal rate of 99.2% for MO and 62.9% for Cr(VI) in deionized water system) by MWCNTs@Fe₃O₄/PEI were achieved. The adsorption process followed a pseudo-second-order model and best fitted to Langmuir isotherms model with q_e values of 1727.6 mg/g for MO and 98.8 mg for Cr(VI) at room temperature. The thermodynamic process of MO and Cr(VI) adsorption is spontaneous and endothermic in nature. MO and Cr(VI) can be easily desorbed from the target adsorbent by using 0.5 M NaOH and no obvious drop in the removal efficiency was observed even after three consecutive adsorption–

desorption cycles, confirming the excellent stability of the as prepared adsorbent for MO removal and implying its great potential in practical applications. The authors recommended MWCNTs@Fe₃O₄/PEI as a promising adsorbent for the simultaneous capture of MO and Cr(VI) from complex wastewater via multiple uptake mechanisms (e.g. electrostatic attraction, $\pi - \pi$ stacking and hydrogen bonding).

The adsorption performance of spent tea leaves (STL) modified with polyethyleneimine on two anionic dyes, namely Reactive Black 5 (RB5) and MO, from simulated wastewater was investigated by Wong *et al.*, (2018). The adsorption study was conducted to analyse the effects of contact time (5-200 min), temperature (25-60 °C), adsorbent dosage (0.01-0.15 g), pH (7-11), and initial dyeconcentration (50-100 mg/L) on the removal of RB5 and MO dyes by PEI-STL. From the results, the adsorption capacities of 71.9 mg/g (RB5) and 62.11 mg/g (MO) on PEI-STL were recorded. The percentage MO removal was increased with time, and the maximum percentage removal (84.1%) was achieved at ~120 min with adsorption capacity of 21.0 mg/g. High adsorptive removals of RB5 and MO onto PEI-STL were observed in acidic medium, and the highest removal was recorded to be at pH 3 for both dyes (100 % removal with adsorption capacity of 25.0 mg/g for RB5, and 91.1% removal with adsorption capacity of 22.78 mg/g for MO). The optimum adsorbent dosage was 0.1 g and no significant improvement was observed beyond the optimum dosage. It was observed that higher temperature promoted the adsorption performance of RB5 dyes, but reduced the adsorption performance of MO where the percentage removal for MO decreased from 88.1% to 61% at elevated temperatures, while the adsorption capacity decreased from 22.1 mg/g to 15.3 mg/g, signifying the exothermic nature of the process. The percentage removal of RB5 (from 98.7% to 43.5%) and MO (from 88.7% to 32.7%) decreased with initial dye concentration. This was accompanied by the decrease of adsorption capacities of STL-AC towards RB5 (24.8 mg/g to 6.7 mg/g) and MO (22.2 mg/g to 1.6 mg/g). Based

on the comparison on the R^2 values, the Temkin model and pseudo-second-order model appears to be the most suitable models in describing adsorption of RB5 and MO onto PEI-STL. From the thermodynamic study, it was reported that RB5 adsorption is endothermic, while MO adsorption is exothermic process. It was proposed that the dyes adsorption proceeds via electrostatic attraction and hydrogen bonding between dyes molecules and adsorbent, while the role of pore filling is minimal.

2.6 Regeneration and reusability of spent-adsorbent

As the regeneration and reusability of the adsorbent is of crucial importance in the economic development, efficient protocols for adsorbate recovery and adsorbent regeneration have to be established; however, common adsorbents vary greatly in their stability and applicability to be regenerated (Alghamdi *et al.*, 2021). Adsorption is very promising method for removal of various pollutants from wastewater. Low cost of adsorbents, simplicity and high removal efficiency are few advantages of the method. In order to make this method more environment friendly and economical, regeneration of adsorbent is very important aspect. Many times, it is also desirable to recover the solute from adsorbent. Thus, the recovery of adsorbate and subsequent regeneration and reuse of adsorbent are important attributes of this process from economy and environmental point of view (Kulkarni *et al.*, 2014).

There are various regeneration techniques like thermal, electrochemical, ultrasonic, chemical methods are reported for regeneration. The need of recovery and regeneration depends on cost of solute and adsorbent and cost of recovery and also on the effect of the solute on the environment and whether it is to be disposal off in water reservoir or atmosphere (Kulkarni *et al.*, 2014).

Nowadays, many studies have been reported on the regeneration of the adsorbents in dyes removal from wastewater or aqueous environment as this technique is highly demanded for choosing the right adsorbent of dyes removal. Generally, if an adsorbent cannot be generated and reused, such materials are not considered as feasible and cost effective from the economic point of view for all industries. This is to ensure the whole cost of adsorption process is reasonably low for all industries.

2.7 Adsorption isotherms

Data analysis of isotherms is one of the most important factors to develop equation which accurately demonstrated the results of the column and that could be applied for column design. In addition, adsorption isotherm can be used to describe how solute interacts with adsorbent; furthermore, it is critical in optimizing the usage of adsorbent. The equilibrium adsorption isotherm is essential in describing the interaction behavior between adsorbate and adsorbent (Agarwal *et al.*, 2016). Once the adsorbate and adsorbent are in contact, adsorption process begins until the equilibrium is reached between the adsorbate on the adsorbent surface and the adsorbate remaining in the aqueous solution. At this stage, the amount of the adsorbate leaving the adsorbent surface will be equal to the amount being adsorbed to the adsorbent surface. The phenomenon that describes the adsorption mechanisms between the adsorbate on the adsorbent surface (that is adsorption amount, Q_e) and the adsorbate in aqueous phase (equilibrium concentration, C_e) is referred to as “adsorption isotherm”. The amount of adsorbate ions per unit mass of the adsorbent (Q_e) and the equilibrium concentration of the adsorbate remaining in the aqueous phase (C_e) can be obtained over a wide range by changing the amount of adsorbent, the initial concentration of solute and the volume of liquid. The equilibrium dye uptake Q_e is calculated by the following equation:

$$Q_e = \frac{(C_i - C_e)V}{m} \quad 2.1$$

where, V is the volume of the solution, C_i and C_e are initial and equilibrium concentrations and m is the dry mass of adsorbent.

There are many adsorptions isotherm models (Langmuir, Freundlich, Brunauer-Emmett-Teller, Redlich-Peterson, Dubinin-Radushkevich, Temkin, Toth, Koble-Corrigan, Sips, Khan, Hill, Flory-Huggins and Radke-Prausnitz isotherm) that have been proposed and investigated in adsorption process. Herein, two important isotherms, i.e., Langmuir isotherm and Freundlich isotherm was selected in this study. These models are briefly reviewed in the following sections.

2.7.1 Langmuir isotherm model

The Langmuir isotherm model is based on the assumption of a monolayer adsorption, where all the sorption sites are identical and energetically equivalent. It assumes that every adsorption site is equivalent and independent of whether or not adjacent sites are occupied. The model is presented by the following equation:

$$\frac{C_e}{Q_e} = \frac{C_e}{Q_{max}} + \frac{1}{Q_{max} b} \quad 2.2$$

where, Q_{max} (mg/g) is the maximum adsorption capacity corresponding to the complete monolayer coverage, C_e (mg/L) is equilibrium concentration of dye, Q_e (mg/g) is equilibrium adsorption capacity, and b (L/mg) is Langmuir constant related to the affinity of adsorbent towards adsorbate. A straight line is obtained when C_e/Q_e is plotted against C_e .

The favourability of an adsorption process can be represented in terms of the dimensionless separation factor, R_L , which is derived as follows:

$$R_L = \frac{1}{1 + bC_0} \quad 2.3$$

where C_0 is the initial concentration of the dye. The separation factor, R_L value is indicative of adsorption favorability. If this value is less than 1, it is favorable ($0 < R_L < 1$) and if the value is more than 1, it is unfavorable ($R_L > 1$) for adsorption (Xin *et al.*, 2015).

2.7.2 Freundlich isotherm model

The Freundlich isotherm is based on multilayer adsorption on heterogeneous surface and there are interactions between the adsorbed molecules. The model also considers mono molecular layer coverage of solute by the adsorbent. However, it assumes the adsorbent has a heterogeneous surface so that binding sites are not identical. The Freundlich equation is expressed as given below:

$$\ln Q_e = \ln K_F + \frac{1}{n} \ln C_e \quad 2.4$$

Where K_F and n are known as Freundlich coefficients which indicate the sorption capacity and favorability of adsorption process, respectively. The Freundlich constants are evaluated from the intercept and the slope, respectively, of the linear plot of $\ln Q_e$ versus $\ln C_e$ based on experimental data (Xin *et al.*, 2015).

2.8 Adsorption kinetic models

Adsorption kinetics models are greatly applied to explain the adsorption process and adsorption mechanism. The study of adsorption kinetics describes the solute uptake rate and evidently this rate controls the residence time of adsorbate uptake at the liquid-solid interface including the diffusion process. In order to understand the adsorption mechanism during the adsorption process, the fitting of the experimental kinetic data by the kinetic models is very important. The commonly used adsorption kinetic models are first-order kinetic model and second-order kinetic equations. The first-order kinetic model suggests that the adsorption is controlled by interface mass transfer, while the

second-order kinetic model indicates the adsorption process is dominated by an interface chemical interaction (Quan *et al.*, 2018).

2.8.1 Pseudo-first-order kinetic model

Lagergren (1898) suggested a pseudo-first-order equation for the sorption of liquid/solid system based on solid capacity. It assumes that the rate of change of sorbate uptake with time is directly proportional to the difference in the saturation concentration and the amount of solid uptake with time. The pseudo-first order rate model is as follows:

$$\ln(Q_e - Q_t) = \ln Q_e - K_1 t \quad 2.5$$

where, K_1 (min^{-1}) is the Lagergren rate constant of adsorption, Q_e (mg/g) is the maximum adsorption capacity, and Q_t (mg/g) is the amount of adsorption at time t (min). The values of K_1 and Q_e are determined from their intercepts and the slopes (Quan *et al.*, 2018).

2.8.2 Pseudo-second-order kinetic model

The pseudo-second-order kinetic model was developed consequent to the pseudo-first-order and it is based on the assumption that the rate-limiting step maybe chemical sorption or chemisorption, involving valence forces through sharing or exchange of electrons between the adsorbate and the adsorbent. The sorption data is also studied by pseudo-second order kinetic which is expressed as follows:

$$\frac{t}{Q_t} = \frac{1}{K_2 Q_e^2} + \frac{t}{Q_e} \quad 2.6$$

where, K_2 is the pseudo-second order rate constant of adsorption (g/mg min), K_2 and Q_e are determined from the intercepts and the slope of the plot of t/Q_t versus t (Quan *et al.*, 2018).

2.9 Adsorbent characterization methods

Several methods such as FTIR, FESEM, XRD and BET techniques are utilized in adsorption studies to study in the depth of molecular composition, thermal stability, functional groups, crystalline material, surface area of the adsorbent materials and etc. In addition, this equipment can project some ideal variables or parameters that are to be used for a good efficiency rate of dye removal. The results that can be obtained from these devices are in the form of either graphs or high-resolution pictures. With that, there can some observations made about the patterns from the diagrams of how the impact of adsorbents from the beginning and its subsequent results. Each pattern will define something and ought to be investigated intently for examination and a few discussions are ought to be made. A few of these characterization methods are briefly in the following sections.

2.9.1 Fourier Transform Infra-Red Spectrometer (FTIR)

Infrared spectroscopy is an essential and crucial characterization technique to elucidate the structure of matter at the molecular scale. The chemical composition and the bonding arrangement of constituents in a homopolymer, copolymer, polymer composite and polymeric materials in general can be obtained using Infrared (IR) spectroscopy. The FTIR spectrometers obtain the IR spectrum by Fourier transformation of the signal from an interferometer with a moving mirror to produce an optical transform of the infrared signal. Numerical Fourier analysis gives the relation of intensity and frequency, that is the IR spectrum. The FTIR technique can be used to analyze gases, liquids, and solids

with minimal preparation. The spectrometer may operate in transmission or reflection, but also in attenuated total reflection (ATR) mode, which have been widely used during the last two decades. An infrared beam is directed onto an optically dense crystal (called a diamond) which has a high refractive index at a specific angle. This internal reflectance will then generate an evanescent wave which acts as a medium to allow extension beyond surface of the crystal into the sample. The result is then sent to a computer which can be programmed to generate a spectrum. Therefore, IR spectrometers have been used to analyze solids, liquids as well as gases by means of transmitting infrared radiation directly towards the sample. ATR technique has revolutionized in the recent years where it is able to be tested onto various solid and liquid samples (Wong *et. al.*, 2018).

2.9.2 Field Emission Scanning Electron Microscopy (FESEM)

FESEM is used to provide the surface topography, composition and other properties of the sample such as electrical conductivity at wider range of magnifications. FESEM is said to be a better version of SEM because of its wider range of magnifications. However, they provide the same functions as in detecting surface topography, composition and morphology of a sample. FESEM provides a clearer and non-distorted image when it is zoomed down to even a resolution of $\frac{1}{2}$ nanometers. This is because FESEM has intensive and high-ended monochromatic electron beam that penetrates the sample giving high resolution of images compared to SEM.

Electrons are sourced and emitted from field emission which are accelerated at a very high speed with high voltage from 0.5 to 30 kV. To observe material under FESEM techniques, the object must first be made suitable to high vacuum and should not alter the vacuum. However, it depends on the material to be scanned, some materials may need to be coated with gold, titanium or palladium while adsorbent materials like polymer and its

composites can be scanned directly if they are in dried and fine powdered form (Boukoussa *et. al.*, 2018).

2.9.3 X-ray Diffraction (XRD)

XRD or X-ray diffraction is an equipment whereby it is high-ended, rapid and non-destructive used for phase recognition of crystalline materials. The main parts of an XRD are X-ray source, sample holder and X-ray detector.

Constructive interferences are produced due to strong interaction of incident rays with crystal material. Bragg's law equation is stated as $n = 2d \sin$. Diffracted radiations possess various patterns which are then detected, processed and transfigure to count rate. The multiple count rates are detected by a detector. Conversion of diffraction peaks to d -spacing could enable the identification of organic matters since organic matters have its own eccentric d -spacing. The width of the peaks is inversely proportional to the crystal size. A thinner peak corresponds to a bigger crystal. A broader peak means that there may be a smaller crystal, defect in the crystalline structure, or that the sample might be amorphous in nature, a solid lacking perfect crystallinity. For smaller samples, the patterns determined using XRD analysis can be used to determine a sample's composition (Alsaiani *et. al.*, 2021).

2.9.4 Brunner-emmett-teller (BET)

The BET theory (abbreviated from Brunner-Emmett-Teller theory) is used to gauge the surface zone of strong or permeable materials. It gives significant data on their physical structure as the territory of a material's surface influences how that strong will communicate with its condition. The surface zone of a material can be changed during both combination and preparation. As a molecule is partitioned (processed) into littler particles, extra surfaces are made, in this way expanding its surface zone.

Correspondingly, when pores are made the molecules inside by disintegration, deterioration, or some their physical or concoction implies, the surface territory is additionally expanded. Materials with many thin pores, for example, initiated carbons, can have surface regions of in excess of 2,000 m² in a solitary gram (Mashkooor *et. al.*, 2020).

Universiti Malaya

CHAPTER 3: RESEARCH METHODOLOGY

3.1 Chemicals and materials

All of the synthetic materials used were of the analytic and reagents grade. Pyrrole (Py) was used as a monomer, obtained in the liquid phase, and purchased from Sigma-Aldrich. The three oxidants used were namely ammonium peroxodisulphate, APS ($(\text{NH}_4)_2\text{SO}_4$), ferric chloride anhydrous (FeCl_3), and ferric chloride hexahydrate ($\text{FeCl}_3 \cdot 6\text{H}_2\text{O}$), all purchased from Sigma-Aldrich while methyl orange (MO) and crystal violet dyes (CV) were purchased from R&M Chemicals. The stock solutions of 300 ppm of both dyes were prepared by dissolving them in deionized water. Polyethylenimine (PEI) (Sigma-Aldrich) with Py was used for the formation of polypyrrole-polyethyleneimine (PPy-PEI) composites. Py was stored in the refrigerator in the absence of light prior to use. HCl and NaOH (Merck) were used to control the pH of the working solution.

Table 3.1: The physical properties of the investigated dyes.

Name	Methyl orange (MO)	Crystal violet (CV)
Molecular formula	$\text{C}_{14}\text{H}_{14}\text{N}_3\text{SO}_3\text{Na}$	$\text{C}_{25}\text{H}_{30}\text{N}_3\text{Cl}$
Molar mass (g/mol)	327.33	407.98
λ_{max} (nm)	464	590

3.2 Methods

The research was carried out in three phases. In the first phase, the polypyrrole-based adsorbents were chemically synthesized at various mole ratios of monomer to oxidant. In the second phase, batch adsorption dyes were carried out at different operating conditions and from here the adsorption efficiency was calculated by measuring the concentration of dyes using an ultra-violet spectrophotometer (UV-1650 PC model). The adsorption experiments were performed under various parameters such as solution pH, initial dye

concentration, contact time, and adsorbent dosage. In the third phase, the prepared adsorbents before and after adsorption were characterized using analytical techniques such as FTIR, FESEM, BET, and XRD. Langmuir and Freundlich's adsorption isotherm models were studied. The kinetic and regeneration studies were also carried out.

3.3 Synthesis of polypyrrole-based adsorbents

3.3.1 Synthesis of polypyrrole

The polypyrrole adsorbents were prepared by chemical oxidative polymerization of pyrrole monomer using $\text{FeCl}_3 \cdot 6\text{H}_2\text{O}$ as an oxidant. Polypyrrole was first prepared with different ratios of pyrrole monomer to oxidant, accordingly (1:0.5, 1:1, 1:2 and 1:3). Briefly, 1.342 g of pyrrole monomer was dissolved in 20 mL deionized water and 5.406 g of oxidant $\text{FeCl}_3 \cdot 6\text{H}_2\text{O}$ (for 1:1 mole ratio of pyrrole monomer to oxidant) was dissolved in another 80 mL deionized water. Then, $\text{FeCl}_3 \cdot 6\text{H}_2\text{O}$ oxidant solution was added to the pyrrole solution and both solutions were simultaneously mixed and allowed to shake at a shaking speed of 150 rpm and 3 h at ambient temperature for complete polymerization. The change of the initial light green color to black indicated the formation of polypyrrole. In order to remove the excess reactants from the polypyrrole solution, it was filtered and washed several times with deionized water, until the filtrate became colorless. The collected polymer product was later dried at 65 °C for 24 h for the following characterization and adsorption experiments. The steps mentioned above were repeated for another two oxidants (anhydrous FeCl_3 and APS) with the different mole ratio of pyrrole monomer to oxidant (1:0.5, 1:1, 1:2 and 1:3) by varying the amount of oxidant accordingly.

Figure 3.1 shows the chemical synthesis of PPy where the propagation step is controlled by a large excess of radical cation formed through oxidation. Due to this, the

hydrogen atom is gradually lost and the polymer chain will multiply until it terminates naturally. The mole ratio of monomer to oxidant affected the quality of the resulting polymer (Brezoi *et al.*, 2010).

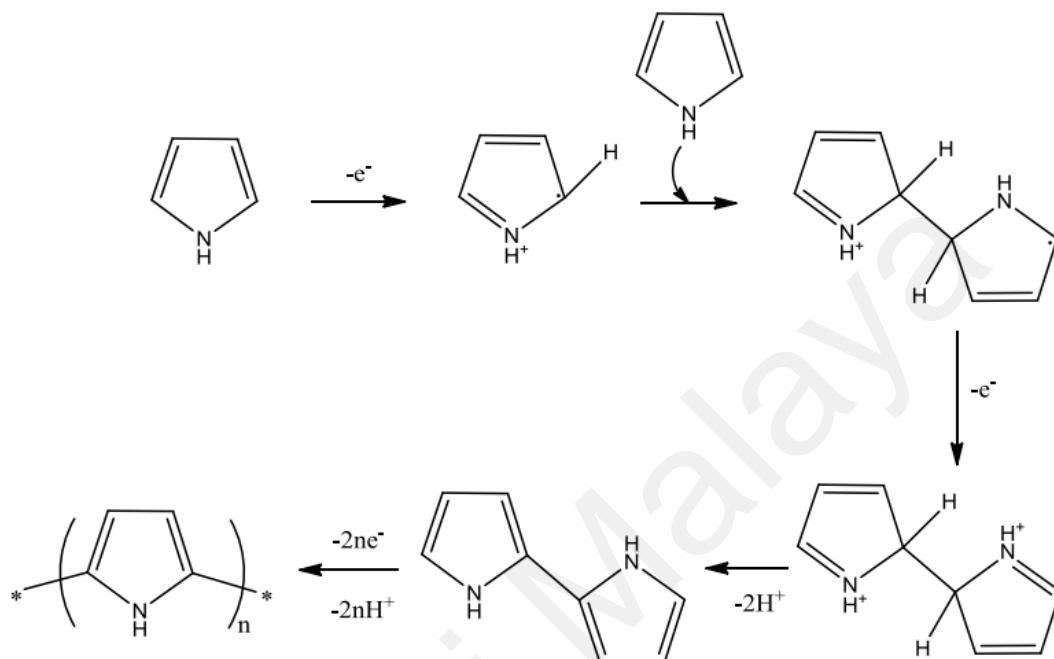


Figure 3.1: Chemical polymerization of pyrrole monomer to form polypyrrole.

3.3.2 Synthesis of PPy-PEI composite adsorbents

For the preparation of the PPy-PEI composite, as shown in Figure 3.2, the pyrrole monomer of 1.342 g, was first dissolved in 20 mL of deionized water. 5.406 g of oxidant $\text{FeCl}_3 \cdot 6\text{H}_2\text{O}$ solution was dissolved with deionized water in another beaker, followed by the addition of 1.0 g polyethyleneimine. Then the mixture was added to the pyrrole solution in order to initiate the polymerization of pyrrole and make up the mixture to 100 mL with deionized water. Then the mixture was allowed to shake at a shaking speed of 150 rpm and 3 h at ambient temperature for complete polymerization and composite preparation. At the end of the polymerization reaction, a black product was obtained confirming the formation of PPy-PEI composite. The reaction mixture was filtered,

washed several times with deionized water and dried at 65 °C for 24 h for the following characterization and adsorption experiments. Again, the steps mentioned above were repeated for another two oxidants (FeCl_3 and APS) with the different mole ratios of pyrrole monomer to oxidant (1:0.5, 1:1, 1:2 and 1:3) by varying the amount of oxidant accordingly.

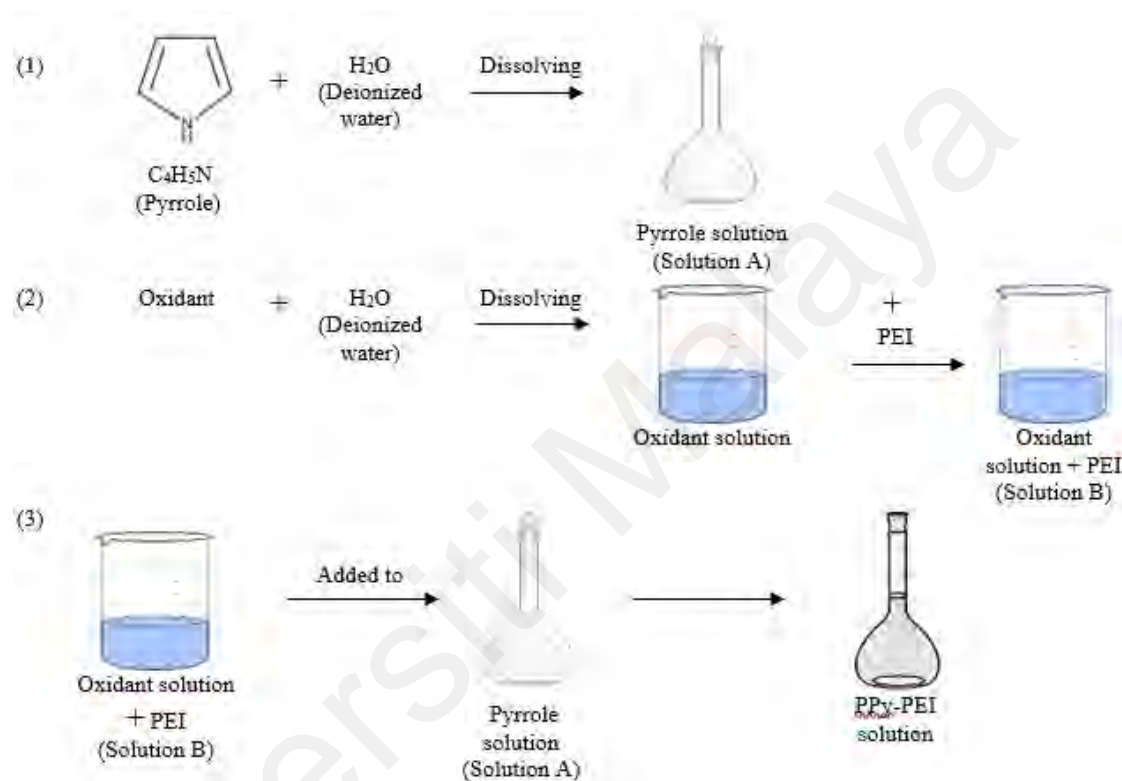


Figure 3.2: Synthesis design of PPy-PEI composite.

3.4 Batch adsorption experiments

The batch experiments were performed to study the adsorption properties of the PPy-based adsorbents for dyes at room temperature. A stock solution of 300 ppm dye was prepared by dissolving appropriate amount of dye in deionized water. All required concentrations of MO and CV dyes for experiments were obtained by successive dilution of the stock solution. Briefly, the highest adsorption efficiency obtained among different

ratios of pyrrole to oxidant (1:0.5, 1:1, 1:2, and 1:3) was subsequently used for the adsorption performance.

For the batch adsorption studies of MO and CV dyes, adsorption was conducted with the prepared adsorbents. Typically, a 50 mL solution of known dye concentration were mixed with composite adsorbent in respective beakers, accordingly. Firstly, the effect of solution pH was varied between 1 to 13. The solution pH was adjusted as necessary by adding 0.1 M solutions of HCl or NaOH. The effect of adsorbent dosage was studied by varying the desired dose of adsorbent between 0.05 to 0.4 g (0.05 g, 0.1 g, 0.15 g, 0.2 g, 0.25 g, 0.3 g, 0.35 g, and 0.4 g). The effect of initial dye concentration was investigated by varying the concentration from 25 to 300 ppm (25 ppm, 50 ppm, 100 ppm, 200 ppm, and 300 ppm). The effect of contact time also was conducted between 30 to 300 min (30 min, 60 min, 120 min, 180 min, 240 min, and 300 min). The isotherm and kinetics parameters were investigated from the obtained experimental data to understand the nature of the adsorption process.

3.5 Ultra-violet spectrophotometer

After the batch adsorption treatments, the solution was filtered to separate the adsorbent from the treated solution. The filtrate of the solution was brought for UV-Vis analysis to measure the UV absorbance of the unknown solution with the wavelengths of 464 nm for MO dye and 590 nm for CV dye, as seen in Table 3.1. All the experiments were replicated and the mean values were calculated. The values of initial and final concentrations of MO and CV dyes before and after adsorption were determined using standard calibration curves of the respective solutions. The determined values were used to calculate the percentage removal of MO and CV dyes according to the following equation:

$$\% \text{ Efficiency} = \left\{ \frac{C_i - C_f}{C_i} \right\} \times 100\%$$

Where, C_i (mg/L) and C_f (mg/L) are the initial and final concentrations of dyes, respectively.

3.6 Regeneration experiments

In order to test the regeneration ability, acidic and alkaline solutions were used to desorb MO and CV dyes on the surface of PPy-based adsorbents. Typically, the spent PPy-based adsorbents powders were put into the flasks. Then, 50 mL of deionized water, 50 mL of 0.1 M HCl, or 50 mL of 0.1 M NaOH solution were applied separately for the regeneration process. Finally, the regenerated adsorbent was reused for further adsorption experiments. The adsorption and desorption were then quantified with a UV-Vis spectrophotometer.

3.7 Characterization

The as-synthesized polypyrrole-based adsorbents have been analysed by different techniques to understand the physicochemical properties, surface morphologies, surface functional groups, and other adsorptive properties. In this study, analytical techniques such as FTIR, XRD, BET, and FESEM were used to further study the dried specimen (yield) by the physical or chemical composition that it contained.

3.7.1 Fourier Transform Infra-Red Spectrometer (FTIR)

This method was done to identify the functional groups present in the conducting polymer before and after the adsorption of dyes. The model of Spectrum 100 FTIR apparatus was used together with a single bounce diamond crystal with a set of range between 4000 cm^{-1} to 525 cm^{-1} , at room temperature.

3.7.2 Field Emission Scanning Electron Microscopy (FESEM)

The surface morphology of the PPy-PEI copolymer-based adsorbents before and after the adsorption of dyes was observed *via* field emission scanning electron microscopy (Hitachi Brand, Model SU 8220), with different magnifications and kV. The finely grounded powder sample was placed evenly on the carbon film and placed on the holder before it is put in the instrument for measurement.

3.7.3 X-ray Diffraction (XRD)

XRD or X-ray diffraction was collected using PANalytical, model Empyrean diffractometer system. The XRD patterns were recorded in the 2θ range of $5-90^\circ$ with a step time of 1.25 sec using Cu K α radiation ($\lambda = 1.5406$).

3.7.4 Brunner-emmett-teller (BET)

The Brunner-Emmett-Teller (BET) was analyzed to study the surface area by using the surface analyzer *via* N₂ adsorption at 77.4 K. The pore structure of this adsorbent was determined by using the t-method.

CHAPTER 4: RESULTS AND DISCUSSION

4.1 Characterization of adsorbents

In this study, the characteristics of the as-synthesized polypyrrole-based adsorbents were studied by FTIR, XRD, BET, and FESEM analyses. Based on the results of the adsorption performance (see detail in section 4.2 adsorption studies), among the different ratios of monomer to oxidant for the preparation of polypyrrole-based adsorbents, the ratio of 1:1 has been chosen for the rest of the experiments as this ratio showed the maximum adsorption of dyes under certain conditions.

4.1.1 BET surface area

Surface area, pore size, and volume distribution are one of the factors for evaluating the adsorption performance of the adsorbent. BET surface area, pore size, and pore volume were measured for PPy-based adsorbents by surface area analyzer (Micromeritics ASAP 2020) *via* N₂ adsorption at 77.4 K. Table 4.1 show the comparative features of BET surface area, pore volume and pore size of various prepared PPy-based adsorbents.

According to the obtained results, it was clearly observed that BET surface area and pore volume of PPy decreased upon increasing the molar concentration of the oxidant. Among the various mole ratio of pyrrole monomer to oxidant (1:0.5, 1:1, 1:2 and 1:3) used to prepare pristine PPy adsorbent, the mole ratio of 1:0.5 produced a higher result BET surface area. However, in comparison of the adsorption performance among the different mole ratios of oxidant, pristine PPy adsorbent of 1:1 mole ratio showed greater adsorption efficiency. Therefore, pyrrole to oxidant mole ratio of 1:1 was used for the batch adsorption experiments as the polymerization with a lower oxidant mole ratio of 1:0.5 produced a very thin and soft powder which appeared very difficult to handle and polymerization was also considered an incomplete process at 1:0.5 mole ratio even

though the BET surface appeared higher than PPy with 1:1 mole ratio. On the other hand, the results also showed the pore volume distribution and BET surface area of the PPy-PEI composite adsorbents with an increase in values compared to the pristine PPy adsorbents. The highest BET surface area of the PPy-PEI composite (1:1) was found to be about 11.85 m²/g, which is much greater than that of the pristine PPy (1:1) of 8.54 m²/g. Overall, the BET surface area of the PPy-PEI composite adsorbent using anhydrous FeCl₃ as the oxidizing agent was found much greater than others. Thus, introducing PEI to PPy greatly improves the surface characteristics of the adsorbent. The increase could be attributed to the successful adsorption of polypyrrole throughout the polyethyleneimine pore matrix and that the oxidant also polymerized pyrrole throughout this pore matrix. The differences in surface area measurements confirmed the successful polymerization of the PPy and PEI unit and also indicated that the anions of the oxidizing agents may have played a different role during polymerization providing a potential route to control the surface size of the resulting PPy-based adsorbent. The higher surface area of the PPy-PEI composite adsorbent provides more binding sites for the adsorption of adsorbate and thus leads to a greater adsorption potential in comparison with that of pristine PPy adsorbent. Similar results have been reported by Mashkoor *et al.*, 2020.

Table 4.1: Characteristics of polypyrrole and composite, surface area measurements and pore volume distribution.

Adsorbent	Ppyrole: oxidant	BET surface area (m ² /g)	Total pore volume (cm ³ /g)	Pore size (Å)
PPy	1:0.5	9.25	0.02603	82.26
PPy	1:1	8.54	0.02283	85.74
PPy	1:2	7.69	0.01257	87.47
PPy	1:3	6.70	0.01205	87.76
PPy-PEI (FeCl ₃)	1:1	11.85	0.02940	52.76
PPy-PEI (FeCl ₃ .6H ₂ O)	1:1	10.25	0.02856	65.37
PPy-PEI (APS)	1:1	9.61	0.02788	71.95

4.1.2 FESEM analysis

To establish the morphology of pristine PPy and PPy-PEI composite adsorbents before and after the adsorption of dye, field emission scanning electron microscope (Hitachi Brand, Model SU 8220) have been used and the micrographs have been investigated at different magnifications for better observation. The FESEM images for PPy-based adsorbents have been shown in the following sections.

4.1.2.1 Pristine PPy adsorbent

Figure 4.1 and Figure 4.2 represent FESEM images of the as-prepared PPy before the adsorption of dye. According to Figure 4.1 (a) and Figure 4.1 (b), the FESEM images of pristine PPy exhibited uniform spheres with an abundance of pores of smooth cloud structure and cauliflower-like compact surface, revealing the success of the synthesized polypyrrole. Figure 4.1 (c) shows higher magnification at x 70 k which clearly shows the microstructure of the prepared PPy fine powder, and the particles tend to form agglomerates because of their high surface area. The surfaces of the material showed the presence of several spherical particles of about internal diameter of 195-345 nm, with a higher magnification of x 130, 000 as shown in Figure 4.2. Several other studies also reported similar scanning images of the characteristics of PPy (Boukoussa *et al.*, 2018; Alghamdi *et al.*, 2019; Zhang *et al.*, 2019; Mashkooor *et al.*, 2020).

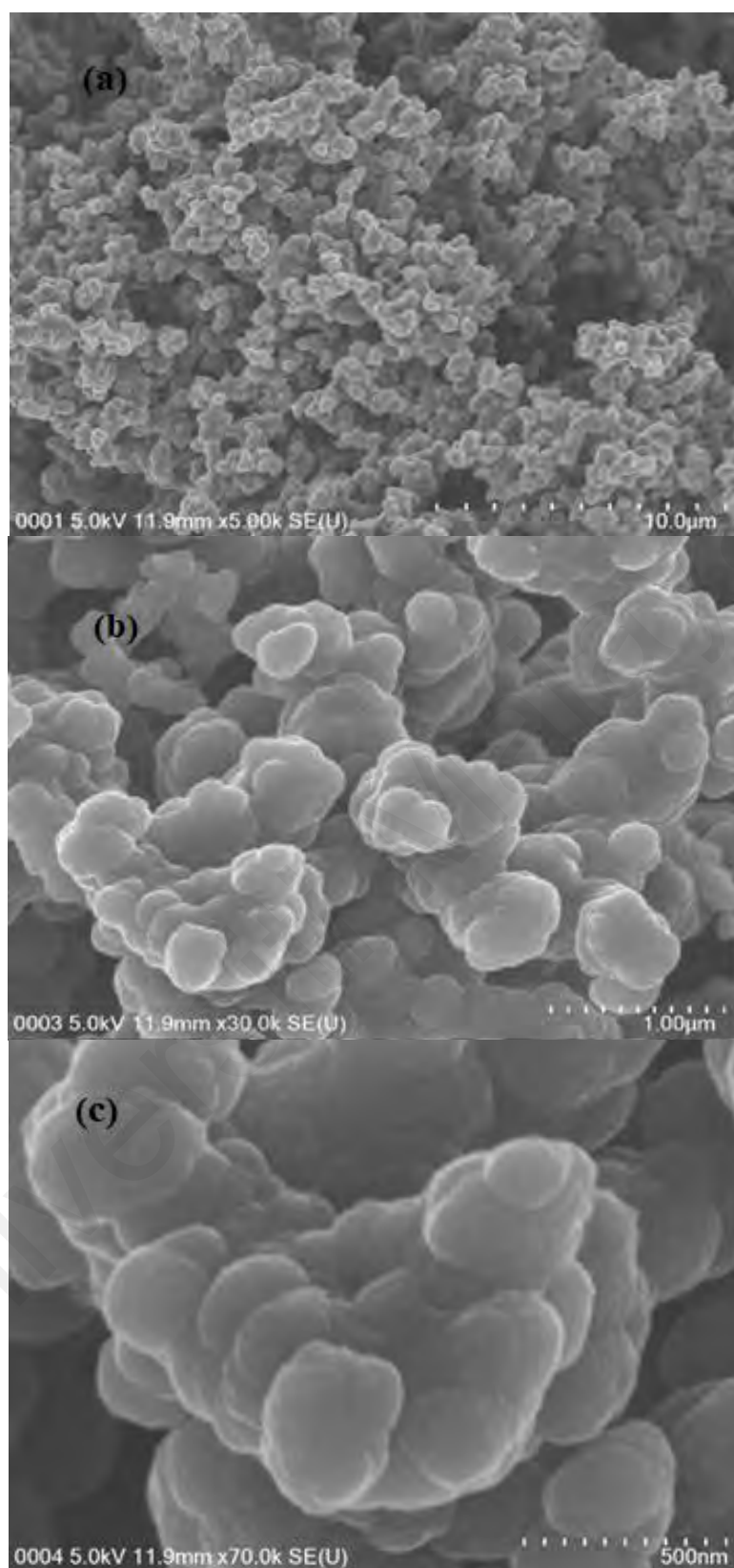


Figure 4.1: FESEM image of PPy before adsorption with different magnifications ((a) $\times 5.00$ k; (b) $\times 30.0$ k; (c) $\times 70.0$ k).

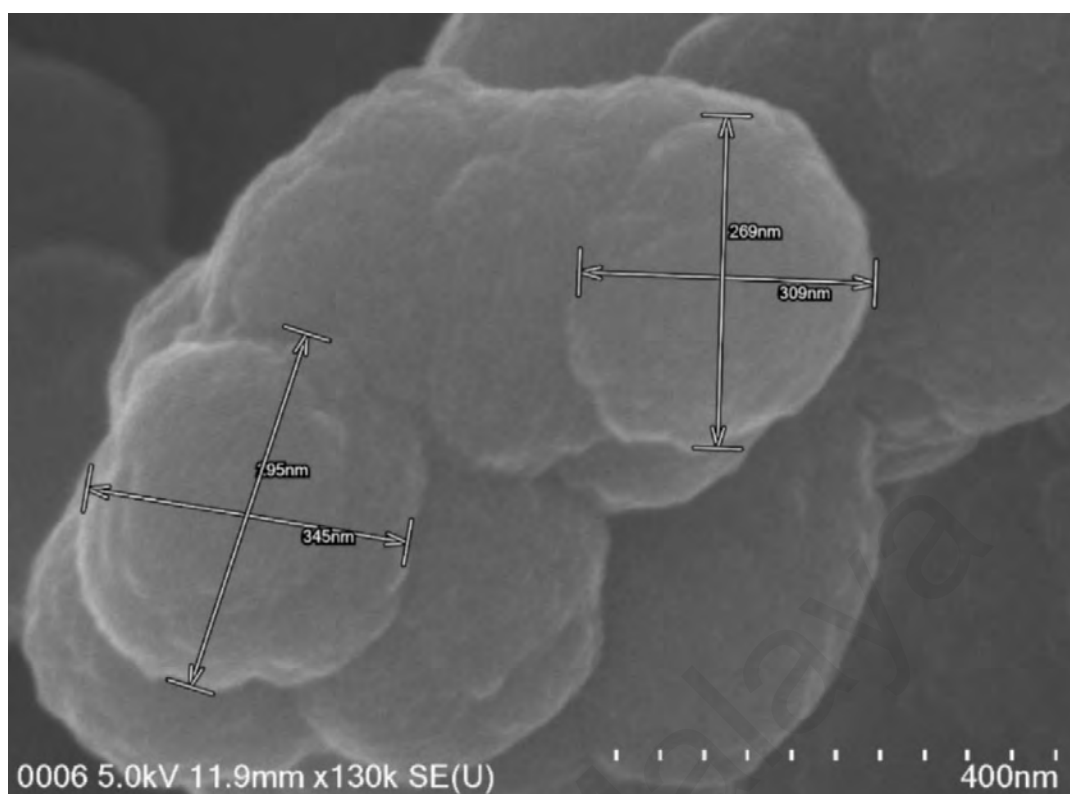


Figure 4.2: FESEM image of PPy before adsorption with internal particle diameter measurement; magnification $\times 130$ k).

Meanwhile, Figure 4.3 and Figure 4.4, represent FESEM images of pristine PPy after dye adsorption. There were few observable FESEM images after dye adsorption on pristine PPy. In Figure 4.3 (a) and Figure 4.3 (b), the FESEM images show roughly several irregularities of the polymer's morphology and thus. From Figure 4.3 (c), with a higher magnification at $\times 70$ k, it can be seen the dye particles as agglomerated on the conducting polymer which indicates the dye adsorbate has successfully been loaded over the surface pores of the adsorbent. Figure 4.4 clearly shows the surface of adsorbed sample becomes denser with an average internal diameter of 172-223 nm, which exhibits the possibility of dye adsorption on the substrate.

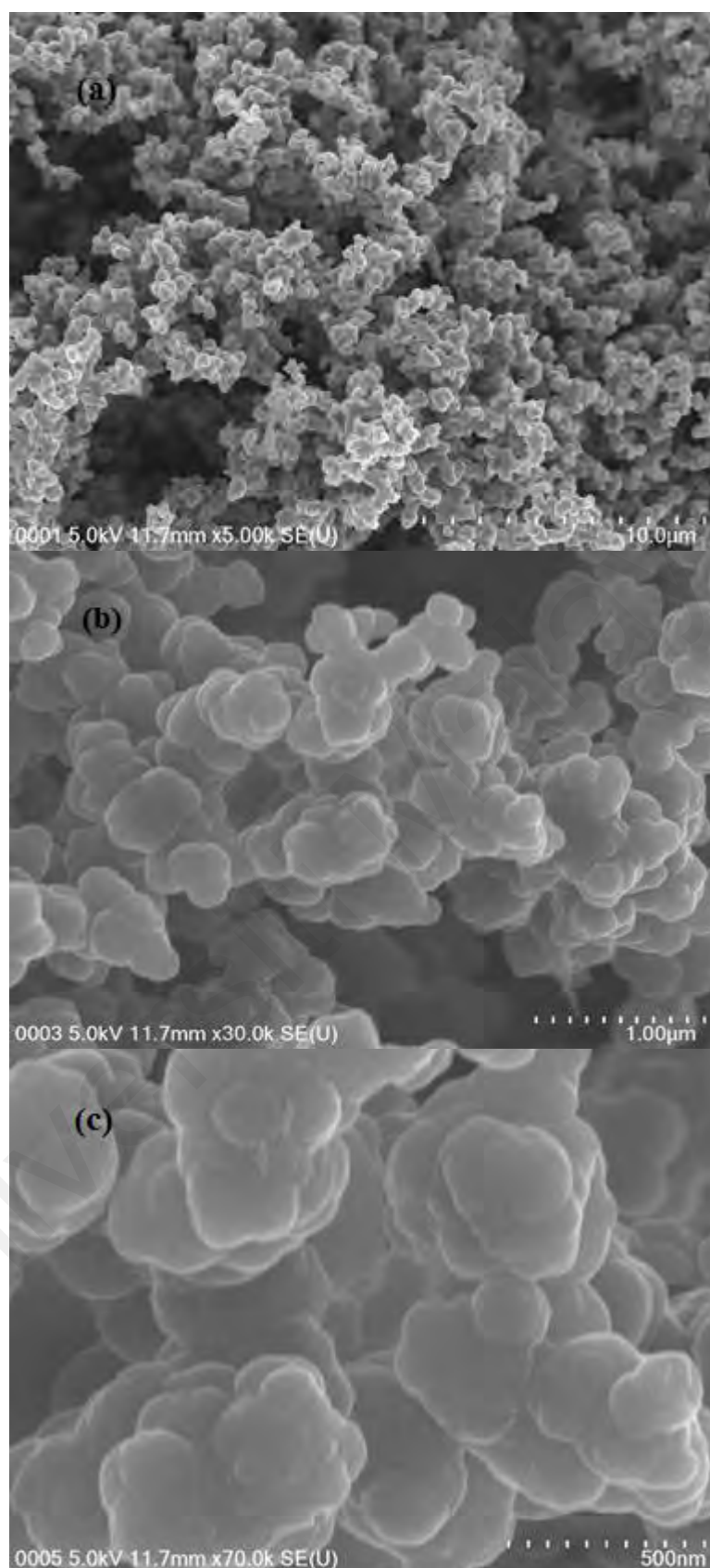


Figure 4.3: FESEM image of PPy after adsorption with different magnifications ((a) $\times 5.00\text{ k}$; (b) $\times 30.0\text{ k}$; (c) $\times 70.0\text{ k}$).

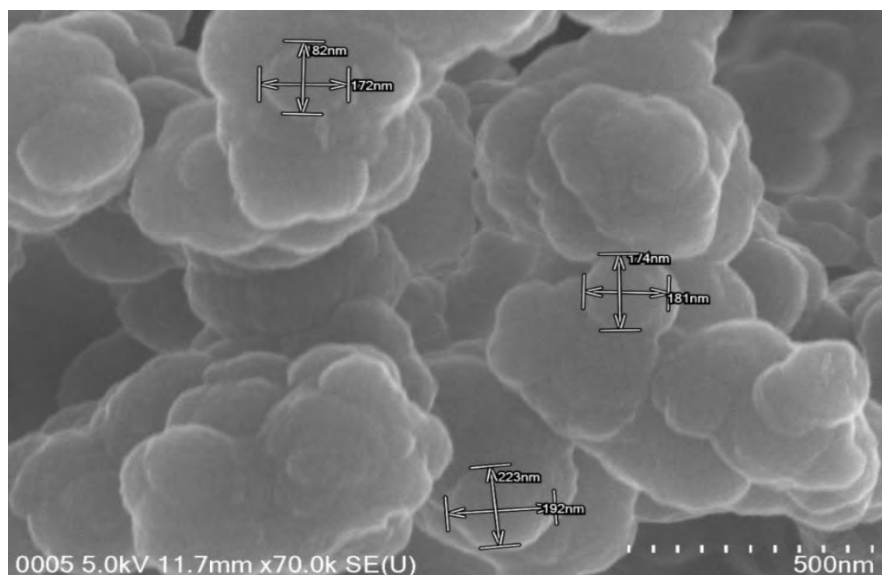


Figure 4.4: FESEM image of PPy after adsorption with internal particle diameter measurement; magnification $\times 70$ k).

4.1.2.2 PPy-PEI composite adsorbent

Figure 4.5 and Figure 4.6 represent FESEM images of the prepared PPy-PEI composite before adsorption of dye. FESEM images before the adsorption process revealed the success of the polymerization of pyrrole and the incorporation of PEI with the Py unit. As before adsorption, the sample only contains pure conducting polymer with PEI composite whereby it has a smooth cloud structure but is rougher than pristine PPy with a simple π - π bonding structure. As seen in Figure 4.5 (a) and Figure 4.5 (b), the particles show similar spherical morphology but are larger in size in comparison with pristine PPy. The images show the structure formed was like a cauli-like flower or the circular holes were evenly distributed on the surface. Figure 4.5 (c) shows higher magnification at $\times 70$ k which clearly shows the microstructure of the prepared composite powder. The image owned homogeneous morphology with an average internal diameter of 491-520 nm, with a higher magnification of $\times 130,000$ as shown in Figure 4.6, thus signifying the great effect of the PEI presence on the size and homogeneity of the particles.

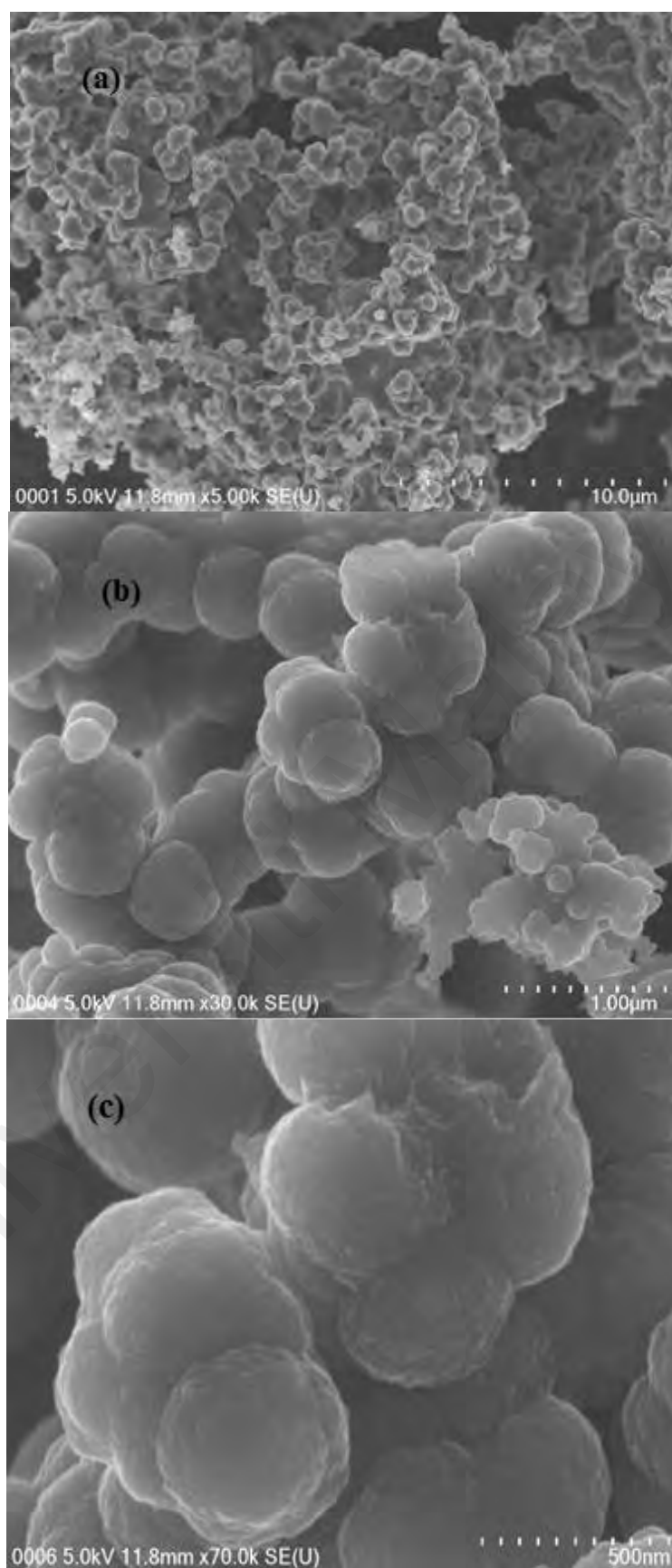


Figure 4.5: FESEM image of PPy-PEI before adsorption with different magnifications ((a) $\times 5.00$ k; (b) $\times 30.0$ k; (c) $\times 70.0$ k).

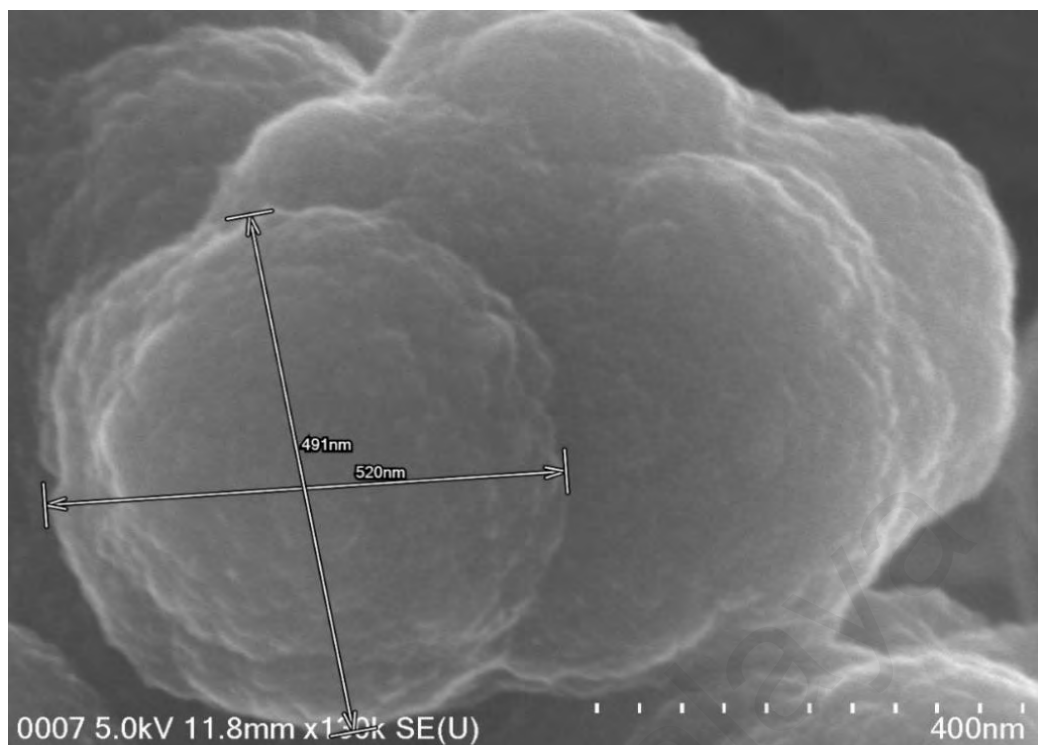


Figure 4.6: FESEM image of PPy-PEI before adsorption with internal particle diameter measurement; magnification $\times 130$ k).

Figure 4.7 and Figure 4.8 represent FESEM images of the PPy-PEI composite after dye adsorption. In Figure 4.7 (a) and Figure 4.7 (b), the FESEM images revealed that the solid PPy-PEI composite had a rough surface, which could increase their specific surface area and active adsorption sites. Thus, the rough surface was favorable for dye removal from an aqueous solution (Xin *et al.*, 2015) and thereby enhancing the adsorption capacity of the dye and reducing the adsorption equilibrium time (Li *et al.*, 2018). The FESEM images also show a unique structure with uniform-shaped pores and bubble-like globules of PPy-based adsorbent that have been formed. Also, it can be presumed that the dye adsorbate has successfully been adsorbed onto the surface pores of the adsorbent as shown in Figure 4.7 (c) with a higher magnification at $\times 70$ k. Figure 4.8 clearly shows the surface of adsorbed sample becomes denser with an average internal diameter of 160-190 nm, which could be referred to as the dye is adsorbed on the substrate. The presence of both adsorbent-adsorbate simply increases the density of surface topography and has a lesser

distance of particles. The adsorption terminology can be said to be the agglomeration of dye adsorbate to be surrounded by the conducting polymer. The presence of a higher amino group on the PEI polymer chain, which stabilizes the particles with severe steric hindrance and static repulsion, is responsible for the decrease in particle diameters. (Li *et al.*, 2013).

Similar micrographs have been observed for CV dye, even before and after the adsorption of the dye. Filled pores and change in the relative morphology of the PPy-PEI composite after the adsorption of MO and CV dyes demonstrate the successful adsorption of both the dye molecules onto the surface of the PPy-PEI composite.

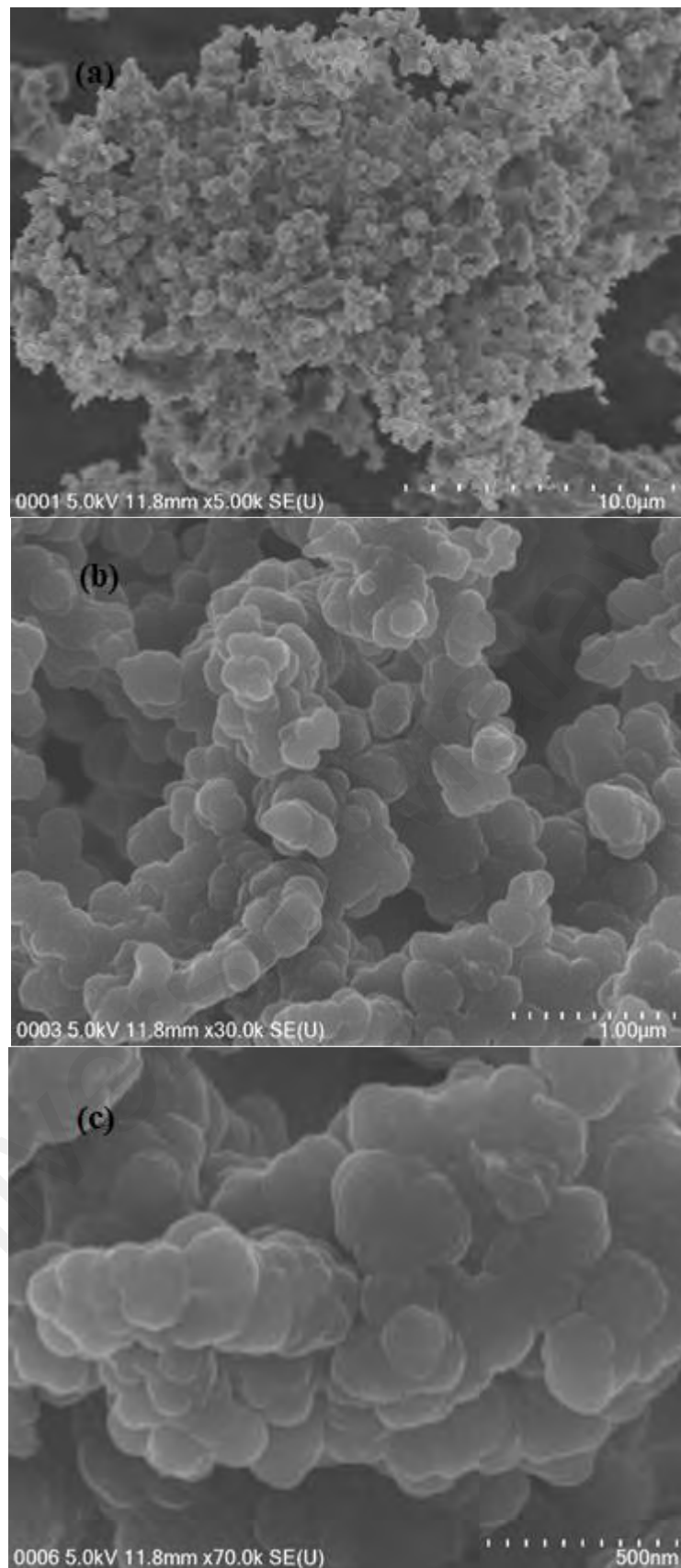


Figure 4.7: FESEM image of PPy-PEI after adsorption with different magnifications ((a) $\times 5.00$ k; (b) $\times 30.0$ k; (c) $\times 70.0$ k).

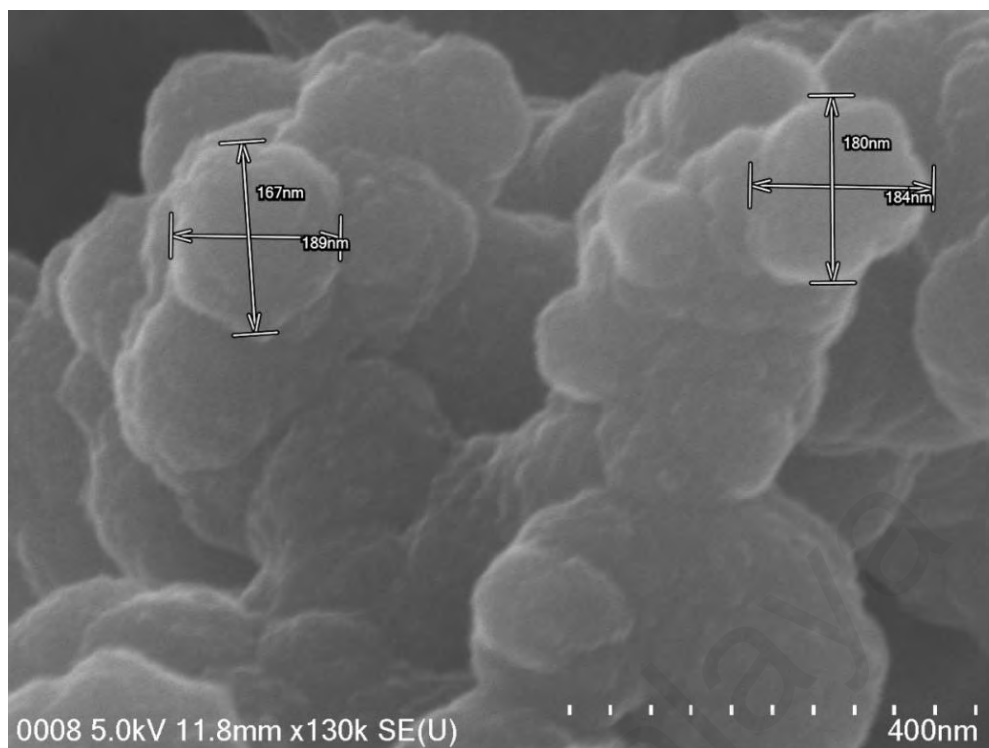


Figure 4.8: FESEM image of PPy-PEI after adsorption with internal particle diameter measurement; magnification $\times 130$ k).

4.1.3 X-ray diffraction (XRD) analysis

The X-ray diffraction patterns of as-prepared polymer powders have been observed to understand the nature of the polymer materials. The crystalline structure of the PPy-PEI composite was characterized by XRD as shown in Figure 4.9 (adsorption of MO dye) and Figure 4.10 (adsorption of CV dye). For comparison purposes, the XRD analysis of the PPy-PEI composite before and after dye adsorption was done and the X-ray diffraction patterns were analysed. In Figure 4.9, the amorphous nature of the as-prepared polymer composite was clearly observed via a broad peak at $2\theta = 26.2^\circ$ which attributed to PPy, suggesting some degree of crystallinity in the PPy. This result further proves the presence of PPy in the structure. After dye adsorption, the broad peak observed has been shifted backward and a new sharp peak has appeared at $2\theta = 25.1^\circ$. From this pattern, the XRD analysis of PPy-PEI after adsorption showed little shift in 2θ value,

indicating the polymer composite has been successfully integrated and MO dye was successfully been adsorbed on the adsorbent surface.

Whereas, in Figure 4.10, the X-ray diffraction pattern indicated that the PPy-PEI was also amorphous in nature. The broad peak was observed at $2\theta = 25.8^\circ$ before adsorption, which was ascribed mainly to the periodicity parallel to the polymer chain. When CV dye was introduced into the polymer composite particles, the peak has been shifted backward which appeared at $2\theta = 24.3^\circ$. The slightly decreased diffraction peak after adsorption indicates the successful adsorption of the studied dye. The X-ray diffraction patterns observed are similar to the previously reported diffraction patterns for polypyrrole and its composite (Alsaiani *et. al.*, 2021; Xin *et. al.*, 2015; Zhang *et. al.*, 2019; Mohamed *et. al.*, 2018).

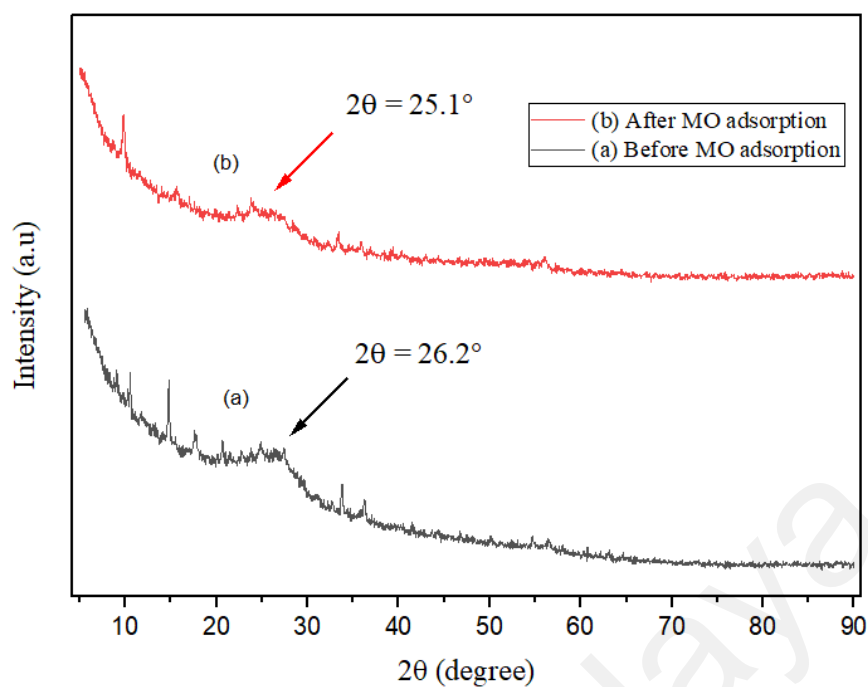


Figure 4.9: XRD diffractograms for PPy-PEI before and after MO dye adsorption.

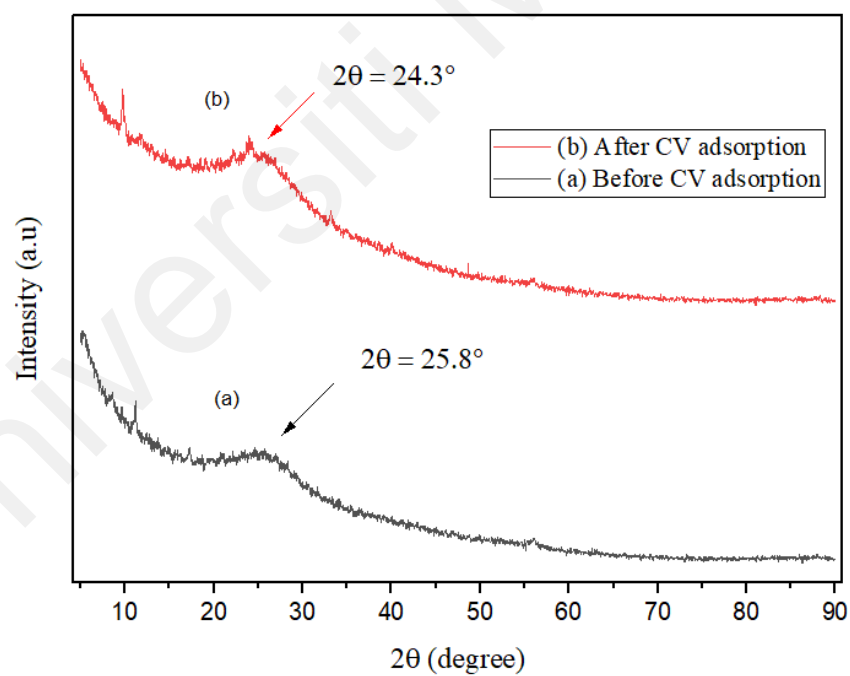


Figure 4.10: XRD diffractograms for PPy-PEI before and after CV dye adsorption.

4.1.4 FTIR analysis

FTIR analysis was used to identify the characteristic peaks of some functional groups and also to confirm the successful synthesis of the as-prepared PPy adsorbents of pristine PPy and PPy-PEI composites adsorbents. The FTIR spectra of both polypyrrole-based adsorbents before and after the adsorption of dyes were shown in the following sections.

4.1.4.1 Pristine PPy adsorbent

The FTIR spectrum of the as-prepared PPy adsorbent before and after dye adsorption were shown in Figure 4.12 (adsorption of MO dye) and Figure 4.14 (adsorption of CV dye), whereas the various bands assigned were summarized in Table 4.3 and Table 4.4, respectively. By comparison, some notable changes were observed in the spectra after dye adsorption whereby all the band positions of the PPy adsorbent before adsorption were markedly shifted to different wavenumbers after the dye adsorption.

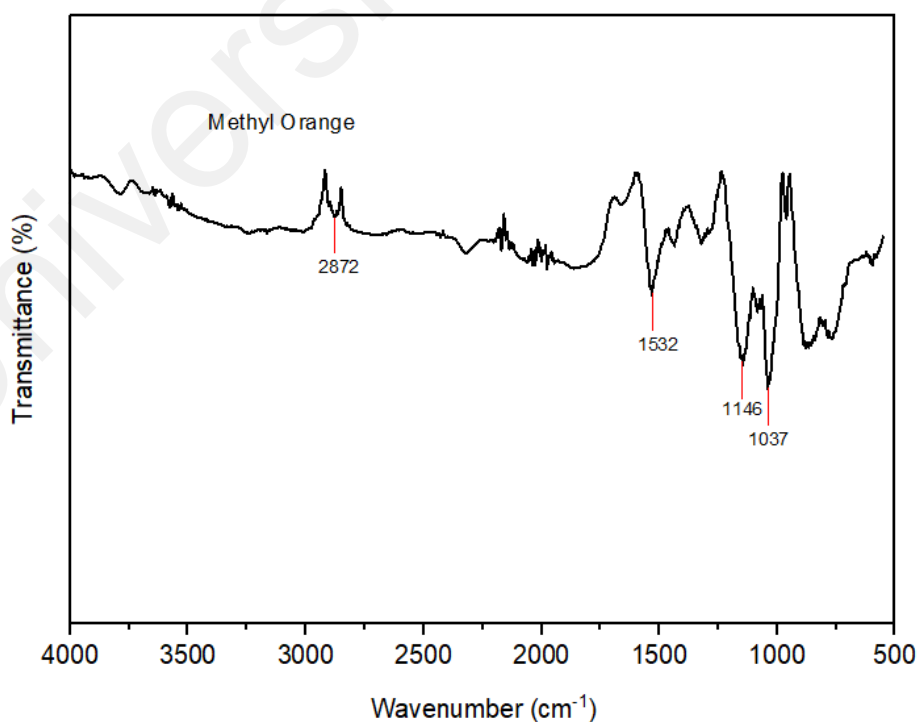


Figure 4.11: FTIR spectrum of MO dye.

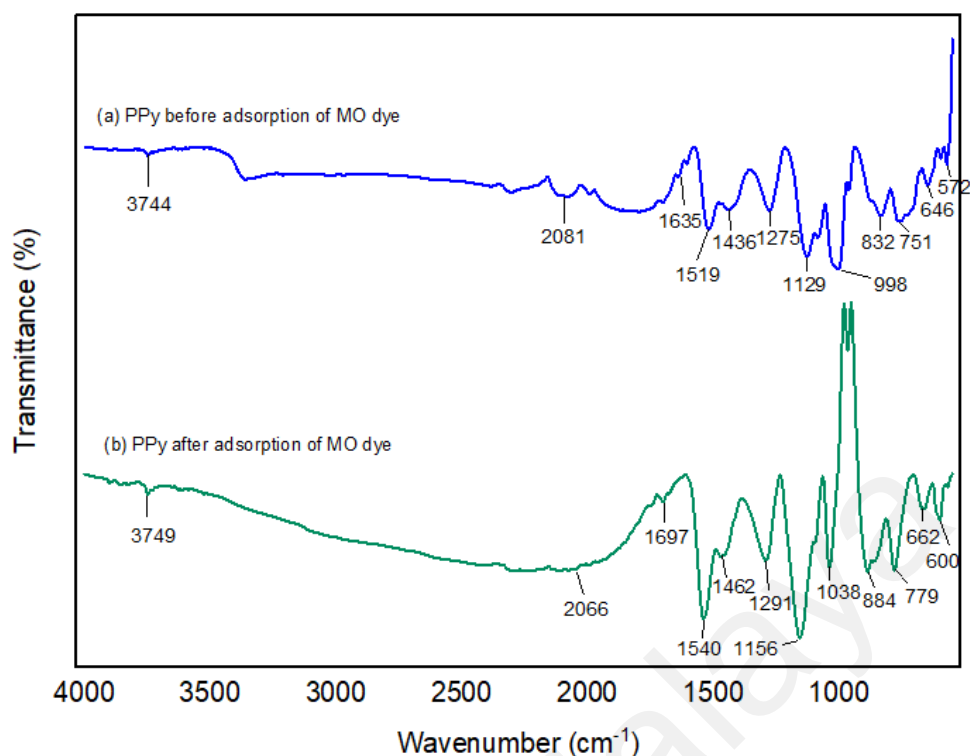


Figure 4.12: FTIR analysis for PPy before and after MO dye adsorption.

Figure 4.11 exhibits the spectrum of MO dye alone. Before the adsorption of MO dye, clearly observable bands were found at 3744 cm^{-1} , 2081 cm^{-1} , 1635 cm^{-1} , 1519 cm^{-1} , 1436 cm^{-1} , 1275 cm^{-1} , 1129 cm^{-1} , 998 cm^{-1} , 832 cm^{-1} , 751 cm^{-1} , 646 cm^{-1} , and 572 cm^{-1} . However, after the adsorption of MO dye, the loaded adsorbent shows some changes in the spectra positions (Figure 4.12). It was found that the bands have been shifted to 3749 cm^{-1} , 2066 cm^{-1} , 1697 cm^{-1} , 1540 cm^{-1} , 1462 cm^{-1} , 1291 cm^{-1} , 1156 cm^{-1} , 1038 cm^{-1} , 884 cm^{-1} , 779 cm^{-1} , 662 cm^{-1} , and 600 cm^{-1} . Generally, the major characteristics peaks that confirm the formation of polypyrrole were those found at 1519 cm^{-1} due to stretching vibrations of C-C=C of the pyrrole ring, the C-N stretching at 1275 cm^{-1} , and the C-H in-plane deformation at 1129 cm^{-1} . However, after the adsorption of MO dye, all those peaks have been shifted to higher wavenumbers, indicating that MO dye was successfully been adsorbed onto the adsorbent surface. Apart from that, it was clearly seen that the peak at 2081 cm^{-1} was assigned to N-H stretching vibration due to the pyrrole ring being found at

lower wavenumber and slightly disappearing after adsorption, endorse to the participation of respective functional groups in the formation of strong chemical bond during the adsorption of dye. The peak at 998 cm^{-1} which may be represents C-N stretching or C-H bending before adsorption, has slightly shifted to a sharp peak at 1038 cm^{-1} after MO uptake. The peak at 1038 cm^{-1} corresponding to S=O stretching vibrations confirm the sulfonic nature of the MO. These changes confirmed the participation of PPy surface functional groups with MO molecules. All the band locations were summarized in Table 4.2, supporting the adsorption of MO dye by PPy adsorbent. Therefore, the spectrum of PPy adsorbent before and after MO adsorption was a good agreement with those reported in the literature (Wong *et. al.*, 2018, Boukoussa *et. al.*, 2018; Mashkoor *et. al.*, 2020; Varga *et. al.*, 2015).

Table 4.2: Chemical bonding for PPy adsorbent before and after adsorption of MO dye.

Type of vibration	Peak position before adsorption (cm^{-1})	Peak position after adsorption (cm^{-1})
O-H stretching	3744	3749
N-H stretching	2081	2066
C=C stretching	1635	1697
C-C=C asymmetric stretch	1519	1540
C=C stretching/C-N stretching	1436	1462
C-N stretching	1275	1291
C-H bending	1129	1156
C-H bending/ S=O stretching	998	1038
C-H bending	832	884
C-H bending	751	779
C-H bending	646	662
C-H bending	572	600

Figure 4.13 shows FTIR spectrum of CV dye alone, whereas Figure 4.14 referred to the FTIR spectra before and after the adsorption of CV dye. All the band assignments were summarized in Table 4.4. Here, before the adsorption of CV dye, the absorption peaks were observed at 3108 cm^{-1} , 1564 cm^{-1} , 1450 cm^{-1} , 1313 cm^{-1} , 1202 cm^{-1} , 1047 cm^{-1} , 924 cm^{-1} , 791 cm^{-1} , 681 cm^{-1} , and 610 cm^{-1} . However, the observable peaks show some changes in the spectra positions and there were also new peaks observed after the adsorption of CV dye. It was found that the bands have been shifted to 3210 cm^{-1} , 1587 cm^{-1} , 1349 cm^{-1} , 1259 cm^{-1} , 1056 cm^{-1} , 942 cm^{-1} , 811 cm^{-1} , 688 cm^{-1} , and 640 cm^{-1} .

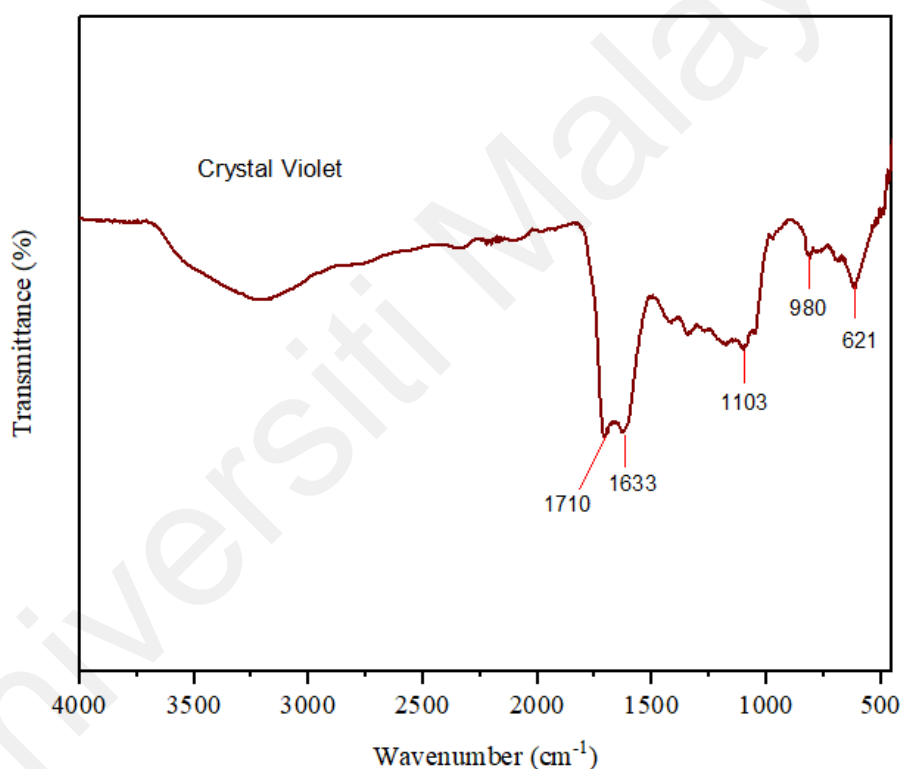


Figure 4.13: FTIR spectrum of CV dye.

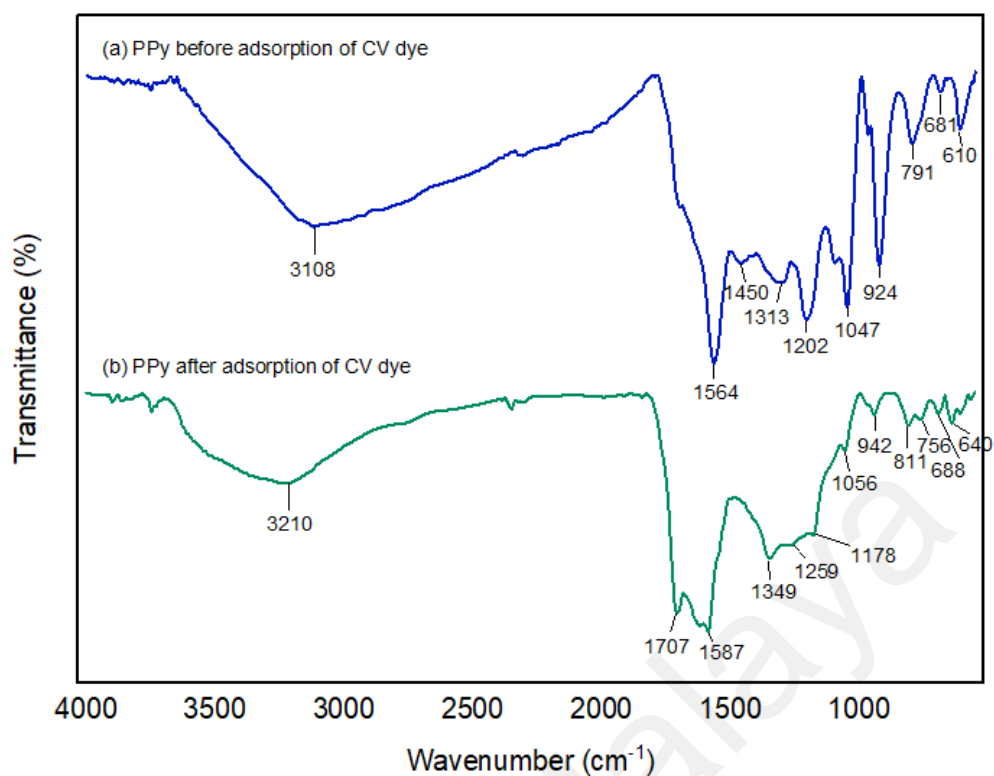


Figure 4.14: FTIR analysis for PPy before and after CV dye adsorption.

The generally notable fundamental peaks that correspond to the formation of polypyrrole were those found at 3108 cm^{-1} due to N-H stretching vibration from the pyrrole ring, 1564 cm^{-1} due to stretching vibrations of C=C, the C-N stretching at 1313 cm^{-1} and 1202 cm^{-1} , and the C-H in-plane deformation at 1047 cm^{-1} . From the spectrum, it can be clearly seen that after the adsorption of CV dye, all those peaks have been shifted to higher wavenumbers. Moreover, some peaks observed before adsorption (1450 cm^{-1} and 1313 cm^{-1}) were merged to 1349 cm^{-1} after CV uptake, and there were some new peaks observed at 1707 cm^{-1} , 1178 cm^{-1} , and 756 cm^{-1} after adsorption which indicate that CV dye was successfully been adsorbed onto the adsorbent surface. A similar behaviour that confirmed the uptake of CV by polymer composite was reported by Loganathan *et al.* (2022), Saad *et al.* (2017), and Sulyman *et al.* (2021). All the band assignments were summarized in Table 4.3, These results could be confirmed that the respective functional groups influenced the adsorption process.

Table 4.3: Chemical bonding for PPy adsorbent before and after adsorption of CV dye.

Type of vibration	Peak position before adsorption (cm ⁻¹)	Peak position after adsorption (cm ⁻¹)
N-H stretching	3108	3210
C=C stretching	-	1707
C=C stretching	1564	1587
C=C stretching/C-N stretching	1450	-
C-N stretching	1313	1349
C-N stretching	1202	1259
C-N stretching	-	1178
C-H bending	1047	1056
C-H bending	924	942
C-H bending	791	811
C-H bending	-	756
C-H bending	681	688
C-H bending	610	640

4.1.4.2 PPy-PEI composite adsorbent

The FTIR spectrum of the as-prepared PPy-PEI composite before and after dye adsorption were shown in Figure 4.15 (adsorption of MO dye) and Figure 4.16 (adsorption of CV dye), respectively. Various bands assigned were summarized in Table 4.5 and Table 4.6, respectively. All the band positions of the PPy-PEI composite before adsorption were markedly shifted to different wavenumbers after the dye adsorption. The shifted results also demonstrated that the polymer composites were successfully formed and the dye has been adsorbed. It has also been observed that some of the band locations of the PPy-PEI composite significantly shifted to other wavenumbers compared to PPy spectrum indicating the successful incorporation of PEI in PPy structure.

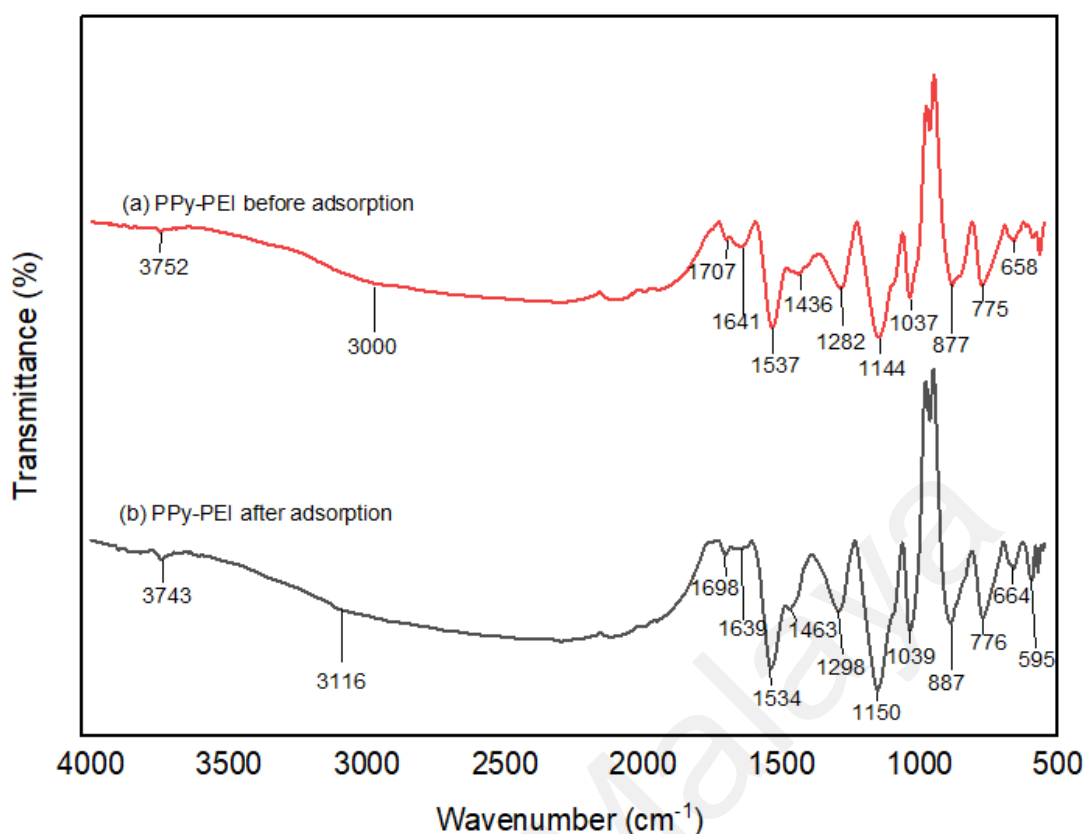


Figure 4.15: FTIR analysis for PPy-PEI before and after MO dye adsorption.

As in Figure 4.15, the bands at 3752 cm^{-1} , 1707 cm^{-1} , 1641 cm^{-1} , and 1537 cm^{-1} observed in the PPy-PEI spectrum before adsorption of MO dye have shifted to lower wavenumbers of 3743 cm^{-1} , 1698 cm^{-1} , 1639 cm^{-1} , and 1534 cm^{-1} , respectively, after adsorption. On the other hand, the bands at 3000 cm^{-1} , 1436 cm^{-1} , 1282 cm^{-1} , 1144 cm^{-1} , 1037 cm^{-1} , 877 cm^{-1} , 775 cm^{-1} and 658 cm^{-1} observed in the PPy-PEI spectrum before adsorption of MO dye have shifted to higher wavenumbers of 3116 cm^{-1} , 1463 cm^{-1} , 1298 cm^{-1} , 1150 cm^{-1} , 1039 cm^{-1} , 887 cm^{-1} , 776 cm^{-1} and 664 cm^{-1} , respectively, after adsorption. The characteristic peaks of considerable intensity at 1537 cm^{-1} which shifted to 1534 cm^{-1} were endorsed to asymmetric stretching vibrations of C-C=C of the pyrrole ring. Apart from that, it was clearly seen that the characteristics of the PPy-PEI polymer composite which were located at 1641 cm^{-1} with a broader peak then shifted to 1639 cm^{-1} and 1282 cm^{-1} which shifted to 1298 cm^{-1} were due to the symmetric N-H bending and also C-N stretching vibration from PEI. These results were assigned to primary amine

groups, therefore confirming the incorporation of PEI with the PPy unit. Thus, indicating the addition of more potential active sites for adsorption, hence achieving higher dye removal. The peak at 1037 cm^{-1} which may be represents C-N stretching before adsorption, has slightly shifted to 1039 cm^{-1} with slightly a sharp peak after MO uptake, suggesting the overlapping with S=O stretching which indicates the SO_3^- involved in MO adsorption. These changes confirmed the participation of PPy-PEI surface functional groups with MO molecules. All the band assignments were summarized in Table 4.4, supporting the adsorption of MO dye by PPy-PEI composite adsorbent. Similar trends have been reported by Huang *et. al.*, (2019); Li *et. al.*, (2018), Nolasco *et. al.*, (2019), and Wong *et. al.*, (2018).

Table 4.4: Chemical bonding for PPy-PEI adsorbent before and after adsorption of MO dye.

Type of vibration	Peak position before adsorption (cm^{-1})	Peak position after adsorption (cm^{-1})
O-H stretching	3752	3743
N-H stretching	3000	3116
C=C stretching	1707	1698
N-H bending	1641	1639
C-C=C asymmetric stretch	1537	1534
C-N stretching	1436	1463
C-N stretching	1282	1298
C-H in plane deformation	1144	1150
S=O stretching	1037	1039
C-H bending	877	887
C-H bending	775	776
C-H bending	658	664
C=C bending	-	595

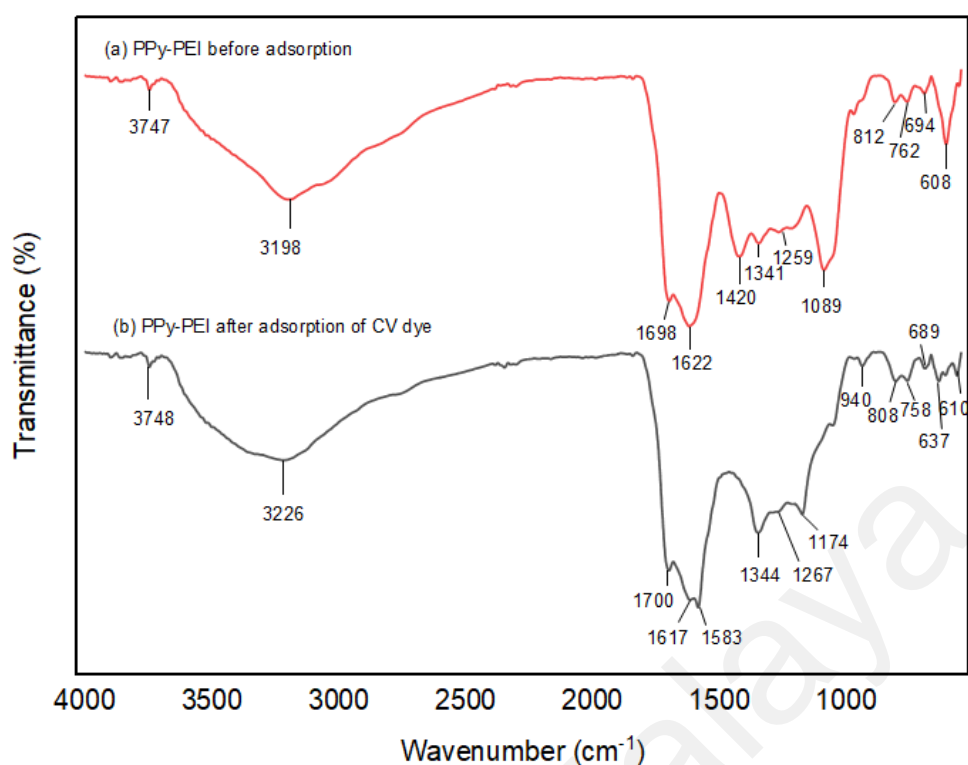


Figure 4.16: FTIR analysis for PPy-PEI before and after CV dye adsorption.

Whereas, in Figure 4.16, the spectrum was referred to as the FTIR spectra before and after the adsorption of CV dye and the band assignments were summarized in Table 4.5. The bands at 3747 cm⁻¹, 3198 cm⁻¹, 1698 cm⁻¹, 1259 cm⁻¹, 1089 cm⁻¹ and 608 cm⁻¹ observed in the PPy-PEI spectrum before adsorption of CV dye have shifted to higher wavenumbers after adsorption which were 3748 cm⁻¹, 3226 cm⁻¹, 1700 cm⁻¹, 1267 cm⁻¹, 1174 cm⁻¹ and 610 cm⁻¹, respectively. Whereas, the bands at 1622 cm⁻¹, 1420 cm⁻¹, 812 cm⁻¹, 762 cm⁻¹, and 694 cm⁻¹ observed in the PPy-PEI spectrum before adsorption of CV dye have shifted to lower wavenumbers of 1617 cm⁻¹, 1344 cm⁻¹, 808 cm⁻¹, 758 cm⁻¹, and 689 cm⁻¹ after adsorption. Wavenumbers at 1622 cm⁻¹ and 1259 cm⁻¹ have shifted to a new band position which were 1583 cm⁻¹ and 1267 cm⁻¹ indicated to the symmetric N-H band and also C-N stretching vibration from PEI, which was assigned to primary amine groups, therefore confirmed the successful preparation of PPy-PEI composite. A new peak at 940 cm⁻¹ was observed after CV dye adsorption, suggesting the dye ion was

successfully loaded on the PPy-PEI composite. A similar behaviour that confirmed the uptake of CV by polymer composite was reported by Huang *et. al.*, (2019), Li *et. al.* (2018), Loganathan *et. al.* (2022), Saad *et. al.* (2017), and Sulyman *et. al.* (2021). Therefore, these changes in band positions indicate the interaction between functionalized amine groups and dye ions and the characteristics peaks from the spectrum demonstrated that the dye ions have been adsorbed successfully by the polymer composite. Moreover, there were subtle differences at the nearly same positions between the IR spectrum of the PPy-PEI composites and that of PPy alone, indicating a new PPy-PEI composite with higher active sites of amine groups.

Table 4.5: Chemical bonding for PPy-PEI adsorbent before and after adsorption of CV dye.

Type of vibration	Peak position before adsorption (cm ⁻¹)	Peak position after adsorption (cm ⁻¹)
O-H stretching	3747	3748
N-H stretching	3198	3226
C=C stretching	1698	1700
N-H bending	1622	1617
C-H bending	1420	1344
C-N stretching	1259	1267
C-N stretching	1089	1174
C-H bending	-	940
C-H bending	812	808
C-H bending	762	758
C-H bending	694	689
C=C bending	-	637
C=C bending	608	610

4.2 Adsorption studies

In this research, MO and CV dyes were selected as a model in order to study the removal of dye materials from aqueous media by new effective conducting polymer-based adsorbents. The main aim of the wastewater treatment process by adsorption was carried out to study the role of polypyrrole conducting polymer and its composite as adsorbents in removing undesirable dyes from the aqueous environment. However, the preparation conditions of PPy-based adsorbent play a major role in its suitable applications and effectiveness. It is useful and necessary to develop a systematic investigation aimed at establishing the relations between the characteristics of the intrinsically conductive polymers and a wide range of preparation variables.

The effects of various parameters such as mole ratio, solution pH, adsorbent dose, contact time, and the initial dye concentration were studied to understand the behavior of the polymer materials during the adsorption process. Moreover, for a practical application, optimization of these factors is very important from the economic and environmental points of view.

4.2.1 Effect of pyrrole to oxidant mole ratios

Preparation conditions of PPy-based adsorbents play a major role in their suitable applications and effectiveness. The various mole ratios of monomer to oxidant and operating conditions were mainly considered for the preparation of these PPy-based adsorbents (pristine PPy and PPy-PEI composite). The adsorption efficiency of both pristine PPy and PPy-PEI composite adsorbents for MO and CV dye removal by using different monomer to oxidant ratios (1:0.5, 1:1, 1:2, and 1:3) were shown in Figure 4.17 and Figure 4.18. Generally, it was observed that the adsorption efficiency of both MO and CV dyes on pristine PPy adsorbent exhibited the maximum of 78.5 % and 45.0 % for

MO and CV, respectively, at 1:1 of monomer to oxidant ratio. Whereas, the maximum adsorption efficiency of MO and CV dyes on PPy-PEI adsorbent was increased to 98.6 % and 70.9 % for MO and CV at the fixed preparation conditions. Although the oxidant controls the polymerization of pyrrole monomers and the yield of the PPy product, it appears also that the adsorption performance of the PPy-based adsorbents depends on the oxidant molarity. It was observed that a higher oxidant to pyrrole mole ratio reduces the removal efficiency for all the studied dyes.

The adsorption efficiency of both MO and CV dyes was found to be the lowest by using 1:0.5 mole ratio of pyrrole to oxidant for all oxidants. Polymerization with a lower monomer to oxidant ratio (1:0.5), produced a very thin and soft powder that appears very difficult to handle. Polymerization also was considered an incomplete process at this mole ratio. The adsorption was found to be rapid in the early stage as it relies on increasing interaction between the additional nitrogen groups from the adsorbent with the dyes. However, as the amount of oxidant increased (1:2 and 1:3), it will result in a decreased percentage of dye removal due to hard and compact polymer that was produced with higher oxidant ratios and fewer active sites available for binding interactions with dyes. A similar trend has been reported by Deng *et. al.*, 2014.

Therefore, the ideal removal of both MO and CV dyes was observed at a mole ratio of 1:1 of pyrrole monomer to oxidant for both types of PPy-based adsorbents. It indicates that the monomer concentration reached the equilibrium state at this point. Consequent to the obtained results, pyrrole to oxidant ratio of 1:1 was used for the next experiments.

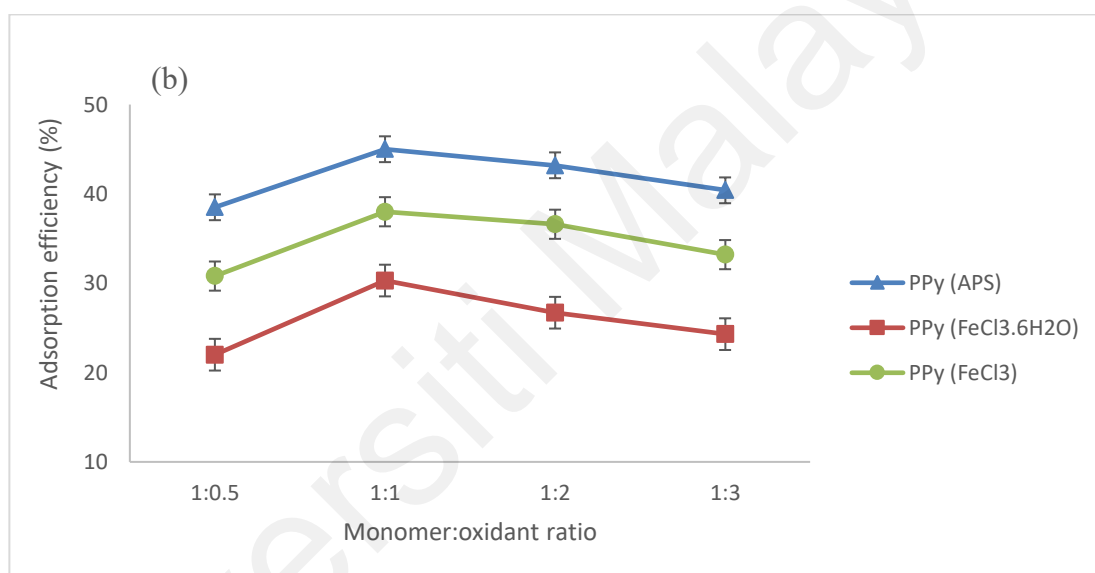
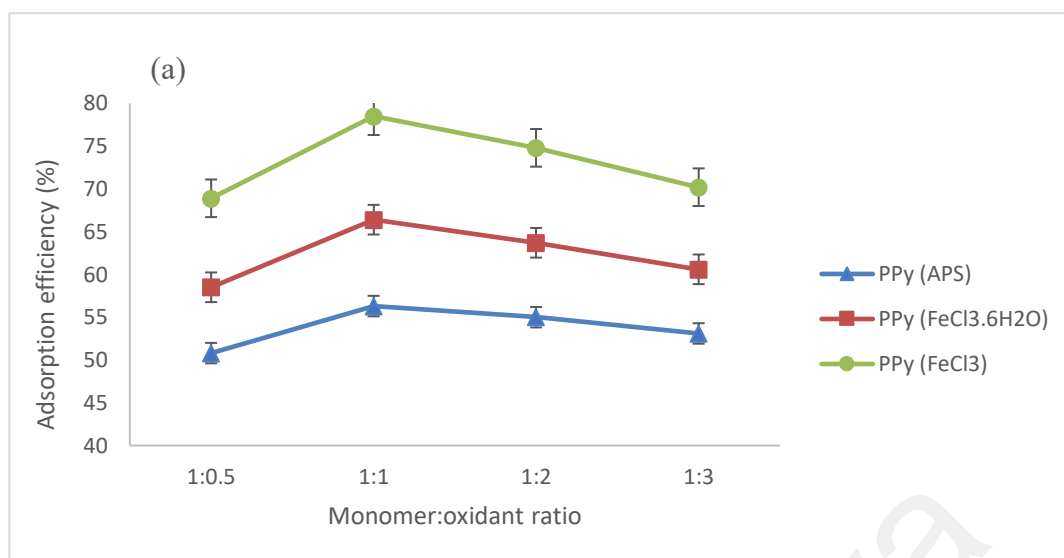


Figure 4.17: Effect of monomer to oxidant ratios by pristine PPy adsorbent on adsorption of (a) MO and (b) CV.

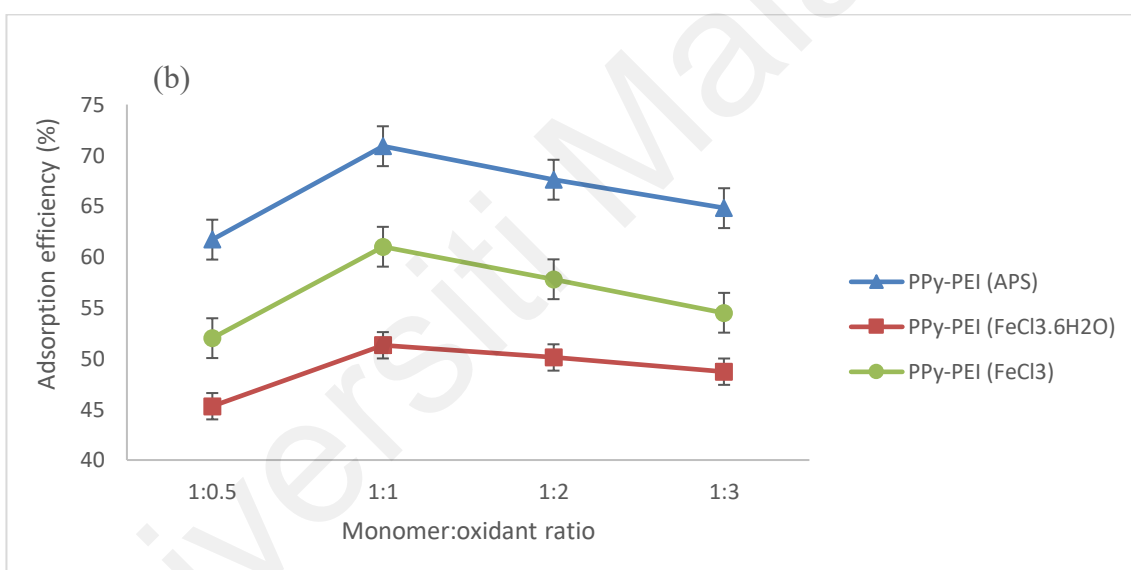
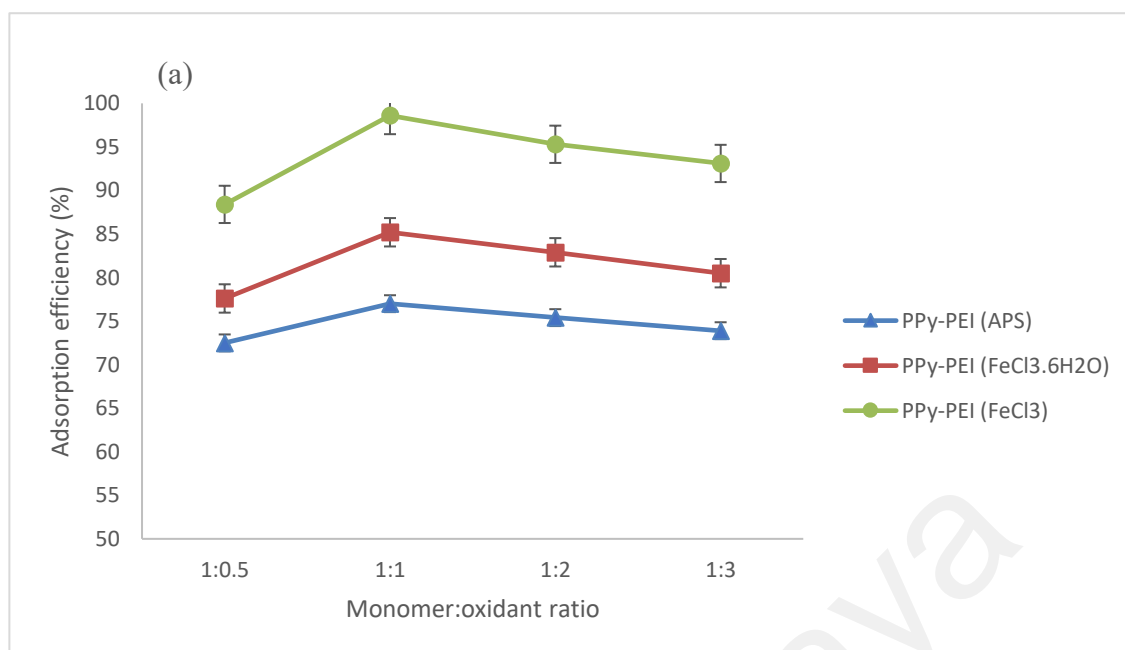


Figure 4.18: Effect of monomer to oxidant ratios by PPy-PEI composite adsorbent on adsorption of (a) MO and (b) CV.

4.2.2 Effect of different oxidants

The oxidant used for the preparation of polymer adsorbent also plays a role in dye adsorption efficiency. PPy-based adsorbent would have excellent adsorption ability with the right oxidant used, but this was rarely reported. As seen in Figure 4.17 or Figure 4.18, it can be clearly observed that the removal of anionic MO dye using FeCl_3 anhydrous as an oxidant exhibited the highest adsorption efficiency of 78.5% for pristine PPy adsorbent and 98.6% for PPy-PEI adsorbent among all oxidants and mole ratios used under certain preparation conditions. Whereas, the removal of cationic CV dye using ammonium persulfate as the oxidant exhibited the highest adsorption efficiency of 45% for pristine PPy adsorbent and 70.9% for PPy-PEI adsorbent under certain preparation conditions. The findings confirmed higher dye removal potential in the presence of FeCl_3 anhydrous and ammonium persulfate as the oxidant for the MO and CV dye, respectively, in comparison to others. Hence, these oxidants have been chosen for studying and comparing the dye removal efficiency for two distinct dyes, MO and CV dyes.

The higher dye adsorption performance obtained in the presence of anhydrous FeCl_3 and ammonium persulfate as the oxidant for MO and CV dyes, respectively, could be attributed to its great surface area. The smaller size and porous particle structure can create bigger surface area and probably increase the adsorption of dye from aqueous solution (Zandevakili and Hamghavandi, 2020). This was also supported by BET surface analysis as shown in Table 4.1 for different oxidizing agents used. Besides, the different in result obtained with different oxidizing agent used could be explained the favourable adsorption of dyes over the adsorbent surface was due to electrostatic interactions between dyes anions or cations with the positively charged surface of the adsorbent in a solution, indicate whether the dyes are highly deprotonated or reverse principle. These describe that the anions of the oxidizing agents may have played a different role of

counterions of altering ion pair interaction. In turn the growth of polypyrrole adsorbent has been confined in different ways during polymerization, providing a potential route to control the adsorption efficiency of dyes from aqueous environment (Zhang *et. al.*, 2014).

4.2.3 Effect of modified adsorbent (PPy-PEI composites)

It was observed that the PPy adsorbent was capable of adsorbing MO and CV dyes from an aqueous solution. However, pristine PPy showed poor adsorption efficiency. In order to enhance the adsorption performance of PPy-based adsorbents for these two dyes, PPy was modified with polyethyleneimine (PEI), a cationic polyelectrolyte containing branched chains of amino groups and highly water-soluble polyamine. For this purpose, batch adsorption experiments were conducted for subsequent adsorption of MO and CV dyes.

4.2.4 Effect of solution pH

4.2.4.1 Pristine PPy adsorbent

The pH of the solution is a very important parameter in the adsorption process, particularly for dye adsorption in determining the surface properties and ionization degree of an adsorbent (Li *et. al.*, 2018). Thus, the effect of pH in the solutions on the adsorption efficiency of 100 ppm of MO and CV dyes were investigated at different pH range between pH 1 and 13. pH values were adjusted by adding 0.1 mol L⁻¹ HCl or 0.1 mol L⁻¹ NaOH solutions. Accordingly, 0.1 g of each PPy adsorbent was treated with 50 mL of MO solution for a contact time of 120 minutes. In the case of CV dye, 0.3 g of each PPy adsorbent was treated with 50 mL of CV solution for a contact time of 180 minutes.

From the result obtained (Figure 4.19 (a)), it was observed that the maximum adsorption efficiency of 100 ppm of MO dye (78 %) was found at pH 3 at a certain dosage

and contact time. Adsorption efficiency increases with the rise of pH solution up to pH 3. However, after this level, the increase in pH causes a decrease in the percentage of sorption. In the case of the removal of 100 ppm of CV dye (Figure 4.19 (b)), it was found the maximum adsorption efficiency of CV dye (44.8 %) was observed at initial pH of 11, after being subjected to modification by NaOH and/or HCl, at a certain dosage and contact time. Likewise, the adsorption efficiency of CV dye increases upon increasing the pH level to the value of 11, after which the increase in pH level decreases the percentage of sorption. A similar trend has been reported by other researchers (Alsaiani *et. al.*, 2021; Alqarni *et. al.*, 2022). Hence, the pH solution was selected at pH 3 and pH 11 for MO and CV adsorption, respectively for all subsequent adsorption experiments.

4.2.4.2 PPy-PEI composite adsorbent

The effect of solution pH on the adsorption efficiency of 100 ppm of MO and CV dyes by PPy-PEI composite has been done at different pH range between 1 to 13 with the same preparation conditions as pristine PPy adsorbent. From Figure 4.19 (a), it can be clearly seen that the adsorption efficiency of 100 ppm of MO dye was the highest at pH 3 (97.8 %). Whereas, the adsorption efficiency of 100 ppm of CV dye exhibited the highest at pH 11 (69.3 %) as seen in Figure 4.19 (b). Therefore, this optimal pH value was employed for further adsorption experiments. From the obtained results, it was observed that PPy-PEI composite adsorbent exhibited higher adsorption performance in a range of pH solutions compared to pristine PPy adsorbent generally due to the effect of PEI having more nitrogen-containing groups in the compounds that can be added to pyrrole structure.

The effect of pH can have an impact on the surface charge on the pristine PPy adsorbent and PPy-PEI composite adsorbent. The functional group $-NH_2$ group in PPy and PEI are considered active sites for the adsorption of dye ions. Depending on the

solution pH, these -NH_2 groups can undergo protonation to NH_3^+ and the extent of protonation will be dependent on the solution pH. In general, at low solution pH, the adsorption efficiency will decrease for cationic CV dye and increase for anionic MO dye. This happens due to the positive charge on the solution interface will increase and the adsorbent surface will appear positively charged, which results in a decrease in adsorption efficiency for cationic dye and an increase for anionic dye. At higher solution pH, adsorption efficiency is more preferable for cationic CV dye but shows a lower efficiency for anionic MO dye. As a result, the cationic dye will show an increase in adsorption efficiency while anionic dye adsorption will decrease (Seow *et. al.*, 2016).

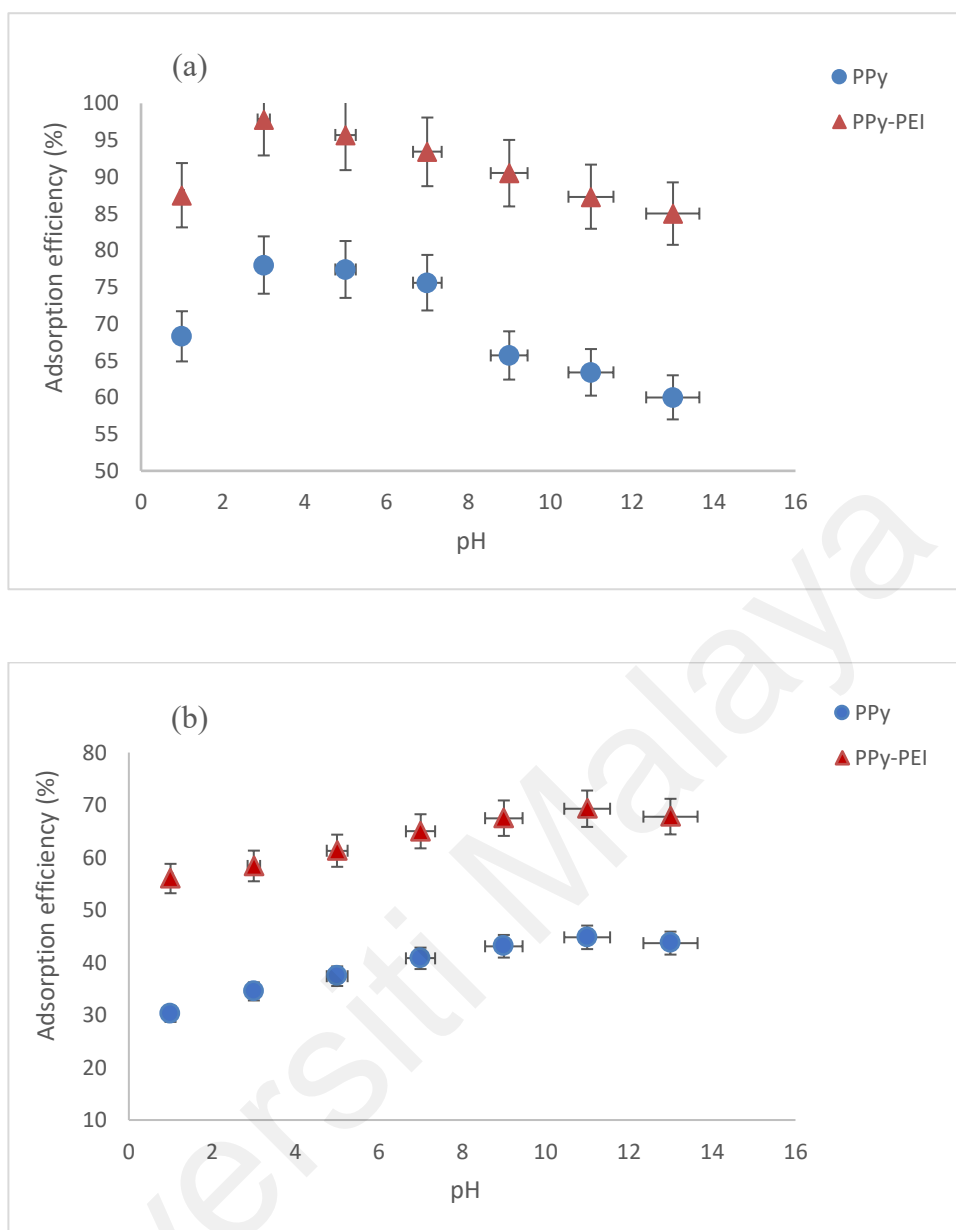


Figure 4.19: Effect of initial solution pH by pristine PPy and PPy-PEI composite adsorbents on adsorption of (a) MO and (b) CV.

4.2.5 Effect of adsorbent dosage

4.2.5.1 Pristine PPy adsorbent

The effect of adsorbent dosage on MO and CV dyes removal was investigated to essentially minimize the doses of PPy-based adsorbents required for the adsorption process. In an era where industries need the saving of amount of adsorbent being used, it is best that the smaller the amount of adsorbent used, the better the adsorption efficiency

or capacity it must be at the industrial scale (Seow *et al.*, 2016). The adsorption process was performed using different pristine PPy adsorbent doses varying from 0.05 to 0.4 g with preparation conditions for MO at the solution of pH 3, 120 min contact time; CV at the solution of pH 11, 180 min contact time. As shown in Figure 4.20 (a), it was observed that MO dye removal exhibited the maximum adsorption efficiency of 79.1 % by using 0.1 g of the prepared adsorbent. However, with an increase in adsorbent doses beyond 0.1 g, it was observed that no further MO could be adsorbed. On the other hand, the maximum adsorption of 44.8 % for CV dye appeared by using 0.3 g of pristine PPy adsorbent dose as seen in Figure 4.20 (b).

A positive correlation was initially observed between the MO and CV dye removal efficiency and the PPy adsorbent dosage due to greater numbers of adsorption active sites being available at higher dosages. However, upon increasing the sorbent dosage, the dye removal efficiency remained almost constant after increasing up to a certain limit, thereby indicating that no further MO could be adsorbed (Li *et. al.*, 2018). Thus, considering the observed removal efficiencies and the desire to keep the adsorbent loading to a minimum during the application, all subsequent adsorption experiments were carried out using a PPy loading of 0.1 g for MO dye removal and 0.3 g for CV dye removal. A similar result has been reported by Mashkooor *et al.*, 2020.

4.2.5.2 PPy-PEI composite adsorbent

Figure 4.18 show the effect of adsorbent dosage on the adsorption of MO and CV dyes by PPy-PEI composite adsorbent. To study the effect of the adsorbent doses of PPy-PEI composite adsorbent on the adsorption of both dyes, the adsorption was performed using different PPy-PEI adsorbent doses from 0.05 to 0.4 g with the same preparation conditions as pristine PPy adsorbent for MO and CV dyes, respectively. From Figure 4.20 (a), it was observed that for MO dye removal, the maximum adsorption efficiency of

98.3 % was exhibited by using 0.1 g of the prepared composite adsorbent with the optimum condition at solution pH 3 for a concentration of 100 ppm MO dye. With the increase in adsorbent doses beyond 0.1 g, the adsorption efficiency remained unaltered. Whereas, for CV dye removal, as shown in Figure 4.20 (b), the maximum adsorption of 69.8 % appeared by using 0.3 g of PPy-PEI adsorbent dose with the optimum condition at solution pH 11 for a concentration of 100 ppm CV dye. The removal efficiency of CV dye gradually increased from 56.5 % to 69.8 % with an increase in adsorbent doses from 0.05 g to 0.3 g of PPy-PEI composite adsorbent, respectively. Here, the PPy-PEI composite adsorbent shows higher adsorption efficiency in adsorbing dye from an aqueous solution by varying the amount of polymer adsorbent.

However, with the increase in adsorbent doses, the polymer adsorbents are likely to aggregate resulting in reduced surface area of the adsorbents and hence the adsorption efficiency is likely to decrease (Aliabadi *et. al.*, 2018). In general, increasing the adsorbent doses will offer more active sites to adsorb more dye ions. However, the higher adsorbent dosage may not be useful due to the saturation of the active sites of the adsorbent once it reached the equilibrium condition and since the aggregation of the polymer adsorbent reduces the active or contact surface area of the adsorbents resulting in lowering the adsorption efficiency (Aliabadi *et. al.*, 2018). Wong *et al.* (2018) has also reported a similar result on the effect of adsorbent dosage on the adsorption of anionic dyes on spent tea leaves modified with polyethyleneimine (PEI-STL).

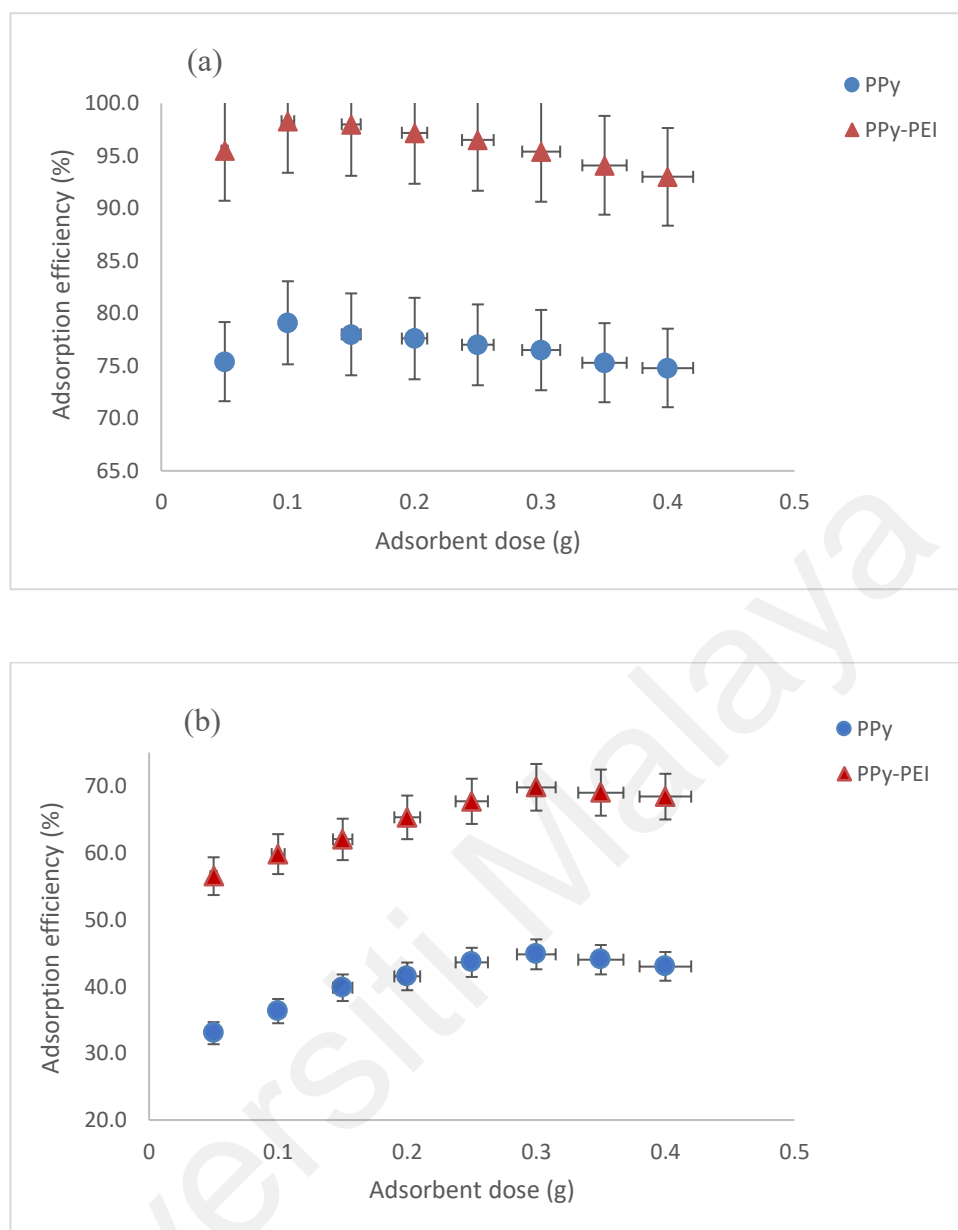


Figure 4.20: Effect of adsorbent dosage by pristine PPy and PPy-PEI composite adsorbents on adsorption of (a) MO and (b) CV.

4.2.6 Effect of contact time

4.2.6.1 Pristine PPy adsorbent

The contact time between the contaminant and the adsorbent is one of the vital variables to investigate the effectiveness of prepared adsorbents for the removal of contaminants, as well as for the practical application of the adsorption process (Sulyman *et. al.*, 2021). The effects of contact time on the adsorption of MO and CV dyes by PPy

adsorbent were investigated at contact times ranging from 30 to 300 min at initial dye concentrations of 100 ppm at an optimum solution pH of 3, a dose of 0.1 g adsorbent for MO dye, and an optimum solution pH of 11 and a dose of 0.3 g adsorbent for CV dye. The results were shown in Figure 4.19. According to Figure 4.21 (a) and (b) for MO and CV adsorption, respectively, generally, the removal efficiency of the dyes was rapid at the first stage of the adsorption time, and thereafter, it slowed down with the increase of contact time until it attained its equilibrium at a contact time of 120 min for the removal of MO dye and 180 min for the removal of CV dye. A further increase in adsorption time shows no significant impact on the rate of adsorption. This phenomenon was due to the fact that a large number of vacant surface sites were available for uptake during the initial stage, and after a period of time, the remaining vacant surface sites were difficult to be occupied due to repulsive forces between the solute molecules on the solid and in aqueous phases (Sulyman *et. al.*, 2021).

4.2.6.2 PPy-PEI composite adsorbent

The adsorption efficiency of 100 ppm MO and CV dyes by PPy-PEI composite adsorbent at optimum pH and adsorbent dosage (MO dye with pH 3 and 0.1 g adsorbent dose; CV dye with pH 11 and 0.3 g adsorbent dose) were measured at a contact time ranging from 30 to 300 min as shown in Figure 4.21. For the removal of MO dye, it was observed the maximum adsorption efficiency of 98.8% was exhibited at a contact time of 120 min, as shown in Figure 4.21 (a). The adsorption of MO dye was found to be very fast during the initial stage and slowly increased up to 120 min, and beyond that time the adsorption efficiency was steady. It showed that the equilibrium has been achieved at this time. This could be described to the fact that there were numbers of vacant surface sites available for the adsorption to take place during the initial stage and the adsorption was initially rapid. The remaining vacant surface sites decreased as the adsorption continued

and they were difficult to occupy due to the repulsive forces between the solute molecules on the solid and bulk phases. Thus, at this stage, the adsorption reached equilibrium.

While for the removal of CV dye, the maximum adsorption efficiency of 70.9 % was achieved at a contact time of 180 min as shown in Figure 4.21 (b). Likewise, the adsorption of CV dye increased with the increase in contact time and became steady with further increase in time, following the similar trend as has been observed for MO dye. The similar trend as obtained results on the effect of contact time on the adsorption of MO and CV dyes by pristine PPy adsorbent and PPy-PEI composite adsorbent have been reported by other researchers (Xin *et al.*, 2015; Agarwal *et al.*, 2016; Zhang *et al.*, 2019; Mashkooor *et al.*, 2020; Alsaiari *et al.*, 2021; Sulyman *et al.*, 2021).

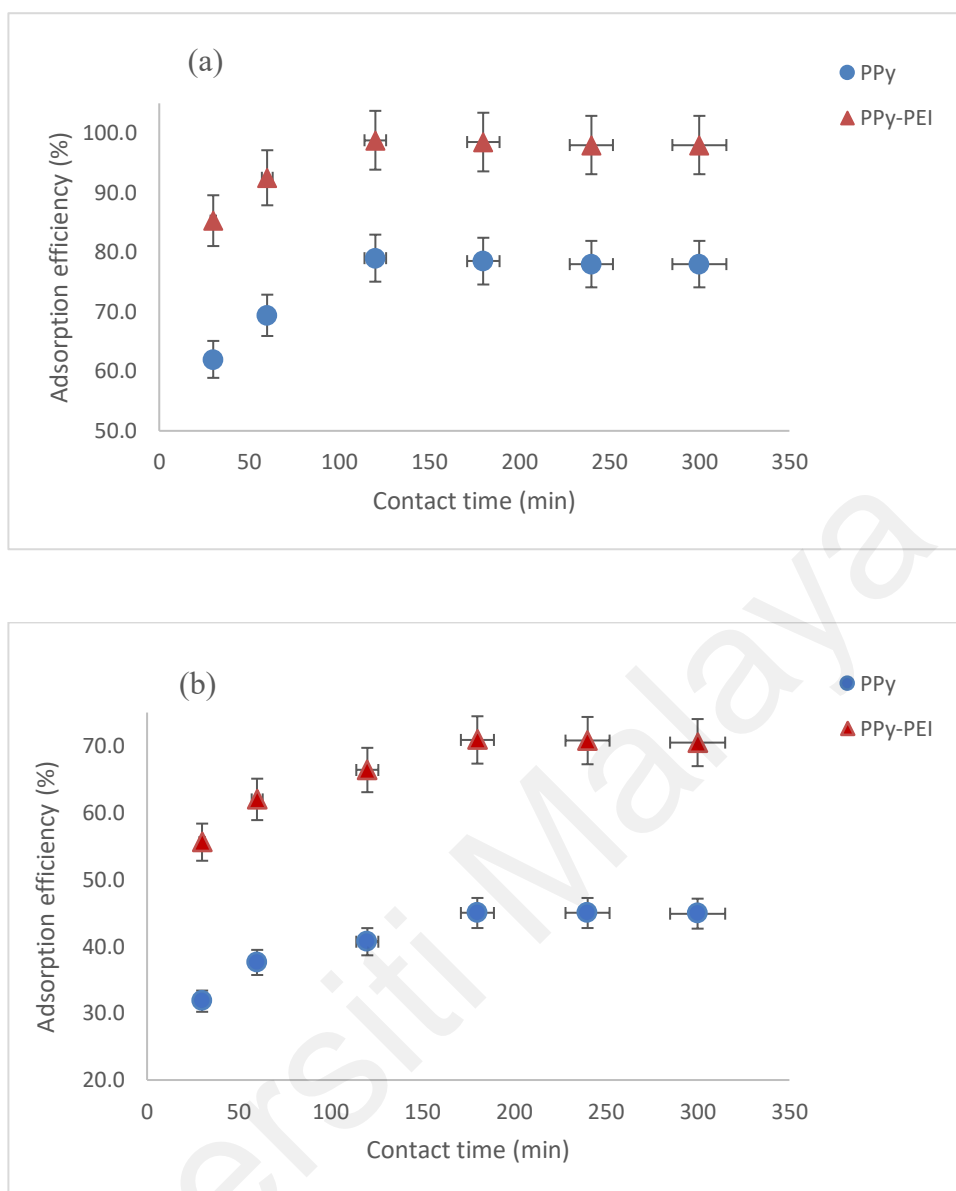


Figure 4.21: Effect of contact time by pristine PPy and PPy-PEI composite adsorbents on adsorption of (a) MO and (b) CV.

4.2.7 Effect of initial dye concentration

4.2.7.1 Pristine PPy adsorbent

Dyes are widely used in the industry, thus their concentrations in wastewater are variable. It is very interesting to study the adsorption behavior of MO and CV dyes containing different initial dye concentrations as the initial concentration of the adsorbate determines the amount of adsorbate ion that is adsorbed on the adsorbent surface (Zhou

et al., 2017). The effect of initial dye concentration on the adsorption of MO and CV dyes by PPy adsorbent were carried out at concentration ranging from 25 to 300 ppm at optimum pH, contact time and adsorbent dosage for each dye, respectively. From Figure 4.22, at lower concentrations, the adsorption efficiency of MO and CV dyes was high. However, upon increasing the dye concentration, the adsorption efficiency decreased. It can be explained due to a lower the dye concentration, the adsorption sites are available (in excess) for the removal of dye molecules, but at higher dye concentrations, the ratio of adsorbent sites is reduced relative to the available dye molecules, and all sites are saturated easily due to the higher dye concentrations (Boukoussa *et al.*, 2018).

4.2.7.2 PPy-PEI composite adsorbent

The effect of initial dye concentrations in the range of 25 to 300 ppm for the removal of MO and CV dyes from aqueous solution has been studied at optimum pH, contact time and adsorbent dosage for each dye, respectively and the results were shown in Figure 4.22. The results show that the adsorption of both MO and CV dyes decreased gradually with the increase in initial concentration from 25 ppm to 300 ppm, respectively. The decrease in adsorption efficiency with the increase in dye concentration may be due to the utilization and saturation of all active sites available on the adsorbent surface for the adsorption at higher concentration, a similar trend as the results obtained by using pristine PPy adsorbent. Several studies that have a similar trend on the effect of initial dye concentration on the adsorption process also have been reported by other researchers (Xin *et. al.*, 2015; Agarwal *et. al.*, 2016; Boukoussa *et al.*, 2018). It shows that the effect of initial dye concentration relies on the immediate relation between the dye concentration and the available binding sites on the adsorbent surface (Seow *et. al.*, 2016).

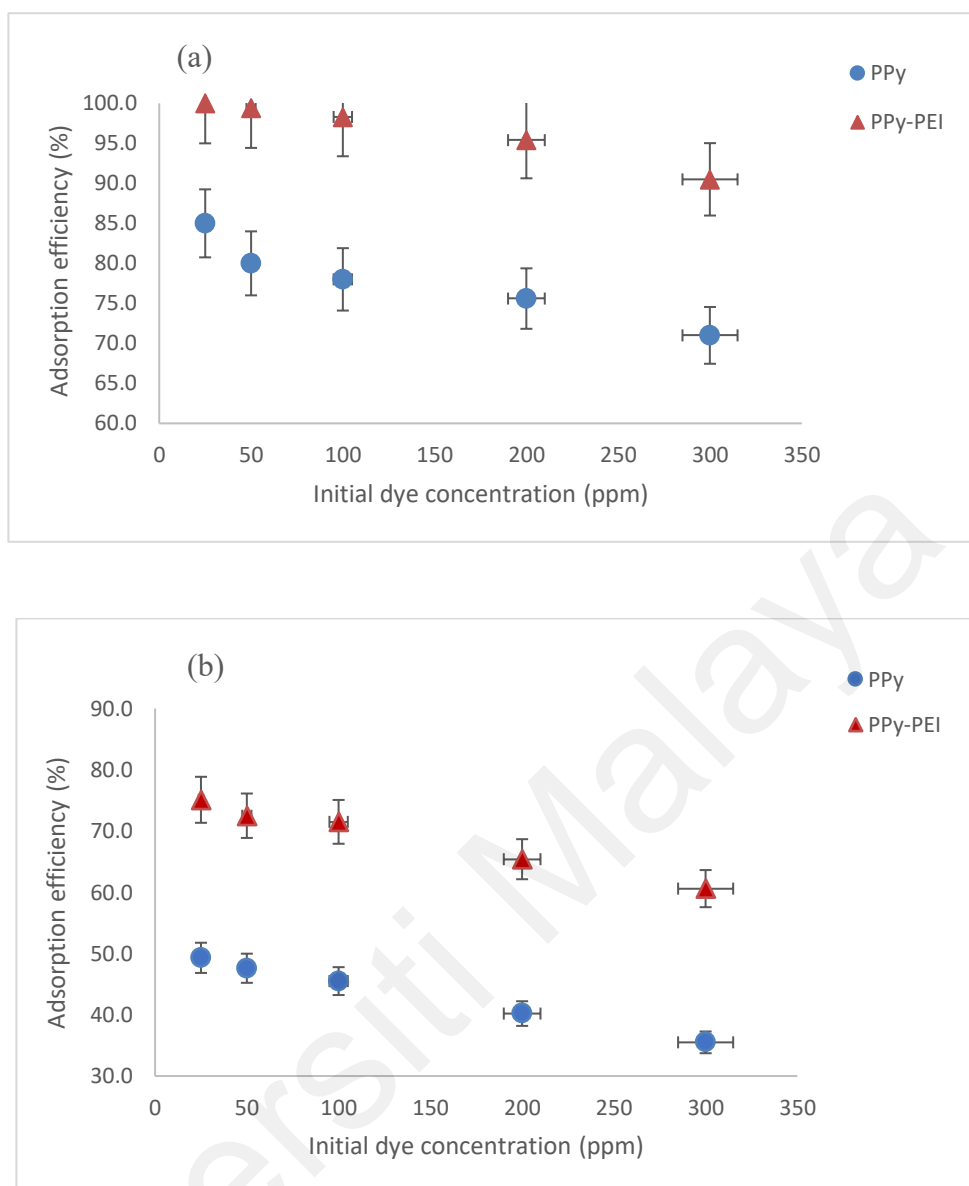


Figure 4.22: Effect of initial dye concentration by pristine PPy and PPy-PEI composite adsorbents on adsorption of (a) MO and (b) CV.

4.2.8 Adsorption kinetic models

The kinetics of adsorption data was processed to understand the dynamics of the adsorption process in terms of the order of rate constant. The knowledge of the adsorption mechanism is not only important in describing the efficiency but also important in designing the future feasibility of the adsorption on large scale (Bhatti *et. al.*, 2020). The kinetic studies of MO and CV dye adsorption were performed using pseudo-first-order and pseudo-second-order kinetics models. The adsorption kinetic data of MO and CV

dyes were shown in Table 4.6 and Table 4.7, respectively. The adsorption kinetic data were described by the Lagergren pseudo-first-order model using the following equation (Quan *et al.*, 2018):

$$\ln(Q_e - Q_t) = \ln Q_e - K_1 t \quad 4.1$$

The Lagergren rate constant of adsorption, K_1 (min^{-1}), the maximum adsorption capacity, Q_e (mg/g), the amount of adsorption at time t (min), Q_t (mg/g) and were calculated for MO and CV dyes. The values of K_1 and Q_e were calculated from the intercepts and the slope of the plot of $\ln(Q_e - Q_t)$ versus t as shown in Figure 4.23. The K_1 values, the correlation coefficients, R^2 , and the predicted and experimental Q_e values were given in Table 4.6. Adsorption kinetics were explained by the pseudo-second-order model developed by (Quan *et al.*, 2018):

$$\frac{t}{Q_t} = \frac{1}{K_2 Q_e^2} + \frac{t}{Q_e} \quad 4.2$$

Where K_2 is the pseudo-second-order rate constant of adsorption (g/mg min). K_2 and Q_e were determined from the intercepts and the slope of the plot of t/Q_t versus t as shown in Figure 4.24, respectively.

Table 4.6: Adsorption kinetic model parameters for MO dye adsorption.

C_0 (ppm)	Q_{exp}	Pseudo-first-order			Pseudo-second-order		
		Q_e	K_1	R^2	Q_e	K_2	R^2
100	49.40	17.9340	0.0111	0.9340	49.7512	0.007566	0.9998
300	94.80	5.7540	0.0175	0.9206	96.1538	0.002287	0.9997

Table 4.7: Adsorption kinetic model parameters for CV dye adsorption.

C_0 (ppm)	Q_{exp}	Pseudo-first-order			Pseudo-second-order		
		Q_e	K_1	R^2	Q_e	K_2	R^2
100	35.45	13.6249	0.0164	0.9696	36.63	0.002705	0.9995
300	75.75	23.0277	0.0144	0.9349	78.74	0.001241	0.9993

As for MO dye, from Figure 4.24 (a), by comparison, the high correlation was obtained by plotting the linearized form of the pseudo-second-order model ($R^2 = 0.9998$ and 0.9997) compared to that of the pseudo-first-order model ($R^2 = 0.9340$ and 0.9206) (Figure 4.23 (a)). It shows that pseudo-second-order fits better for MO dye adsorption. Similarly, for CV dye, the high correlation obtained by plotting the linearized form of the pseudo-second-order model ($R^2 = 0.9995$ and 0.9993) (Figure 4.24 (b)) compared to that of the pseudo-first-order model ($R^2 = 0.9696$ and 0.9349) (Figure 4.23 (a)) presented pseudo-second-order fits well for CV dye adsorption, suggesting that the diffusion is the physisorption mechanism for both MO and CV dyes which may be controlled by the diffusion process and is due to the operation of weak forces between species (Naushad *et al.*, 2013). In this process, the adsorbed molecule is not affixed to a particular site on the solid surface, it is free to move over the surface. Typically, there are a large number of vacant adsorbent sites available for the MO and CV molecules to be adsorbed in the initial stages of the adsorption, after which repulsive forces and the diffusion process may be prominent, lowering the rate of adsorption. Three adsorption steps can be distinguished by ignoring the adsorbate transfer from the liquid film's bulk to the adsorbent nearby: The process of external adsorbate mass transfer across the liquid film to the adsorbent exterior surface is known as the outer (or boundary layer) diffusion. The inner (or intra-particle) diffusion is the transport of adsorbate particles from the adsorbent exterior surface to its internal pores (Alghamdi *et al.*, 2019). Moreover, the calculated Q_e values from the pseudo-second-order kinetics model were much nearer to the experimental ones.

Therefore, the pseudo-first-order kinetics was not suitable for explaining the rate processes.

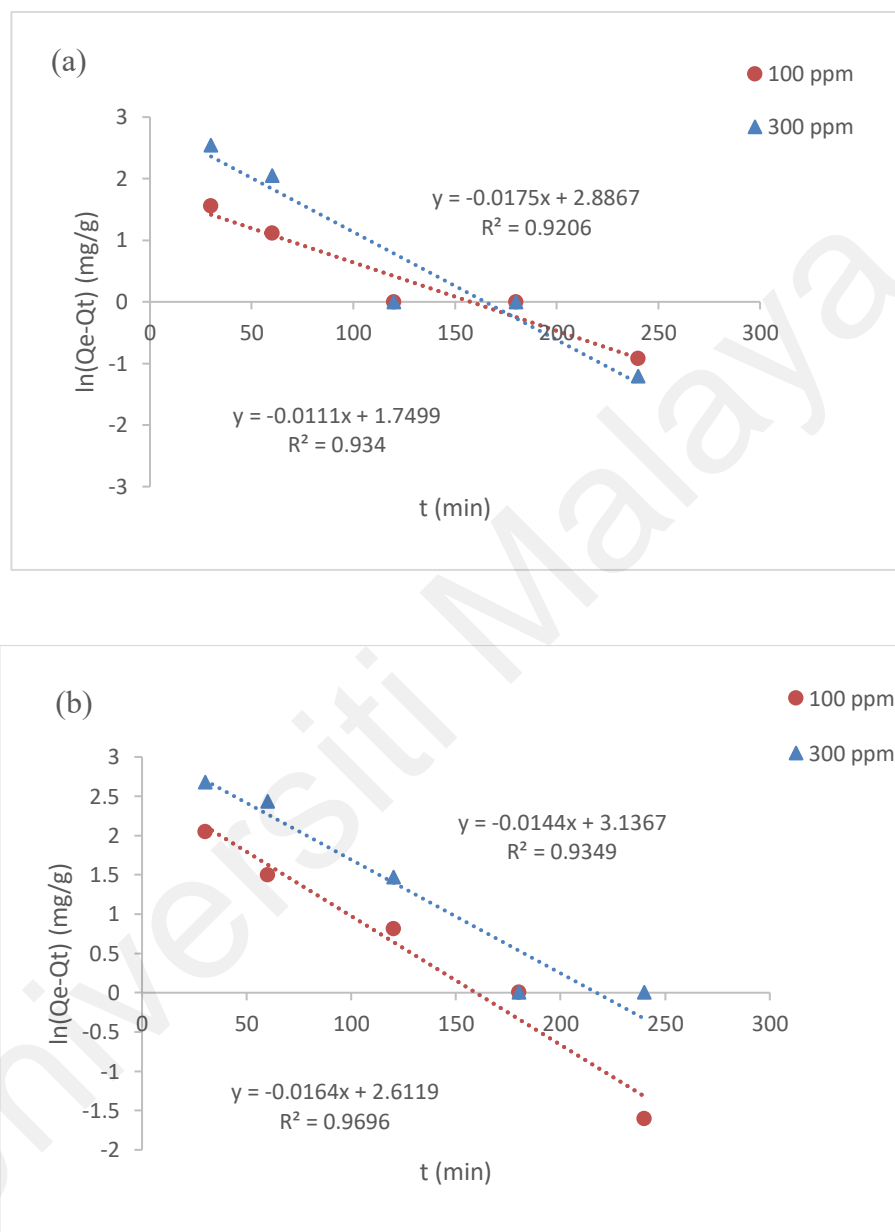


Figure 4.23: Pseudo-first-order kinetic model for the adsorption of (a) MO and (b) CV.

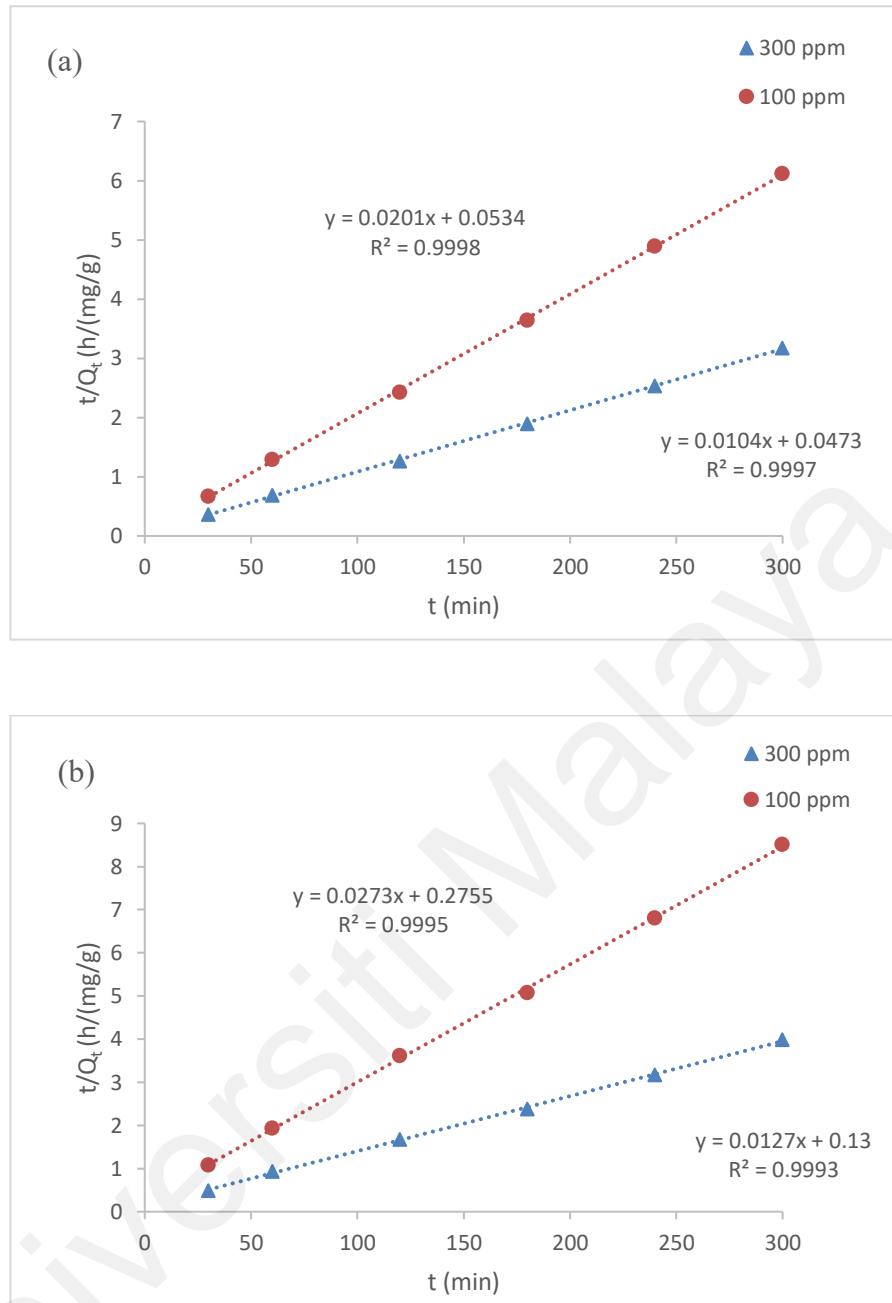


Figure 4.24: Pseudo-second-order kinetic model for the adsorption of (a) MO and (b) CV.

4.2.9 Adsorption isotherm models

In order to describe the interaction between adsorbate and an adsorbent, to design and operate an adsorption system successfully, thus equilibrium adsorption isotherm data is important (Agarwal *et al.*, 2016). An adsorption isotherm is a plot related to the equilibrium concentration of an adsorbate on the surface of an adsorbent, Q_e , to the concentration of the adsorbate in the solution, C_e . The results of adsorption data were

used in two common models (Langmuir and Freundlich) for the isotherms analysis. Table 4.8 and Table 4.9 presented all the values related to both the Langmuir and Freundlich models for MO and CV dye adsorption at temperatures of 27 °C, 40 °C and 60 °C, respectively. Adsorption isotherms can be used to describe how the solute interacts with the adsorbent, furthermore, it is critical in optimizing the usage of adsorbent for the removal of dyes from aqueous solution (Agarwal *et al.*, 2016). The Langmuir adsorption isotherm assumes that the surface of the adsorbents is energetically identical and one active site can only be occupied by one adsorbate molecule, revealing that a monolayer of adsorbates covers the surface of the homogeneous adsorbent (Chen *et al.* 2019). The equation of the Langmuir isotherm model is as follows (Xin *et al.* 2015):

$$\frac{C_e}{Q_e} = \frac{C_e}{Q_m} + \frac{1}{Q_m b} \quad 4.3$$

Where, Q_m (mg/g) is the maximum monolayer adsorption capacity, C_e (mg/L) is the equilibrium concentration of dye (MO or CV), Q_e (mg/g) is the equilibrium adsorption capacity corresponding to complete monolayer coverage on the surface, and b (L/mg) is the Langmuir equilibrium constant. The Langmuir isotherm model of MO and CV dyes at three different temperatures (27 °C, 40 °C and 60 °C) were shown in Figure 4.25. A straight line was obtained when C_e/Q_e was plotted against C_e . The values of Q_m and b were calculated from the slopes and intercepts. The essential feature of Langmuir adsorption isotherm is the dimensionless separation factor, R_L , which is derived as follows (Xin *et al.* 2015):

$$R_L = \frac{1}{1+bC_0} \quad 4.4$$

The initial concentration of the dye was represented as C_0 . The separation factor, R_L value is indicative of adsorption favorability. If the value is less than 1, it is favorable ($0 <$

$R_L < 1$) and if the value is more than 1, it is unfavorable ($R_L > 1$) for adsorption (Xin *et al.* 2015).

The Freundlich model is an empirical equation, applied to non-ideal and multi-layer adsorption on heterogeneous surfaces (Chen *et al.* 2019). The equilibrium adsorption data were also fitted to the Freundlich model (Figure 4.26), where the solute is assumed to be adsorbed onto a heterogeneous surface. The Freundlich model is expressed as given below (Xin *et al.* 2015):

$$\ln Q_e = \ln K_F + \frac{1}{n} \ln C_e \quad 4.5$$

Where K_F and n are known as Freundlich coefficients, indicating the sorption capacity and favorability of the adsorption process, respectively. The linearized Freundlich adsorption isotherm was estimated from the equation above. A straight line was obtained when $\ln Q_e$ was plotted against $\ln C_e$ and, n and K_F were calculated from the slopes and intercepts.

Table 4.8: Adsorption isotherm model parameters for MO dye adsorption.

Temp. (°C)	Langmuir				Freundlich		
	Q_m	b	R_L	R^2	K_F	n	R^2
27 °C	232.56	0.0444	0.1838	0.9998	13.088	1.432	0.9894
40 °C	192.31	0.0763	0.1159	0.9994	17.875	1.616	0.9859
60 °C	169.49	0.1408	0.0663	0.9984	25.363	1.879	0.9788

Table 4.9: Adsorption isotherm model parameters for CV dye adsorption.

Temp. (°C)	Langmuir				Freundlich		
	Q_m	b	R_L	R^2	K_F	n	R^2
27 °C	142.86	0.0889	0.1011	0.9994	18.525	2.069	0.9682
40 °C	140.85	0.1162	0.0792	0.9945	22.527	2.253	0.9878
60 °C	138.89	0.1506	0.0623	0.9947	25.891	2.372	0.9875

All the adsorption isotherm parameters obtained from these models and the values of the correlation coefficient (R^2) are depicted in Table 4.8 for MO dye and Table 4.9 for CV dye. From the results obtained, it was observed that the correlation coefficients (R^2) shown by the Langmuir model are higher than the Freundlich model suggested that the adsorption sites onto the PPy-PEI adsorbent was homogeneous and it was a monolayer interaction between the composite surface and adsorbates. This was an indication of the behavior of the composite adsorption monolayer besides active sites homogeneity. Also, it showed that the different active sites on the composite surface have energetically equivalent properties. The values of Q_m as found at various temperatures, are also given in the table. The decreasing trend of Q_m with increasing temperature specified that the increase of temperature did not favor the removal of dyes might be due to the exothermic nature of the process (Mashkoor *et al.*, 2020). In addition, it was observed that R_L values (in the range of 0–1) as shown in Table 4.8 and Table 4.9, indicating that the adsorption process of the resulting adsorbent towards the investigated adsorbates was favourable. Note that the extremely high adsorption capacity of MO on PPy-PEI adsorbent was mainly assigned to the synergistic effect of multiple uptake mechanisms (such as electrostatic attraction, $\pi - \pi$ stacking and hydrogen bond) contributed from the PEI molecules with a high cationic charge density (Chen *et al.*, 2019).

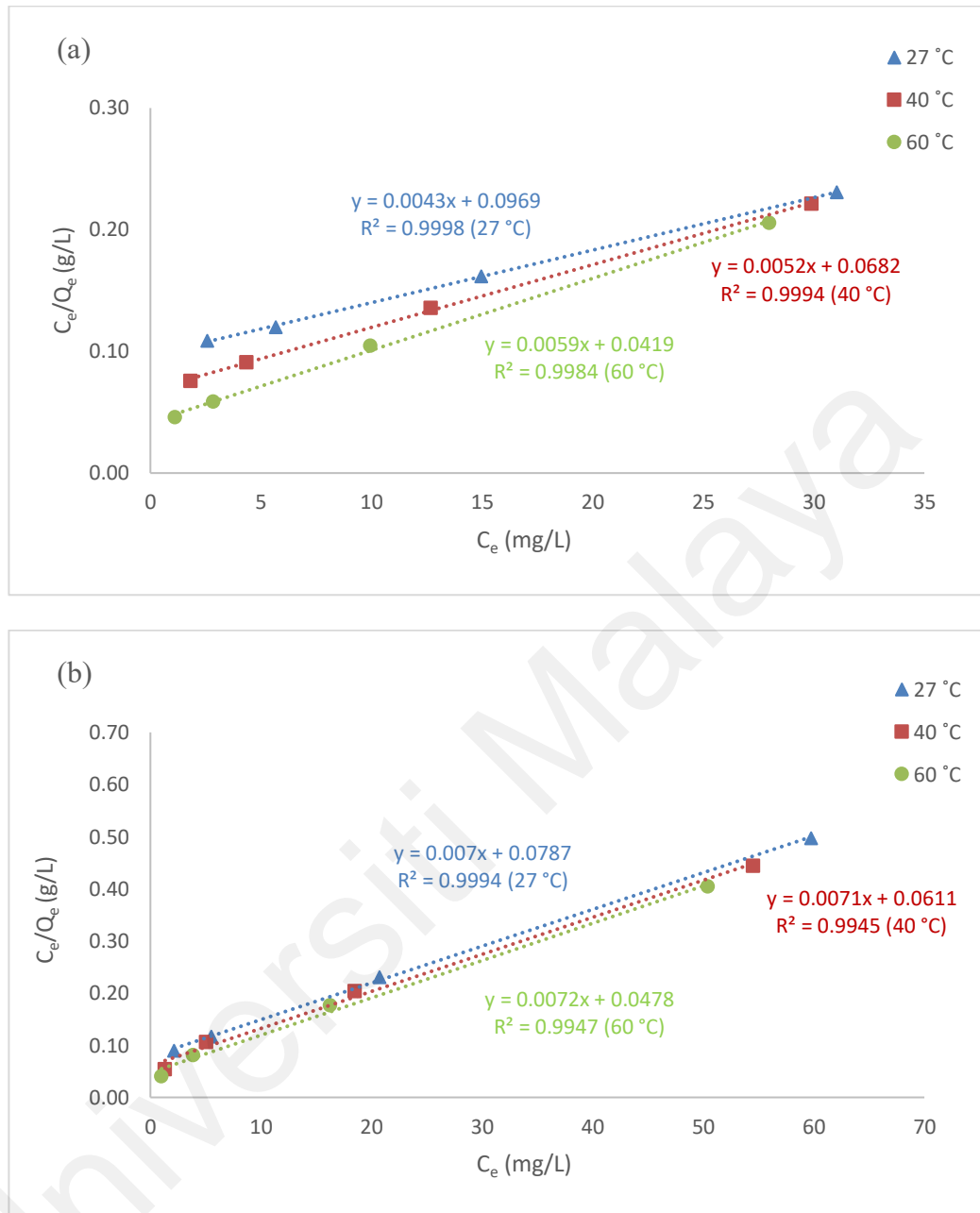


Figure 4.25: Langmuir isotherm model for the adsorption of (a) MO and (b) CV.

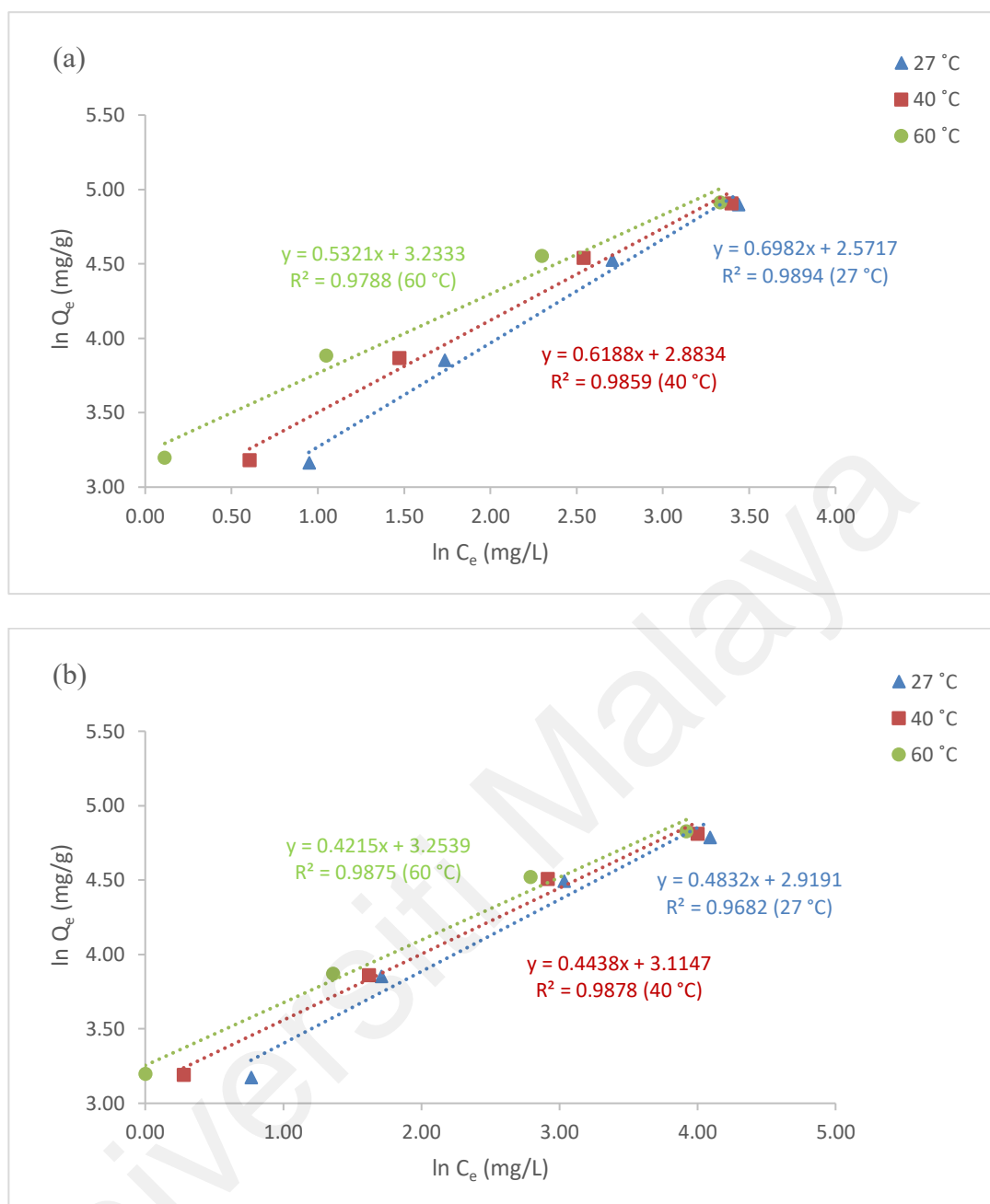


Figure 4.26: Freundlich isotherm model for the adsorption of (a) MO and (b) CV.

In this context, it is valuable to mention that a number of composites based on PPy and/or PEI adsorbents have also been reported to be obeyed Langmuir model for the adsorption of CV and MO dyes (Boukoussa *et al.*, 2018; Wang *et al.*, 2018; Chen *et al.*, 2019; Xu *et al.*, 2019; Mashkoor *et al.*, 2020; Alsaiani *et al.*, 2021; Alghamdi *et al.*, 2021). Thus, PPy-PEI composite adsorbent can be considered to be a promising adsorbent for the treatment of MO and CV dyes from wastewater.

4.3 Regeneration and repeatability studies

The regeneration study is a crucial parameter for evaluating the economic feasibility of the adsorbent. So facile regeneration of an adsorbent was important for its industrial applications (Salama *et al.*, 2017). The regeneration experiment was carried out with 50 mL of 0.1 M HCl or 50 mL of 0.1 M NaOH solution and distilled water separately. It was revealed that the spent adsorbent can be easily regenerated and reused.

As can be seen in Figure 4.27 and Figure 4.28, it shows that the cycles of adsorption and repeatability processes were successfully conducted three times for both dyes. Several attempts were done to regenerate MO and CV dyes from the adsorbed PPy-PEI composite powder by 0.1 M HCl and 50 mL of 0.1 M NaOH solution, separately. From the experiment, it was observed that desorption of MO would be triggered in the basic solution and the regeneration by using 0.1 M NaOH showed the better performance. In contrast for CV, the regeneration by using 0.1 M HCl showed better efficiency due to the effect of surface charge on the adsorption and it could be employed to realize desorption of the adsorbed dye (Xin *et al.*, 2015). From Figure 4.27, MO dye adsorption efficiency decreased from 98.6 % to 94.7 % after three cycles, while as seen in Figure 4.28, CV dye adsorption efficiency decreased from 70.9 % to 64.4 % also after three adsorption-desorption cycles. This decrease was due to the increase of dye ions attached to the adsorbent via strong chemical interaction after each cycle. From the results obtained, the removal efficiency is remaining high after three cycles which indicate that PPy-PEI composite is suitable for recyclability and repeatedly as an efficient adsorbent for MO and CV dyes removal. A similar finding has been reported by Xin *et al.*, 2015 for the desorption experiment.

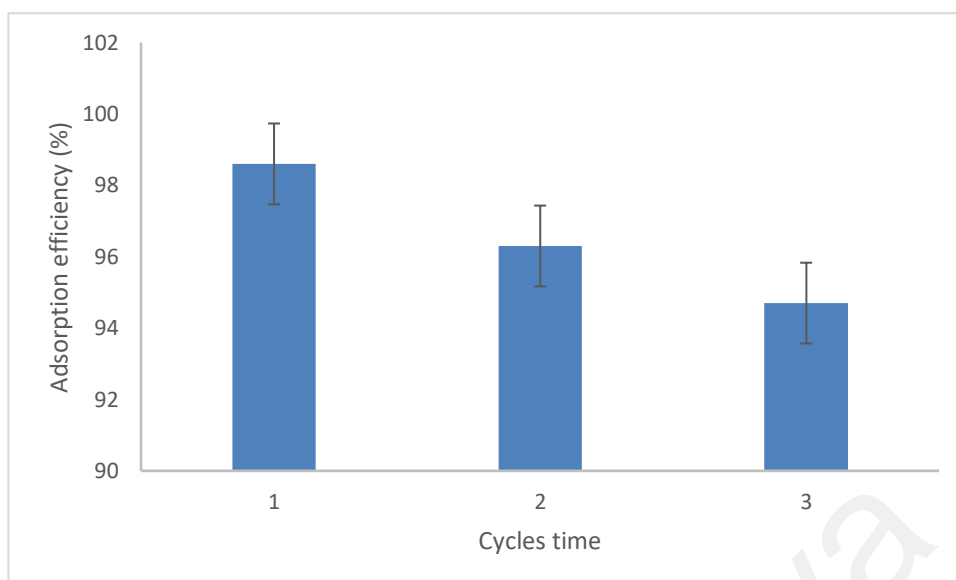


Figure 4.27: Reusability of PPy-PEI adsorbent for MO adsorption.

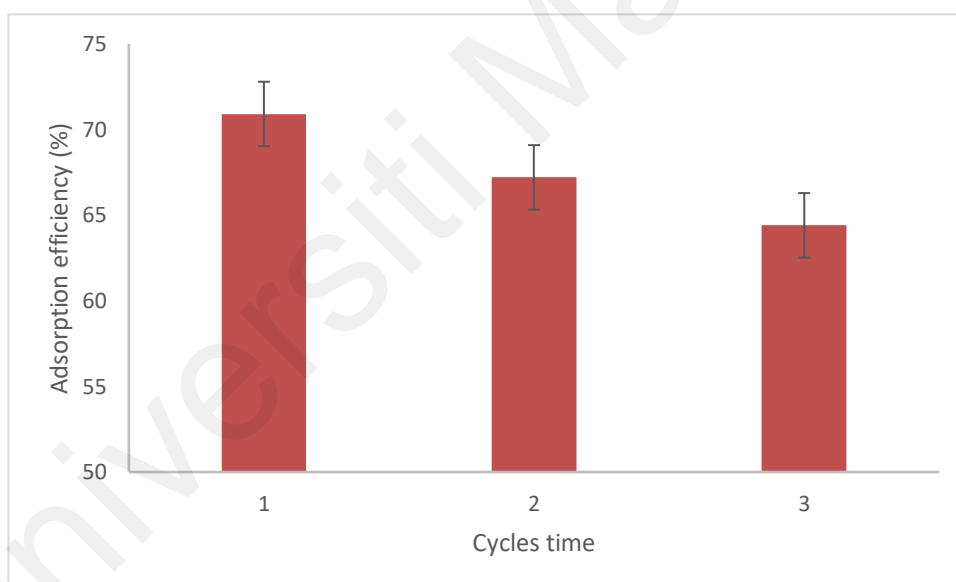


Figure 4.28: Reusability of PPy-PEI adsorbent for CV adsorption.

CHAPTER 5: CONCLUSIONS

5.1 Conclusion

In this study, conducting polymer-based adsorbents (pristine polypyrrole and polypyrrole-polyethyleneimine composites) were successfully synthesized via chemical oxidative polymerization in presence of three different types of oxidants, i.e., $\text{FeCl}_3 \cdot 6\text{H}_2\text{O}$, anhydrous FeCl_3 , and $(\text{NH}_4)_2\text{S}_2\text{O}_8$, respectively, under different polymerization conditions. Moreover, their adsorption efficiencies were evaluated for the removal of selected dyes such as anionic methyl orange dye and cationic crystal violet dye from aqueous solution.

The prepared PPy-based adsorbents were characterized by BET, FESEM, FTIR and XRD techniques before and after the adsorption of selected dyes. The pore volume distributions and surface area measurements of the prepared PPy-based adsorbents were examined by BET, surface morphology was performed by FESEM, the crystalline structure was investigated by XRD, and the various surface functional groups of the prepared adsorbents were identified by FTIR technique. The highest BET surface area of the PPy-PEI composite of 1:1 pyrrole monomer to oxidant ratio was found to be greater than that of the pristine PPy.

Among the various PPy-based adsorbents prepared, the ideal removal of both MO and CV dyes were observed at mole ratio of 1:1 of pyrrole monomer to oxidant for both types of PPy-based adsorbents. Also, among the different oxidizing agents used, the findings confirmed higher in dye removal potential in the presence of anhydrous FeCl_3 and ammonium persulfate as the oxidant for the MO and CV dye, respectively, in comparison to others. The PPy-PEI composite adsorbent has exhibited high adsorption efficiency compared to the pristine PPy adsorbent for the removal of methyl orange and

crystal violet dyes from aqueous solution. The incorporation of PEI with Py unit extremely improved the adsorption of anionic methyl orange and cationic crystal violet dye due to the availability of a higher number of nitrogen atoms present in the polypyrrole-polyethyleneimine structure.

It has been found that the batch adsorption parameters such as solution pH, adsorbent dosage, contact time, and initial dye concentration played an important role in the adsorption of both dyes which was conducted at room temperature. The maximum removal performance for MO dye obtained at the optimum conditions by PPy-PEI composite shows higher than pristine PPy. A similar trend was obtained using pristine PPy and PPy-PEI composite for the removal performance of CV dyes. From the results obtained, the optimum conditions for the adsorption of known concentration dye (100 ppm) MO dye were found to be at pH 3, adsorbent dosage of 0.1 g and with a contact time of 120 minutes. Whereas, for 100 ppm concentration of CV dye, the adsorption efficiency exhibited high at pH 11, an adsorbent dosage of 0.3 g and contact time of 180 minutes. However, the PPy-based adsorbents presented high adsorption performance toward MO than CV dye which may be attributed to the interaction between the anionic dye molecule and protonated amine groups of polypyrrole and polyethyleneimine structure.

The adsorption data for MO and CV dyes have been found to be well-fitted to the Langmuir isotherm model with the maximum monolayer sorption capacity of MO dye higher than CV dye and followed the pseudo-second-order kinetic model for both dyes. In addition, it was observed that the adsorption process of the resulting adsorbent towards the investigated adsorbates was favorable. The regeneration studies were also carried out and it was observed that desorption of MO would be triggered in basic solution and the regeneration by using 0.1 M NaOH showed a better performance. The adsorption

efficiency remained high after three adsorption-desorption cycles. In contrast for CV, the regeneration by using 0.1 M HCl showed better adsorption efficiency also after three adsorption-desorption cycles.

Summarily, the current study shows that polypyrrole composite adsorbent is more effective to treat wastewater to remove MO and CV dyes than the pristine polypyrrole adsorbent. Finally, it was concluded that the PPy-PEI composite appears as an interesting new adsorbent for dye removal from aqueous environment. The low cost, ease of preparation and higher adsorption efficiency towards anionic and cationic dye encourages this PPy-PEI composite adsorbent to be used to treat wastewater.

5.2 Suggestions for future works

In this study, the removal of methyl orange and crystal violet dyes from aqueous solution by polypyrrole-based adsorbents via adsorption process have been examined. Based on the obtained results, further works could be suggested which may include:

- The choice of another oxidant/dopant varies and may be worth studying for adsorption.
- Applications of other adsorptive materials could be employed during the synthesis of polypyrrole to enhance its adsorption performance.
- The composite materials used in the current study can be investigated for the adsorption of other anionic or cationic dyes.
- Studies with real industrial wastewater containing various pollutants of dyes are advocated for future studies.
- Adsorption capacity of regenerated polymer composite in the current study should be further evaluated for industrial applications.

REFERENCES

- Agarwal, S., Tyagi, I., Gupta, V. K., Golbaz, F., Golikand, A. N. and Moradi, O. (2016). Synthesis and characteristics of polyaniline/zirconium oxide conductive nanocomposite for dye adsorption application. *Journal of Molecular Liquids*, 218:494-498.
- Alaor, V. F., Raíssa, X. K., Natália, N. J., Luana, V. T., André, R. F. A. and Gabriela, S. R. (2021). Optimization of cationic dye removal using a high surface area-activated carbon from water treatment sludge. *Bulletin of Materials Science*, 44:41.
- Alghamdi, A. A, Al-Odayni, A., Saeed, W. S, Almutairi, M. S., Alharthi, F. A., Aouak, T. and Al-Kahtani, A. (2019). Adsorption of azo dye methyl orange from aqueous solutions using alkali-activated polypyrrole-based graphene oxide. *Molecules*, 24:3685.
- Alghamdi, A. A, Al-Odayni, A., Abduh, N. A. Y., Alramadhan, S. A., Aljboar, M. T. and Saeed, W. S. (2021). Adsorptive performance of polypyrrole-based KOH-activated carbon for the cationic dye crystal violet: Kinetic and equilibrium studies. *Adsorption Science and Technology*, 5527594.
- Aliabadi, R. S. and Mahmoodi, N. O. (2018). Synthesis and characterization of polypyrrole, polyaniline nanoparticles and their nanocomposite for removal of azo dyes; sunset yellow and Congo red. *Journal of Cleaner Production*, 179:235-245.
- Alqarni, S. A. (2022). The performance of different AgTiO₂ loading into Poly(3-nitrothiophen) for efficient adsorption of hazardous brilliant green and crystal violet dyes. *International Journal of Polymer Science*, 4691347.
- Alsaieri, N. S, Amari, A., Katubi, K. M, Alzahrani, F. M., Rebah, F. B. and Tahoona, M. A. (2021). Innovative magnetite based polymeric nanocomposite for simultaneous removal of methyl orange and hexavalent chromium from water. *Processes*, 9:576.

- Amode, J.O., Santos, J.H., Md. Alam, Z., Mirza, A. H. and Mei, C. C. (2016). Adsorption of methylene blue from aqueous solution using untreated and treated (*Metroxylon spp.*) waste adsorbent: equilibrium and kinetics studies. *International Journal Indian Chemical*, 7:333–345.
- An, F. J. and Gao, B. J. (2007). Chelating adsorption properties of PEI/SiO₂ for plumbum ion. *Journal of Hazardous Material*, 145:495–500.
- Ansari, R., Keivani, M. B., and Delavar, A. F. (2011). Application of polypyrrole coated onto wood sawdust for the removal of carmoisine dye from aqueous solutions. *Journal of Applied Polymer Science*, 122(2):804-812.
- Ansari, R. and Mosayebzadeh, Z. (2011). Application of polyaniline as an efficient and novel adsorbent for azo dyes removal from textile wastewaters. *Chemical Papers*, 65(1):1-8.
- Ansari, R., Tehrani, M. S. and Keivani, M. B. (2013). Application of polythiophene–sawdust nano-biocomposite for basic dye removal using a continuous system. *Journal of Wood Chemistry & Technology*, 33(1):19-32.
- Arkas, M and Tsiourvas, D. (2009). Organic/inorganic hybrid nanospheres based on hyperbranched poly(ethyleneimine) encapsulated into silica for the sorption of toxic metal ions and polycyclic aromatic hydrocarbons from water. *Journal of Hazardous Material*, 170:35-42.
- Ayad, M. M., Amer, W. A., Zaghlol, S., Minisy, I. M., Bober, P. and Stejskal, J. (2018). Polypyrrole-coated cotton textile as adsorbent of methylene blue dye. *Chemical Papers*, 72:1605-1618.
- Bai, L., Li, Z., Zhang, Y., Wang, T., Lu, R., Zhou, W. and Zang, S. (2015). Synthesis of water-dispersible graphene-modified magnetic polypyrrole nanocomposite and its ability to efficiently adsorb methylene blue from aqueous solution. *Chemical Engineering Journal*, 279:757-766.

- Bhatti, H. N., Safa, Y., Yakout, S. M., Shair, O. H., Iqbal, M. and Nazir, A. (2020). Efficient removal of dyes using carboxymethyl cellulose/alginate/polyvinyl alcohol/rice husk composite: Adsorption/desorption, kinetics and recycling studies. *International Journal of Biological Macromolecules*, 150:861-870.
- Bhaumik, M., McCrindle, R. I., Maity, A., Agarwal, S. and Gupta, V. K. (2016). Polyaniline nanofibers as highly effective re-usable adsorbent for removal of reactive black 5 from aqueous solutions. *Journal of Colloid and Interface Science*. 466:442-451.
- Binaeian, E., Tayebi, H. A., Shokuhi Rad, A. and Afrashteh, S. (2018). Adsorption of acid blue on synthesized polymeric nanocomposites, PPy/MCM-41 and PANi/MCM-41: Isotherm, thermodynamic and kinetic studies. *Journal of Macromolecular Science Part A-Pure Applied Chemistry*, 55:269-279.
- Boukoussa, B., Hakiki, A., Moulai, S., Chikh, K., Kherroub, D. E., Bouhadjar, L., Guedal, D., Messaoudi, K., Mokhtar, F. and Hamacha, R. (2018). Adsorption behaviors of cationic and anionic dyes from aqueous solution on nanocomposite polypyrrole/SBA-15. *Journal of Materials Science*, 53:7372–7386
- Brezoi, D. (2010). Polypyrrole films prepared by chemical oxidation of pyrrole in aqueous FeCl₃ solution. *Journal of Science and Arts*, 1(12):53-58.
- Chafai, H., Laabd, M., Elbariii, S., Bazzaoui, M. and albourine, A. (2016). Study of congo red adsorption on the polyaniline and polypyrrole. *Journal of Dispersion Science and Technology*, 38(6): 832-836.
- Chen, B., Yue, W., Zhao, H., Long, F., Cao, Y. and Pan, X. (2019). Simultaneous capture of methyl orange and chromium(VI) from complex wastewater using polyethyleneimine cation decorated magnetic carbon nanotubes as a recyclable adsorbent. *RSC Advances*, 9:4722.
- Cheruiyot, G. K., Wanyonyi, W., Kiplimo, J. J. and Maina, E. N. (2019). Adsorption of toxic crystal violet dye using coffee husks:Equilibrium, kinetics and thermodynamics study. *Scientific African*, 5:00116.

Christie, R. M. (2007). Environmental aspects of textile dyeing: *Elsevier*.

Das, R., Bhaumik, M., Giri, S. and Maity, A. (2017). Sonocatalytic rapid degradation of Congo red dye from aqueous solution using magnetic Fe⁰/polyaniline nanofibers. *Ultrasonics Sonochemistry*, 37:600-613.

Deb, A., Kanmani, M., Debnath, A., Bhowmik, K. L. and Saha, B. (2019). Ultrasonic assisted enhanced adsorption of methyl orange dye onto polyaniline impregnated zinc oxide nanoparticles: kinetic, isotherm and optimization of process parameters. *Ultrasonics Sonochemistry*, 54:290-301.

Deng, J., Wang, X., Guo, J. and Liu, P. (2014). Effect of the oxidant/monomer ratio and the washing post-treatment on electrochemical properties of conductive polymers. *Industrial and Engineering Chemistry Research*, 53:1380-13689.

Dutta, S., Gupta, B., Srivastava, S. K. and Gupta, A. K. (2021). Recent advances on the removal of dyes from wastewater using various adsorbents: a critical review. *Material Advances*, 2:4497.

Essandoh, M., Garcia, R. A., Palochik, V. L., Gayle, M. R. and Liang, C. (2021). Simultaneous adsorption of acidic and basic dyes onto magnetized polypeptidylated-Hb composites. *Separation and Purification Technology*, 255:117701.

Feng, J., Li, J., Lv, W., Xu, H., Yang, H., and Yan, W. (2014). Synthesis of polypyrrole nano-fibers with hierarchical structure and its adsorption property of Acid Red G from aqueous solution. *Synthetic Metals*, 191:66-73.

Ganea, I. V., Nan, A., Baci, C. and Turcu, R. (2021). Effective Removal of Crystal Violet Dye Using Neoteric Magnetic Nanostructures Based on Functionalized Poly(Benzofuran-co-Arylacetic Acid): Investigation of the Adsorption Behaviour and Reusability. *Nanomaterials*, 11:679.

- Ghorbani, M., and Eisazadeh, H. (2013). Removal of COD, color, anions and heavy metals from cotton textile wastewater by using polyaniline and polypyrrole nanocomposites coated on rice husk ash. *Composites Part B: Engineering*, 45(1):1-7.
- Gupta, V. K. and Suhas. (2009). Application of low-cost adsorbents for dye removal-a review. *Journal of Environmental Management*, 90(8):2313-2342.
- Habiba, U., Joo, T. C., Siddique, T. A., Salleh, A., Ang, B. C. and Afifi, A. M. (2017). Effect of degree of deacetylation of chitosan on adsorption capacity and reusability of chitosan/polyvinyl alcohol/TiO₂ nano composite. *International Journal of Biological Macromolecules*, 104:1133-1142.
- Haitham, K., Razak, S. and Nawawi, M. A. (2019). Kinetics and isotherm studies of methyl orange adsorption by a highly recyclable immobilized polyaniline on a glass plate. *Arabian Journal of Chemistry*, 12(7):1595-1606.
- Hao, M., Qiu, M., Yang, H., Hu, B. and Wang, X. (2021). Recent advances on preparation and environmental applications of MOF-derived carbons in catalysis. *Science of the Total Environment*, 760:143333.
- Hasani, T. and Eisazadeh, H. (2013). Removal of Cd (II) by using polypyrrole and its nanocomposites. *Synthetic Metals*, 175:15-20.
- Hasan, M., Rashid, M. M., Al Mesfer, M. K., Danish, M., et al. (2019). Fabrication of polyaniline/activated carbon composite and its testing for methyl orange removal: optimization, equilibrium, isotherm and kinetic study. *Polymer Testing*, 77: 105909.
- Huang, Y., Li, J., Chen, X. and Wang, X. (2014). Applications of conjugated polymer-based composites in wastewater purification. *RSC Advances*, 4(107):62160-62178.
- Huang, B., Liu, Y., Li, B., Wang, H. and Zeng, G. (2019). Adsorption mechanism of polyethyleneimine modified magnetic core-shell Fe₃O₄@SiO₂ nanoparticles for anionic dye removal. *RSC Advances*, 9:32462-32471.

- Iqhrammullah, M., Marlina and S., Nur. (2020). Adsorption behaviour of hazardous dye (methyl orange) on cellulose-acetate polyurethane sheets. *IOP Conference Series: Materials Science and Engineering*, 845:012035.
- Jadhav, S. A., Patil, V. S., Shinde, P. S., Thoravat, S. S., & Patil, P. S. (2020). A short review on recent progress in mesoporous silicas for the removal of metal ions from water. *Chemical Papers*, 74:4143-4157.
- Kamran, U., Bhatti, H. N., Iqbal, M., Jamil, S. and Zahid, M. (2019). Biogenic synthesis, characterization and investigation of photocatalytic and antimicrobial activity of manganese nanoparticles synthesized from *Cinnamomum verum* bark extract. *Journal of Molecular Structure*, 1179:532-539.
- Katheresan, V., Kansedo, J. and Lau, S. Y. (2018). Efficiency of various recent wastewater dye removal methods: A review. *Journal of Environmental Chemical Engineering*, 6:4676-4697.
- Kim, J. O., Lee, S. M. and Jeon, C. (2014). Adsorption characteristics of seicite for cesium ions from an aqueous solution. *Chemical Engineering Research and Design*, 92:368-374.
- Kulkarni, S. and Kaware, J. (2014). Regeneration and recovery in adsorption-a review. *International Journal of Innovative Science, Engineering & Technology*, 1(8):61-64.
- Kumar, V., Saharan, P., Sharma, A.K., Kaushal, I., and Dhuan, S (2020a). Silver embellished PANI/CNT nanocomposite for antimicrobial activity and sequestration of dye based on RSM modelling. *Environmental Technology*, 41(23):2991-3003.
- Kumar, V., Saharan, P., Sharma, A.K., Umar, A., Kaushal, I., Mittal, A., Al-Hadeethi Y and Rashad, B (2020b). Silver doped manganese oxide-carbon nanotube nanocomposite for enhanced dye-sequestration: Isotherm studies and RSM modelling approach. *Ceramic International*, 46(8):10309-10319.
- Li, J., Feng, J. and Yan, W. (2013). Excellent adsorption and desorption characteristics of polypyrrole/TiO₂ composite for Methylene Blue. *Applied Surface Science*, 279:400-408.

- Li, X., Wang, Z., Ning, J., Gao, M., Jiang, W., Zhou, Z. and Li, G. (2018). Preparation and characterization of a novel polyethyleneimine cation-modified persimmon tannin bioadsorbent for anionic dye adsorption. *Journal of Environmental Management*, 217: 305-314.
- Li, Y. (2015). Conducting Polymers. *Organic Optoelectronic Materials*, 2:23-50.
- Li, Z., Hanafy, H., Zhang, L., Sellaoui, L., Schadeck Netto, M., Oliveira, M. L. S., Seliem, M. K., Luiz Dotto, G., Bonilla-Petriciolet, A. and Li, Q. (2020). Adsorption of congo red and methylene blue dyes on an ashitaba waste and a walnut shell-based activated carbon from aqueous solutions: Experiments, characterization and physical interpretations. *Chemical Engineering Journal*, 388:124263.
- Liu, X., Zhang, J., Cheng, Y., Zhao, X., Dai, Z. and Liu, G. (2021). Efficient removal of crystal violet by polyacrylic acid functionalized ZIF-67 composite prepared by one-pot synthesis. *Colloids and Surfaces A: Physicochemical and Engineering Aspects*, 631:127655.
- Loganathan, M., Raj, A. S., Murugesan, A., Kumar, P. S. (2022). Effective adsorption of crystal violet onto aromatic polyimide: Kinetics and isotherm studies. *Chemosphere*, 304:135332.
- Ma, F.-f., Zhang, D., Zhang, N., Huang, T., and Wang, Y. (2018). Polydopamine-assisted deposition of polypyrrole on electrospun poly(vinylidene fluoride) nano-fibers for bidirectional removal of cation and anion dyes. *Chemical Engineering Journal*, 354:432-444.
- Mallakpour, S. and Hatami, M. (2019). An effective, low-cost and recyclable bio-adsorbent having amino acid intercalated LDH@Fe₃O₄/PVA magnetic nanocomposites for removal of methyl orange from aqueous solution. *Applied Clay Science*, 174:127-137.
- Maqbool, M., Bhatti, H. N., Sadaf, S., Zahid, M. and Shahid, M. (2019). A robust approach towards green synthesis of polyaniline-Scenedesmus biocomposite for wastewater treatment applications. *Materials Research Express*, 6(5):055308.

- Mashkoo, F. and Nasar, A. (2020). Facile synthesis of polypyrrole decorated chitosan-based magsorbent: Characterizations, performance, and applications in removing cationic and anionic dyes from aqueous medium. *International Journal of Biological Macromolecules*, 161:88-100.
- Mashkoo, F. and Nasar, A. (2020). Polyaniline/*Tectona grandis* sawdust: A novel composite for efficient decontamination of synthetically polluted water containing crystal violet dye. *Groundwater for Sustainable Development*, 8:390-401.
- Mohamed, F., Abukhadra, M. R. and Shaban, M. (2018). Removal of safranin dye from water using polypyrrole nanofiber/Zn-Fe layered double hydroxide nanocomposite (PPy NF/Zn-Fe LDH) of enhanced adsorption and photocatalytic properties. *Science of the Total Environment*, 640-641:352-363.
- Momina and Ahmad., K. (2021). Study of different polymer nanocomposites and their pollutant removal efficiency: A review. *Polymer*, 217:123453.
- Naushad, M., and ALOthman, Z. A. (2013). Equilibrium and kinetics studies in adsorption of toxic metal ions for wastewater treatment. *Ion Exchange, Adsorption, and Solvent Extraction*, 8:146-182.
- Nolasco J. E. T., Caneba, E. N. O., Edquila, K. M. V., Espita, J. I. C. and Perez, J. V. D. (2019). Kinetics and isotherm studies of methyl orange adsorption using polyethyleneimine-graphene oxide polymer nanocomposite beads. *Key Engineering Materials*, 801:304-310.
- Noreen S., Bhatti, H. N., Iqbal, M., Hussain, F. and Sarim, F. M. (2020). Chitosan, starch, polyaniline and polypyrrole biocomposite with sugarcane bagasse for the efficient removal of Acid Black dye. *International Journal of Biological Macromolecules*, 147:439-452.
- Qi, X., Zeng, Q., Tong, X., Su, T., Xie, L., Yuan, K., Xu, J. and Shen, J. (2021). Polydopamine/montmorillonite-embedded pullulan hydrogels as efficient adsorbents for removing crystal violet. *Journal of Hazardous Materials*, 402:123359.

- Quan, X., Sun, Z., Meng, H., Han, Y., Wu, J., Xu, J., Xu, Y. and Zhang, X. (2018). Polyethyleneimine (PEI) incorporated Cu-BTC composites: extended applications in ultra-high efficient removal of congo red. *Journal of Solid State Chemistry*, 270:231-241.
- Rahchamani, J., Mousavi, H. Z. and Behzad, M. (2011). Adsorption of methyl violet from aqueous solution by polyacrylamide as an adsorbent: Isotherm and kinetic studies. *Desalination*, 267:256-260.
- Rahman, F. B. A. and Akter, M. (2016). Removal of dyes from textile wastewater by adsorption using shrimp shell. *International Journal of Waste Resources*, 6(3):244.
- Rathore, B. S., Chauhan, N. P. S., Rawal, M. K., Ameta, S. C. and Ameta, R. (2019). Chitosan–polyaniline–copper(II) oxide hybrid composite for the removal of methyl orange. *Polymer Bulletin*, 77(9):4833-4850.
- Saad, M., Tahir, H., Khan, J., Hameed, U. and Saud, A. (2017). Synthesis of polyaniline nanoparticles and their application for the removal of Crystal Violet dye by ultrasonicated adsorption process based on response surface methodology. *Ultrasonics Sonochemistry*, 34:600-608.
- Safa, Y., Tariq, S. R., Bhatti, H. N., Sultan, M., Bibi, I., and Nouren, S. (2018). Synthesis and characterization of sugarcane bagasse/zinc aluminium and apple peel/zinc aluminium biocomposites: Application for removal of reactive and acid dyes. *Membrane Water Treatment*, 9(5):301-307.
- Saharan, P., Sharma, A. K., Kumar, V. and Kaushal, I. (2019). Multifunctional CNT supported metal doped MnO₂ composite for adsorptive removal of anionic dye and thiourea sensing. *Material Chemistry and Physics*, 221:239-249.
- Salama, A. (2017). New sustainable hybrid material as adsorbent for dye removal from aqueous solutions. *Journal of Colloid and Interface Science*, 487:348-353.

- Salama, A. (2017). Preparation of CMC-g-P(SPMA) super adsorbent hydrogels: Exploring their capacity for MB removal from waste water. *International Journal of Biological Macromolecules*, 106:940-946.
- Senguttuvan, S., Janaki, V., Senthilkumar, P. and Kamal-Kannan, S. (2022). Polypyrrole/zeolite composite – A nanoadsorbent for reactive dyes removal from synthetic solution. *Chemosphere*, 287:132164.
- Seow, T. W. and Lim, C. K. (2016). Removal of dye by adsorption: A review. *International Journal of Applied Engineering Research*, 11(4):2675-2679.
- Shahabuddin, S., Sarih, N. M., Mohamad, S., Atika Baharin, S. N. (2016). Synthesis and characterization of Co₃O₄ nanocube-doped polyaniline nanocomposites with enhanced methyl orange adsorption from aqueous solution. *RSC Advances*, 6:43388-43400.
- Shanehsaz, M., Seidi, S., Ghorbani, Y. and Shoja, S. M. R. (2015). Polypyrrole-coated magnetic nanoparticles as an efficient adsorbent for RB19 synthetic textile dye: Removal and kinetic study. *Spectrochimica Acta Part A: Molecular and Biomolecular Spectroscopy*, 149:481-486.
- Sharma, P., Kaur, H., Sharma, M., and Sahore, V. (2011). A review on applicability of naturally available adsorbents for the removal of hazardous dyes from aqueous waste. *Environmental Monitoring Assess*, 183(1-4):151-195.
- Shen, J., Wang, R., Liu, Q., Yang, X., Tang, H. and Yang, J. (2019). Accelerating photocatalytic hydrogen evolution and pollutant degradation by coupling organic co-catalysts with TiO₂. *Chinese Journal of Catalysis*, 40:380-389.
- Shirmardi, M., Mesdaghinia, A., Mahvi, A. H., Nasser, S., and Nabizadeh, R. (2012). Kinetics and Equilibrium Studies on Adsorption of Acid Red 18 (Azo-Dye) Using Multiwall Carbon Nanotubes (MWCNTs) from Aqueous Solution. *E-Journal of Chemistry*, 9(4):2371-2383.

- Shirsath, S. R., Patil, A. P., Bhanvase, B. A. and Sonawane, S. H. (2015). Ultrasonically prepared poly(acrylamide)-kaolin composite hydrogel for removal of crystal violet dye from wastewater. *Journal of Environmental Chemical Engineering*, 3:1152-1162.
- Sivamani, S., Manimaran, D. R., Banupriya, A., Prathap, N., Vasu, G. and Kanakasabai, P. (2021). A comprehensive review on liquid-liquid extraction-based systems in treatment of textile wastewater. *Indian Journal of Science and Technology*, 14(33):2646-2662.
- Smita, J., Dipika, J., and Shraddha, K. (2016). Polyaniline for removal of methyl orange dye from waste water. *International Journal of Science Engineering Management*, 1-6.
- Soliman, N. and Moustafa, A. (2020). Industrial solid waste for heavy metals adsorption features and challenges; a review. *Journal of Materials Research and Technology*, 9(5):10235-10253.
- Sulyman, M., Kucinska-Lipka, J., Sienkiewicz, M. and Gierak, A. (2021). Development, characterization and evaluation of composite adsorbent for the adsorption of crystal violet from aqueous solution: Isotherm, kinetics, and thermodynamic studies. *Arabian Journal of Chemistry*, 14:103115.
- Susanti, Y. D., Afifah, N, and Saleh, R. (2021). Preparation of LaMnO₃/TiO₂/NGP composites for methylene blue dye removal via adsorption and photosonocatalysis. *Journal of Physics*, 1725:012003.
- Varga, M., Kopecka, J, Moravkova, Z., Knvka, I., Trchova, M., Stejskal, J. and Prokes, J. (2015). Effect of oxidant on electronic transport in polypyrrole nanotubes synthesized in the presence of methyl orange. *Journal of Polymer Science, Part B: Polymer Physics*, 53:1147-1159.
- Wang, L., Zhang, M., Huang, Q., Zhao, C., Luo, K. and Lei, M. (2018). Fabrication of ACF/GO/PEI composite for adsorption of methyl orange from aqueous solution. *Journal of nanoscience and nanotechnology*, 18(3):1747-1756.

- Wong, S., Tumari, H. H., Ngadi, N., Mohamed, N. B., Hassan, O., Mat, R., and Amin, N. A. S. (2018). Adsorption of anionic dyes on spent tea leaves modified with polyethyleneimine (PEI-STL). *Journal of Cleaner Production*, 206:394-406.
- Wu, Z., Wang, X., Yao, J., Zhan, S., Li, H., Zhang, J. and Qiu, Z. (2021). Synthesis of polyethyleneimine modified CoFe₂O₄-loaded porous biochar for selective adsorption properties towards dyes and exploration of interaction mechanisms. *Separation and Purification Technology*, 277:119474.
- Xin, Q., Fu, J., Chen, Z., Liu, S., Yan, Y., Zhang, J. and Xu, Q. (2015). Polypyrrole nanofibers as a high-efficient adsorbent for the removal of methyl orange from aqueous solution. *Journal of Environmental Chemical Engineering*, 3(3):1637-1647.
- Yadav, A. K., Jain, C. K. and Malik, D. S. (2014). Toxic characterization of textile dyes and effluents in relation to human health hazards. *Journal of Sustainable Environmental Research*, 3(1):95-102.
- Yang, Q., Ren, S., Zhao, Q., Lu, R., Hang, C., Chen, Z. and Zheng, H. (2018). Selective separation of methyl orange from water using magnetic ZIF-67 composites. *Chemical Engineering Journal*, 333:49-57.
- Yao, L., Yang, H., Chen, Z., Qiu, M., Hu, B. and Wang, X. (2020). Bismuth oxychloride-based materials for the removal of organic pollutants in wastewater. *Chemosphere*, 273:128576.
- Zandevakili, S. and Hmghavandi, M. R. (2020). Effect of oxidizing agents on adsorption capacity of lithium ion sieve nanoparticles. *Inorganic and Nano-Metal Chemistry*, 50(5): 382-388.
- Zare, E. N., Motahari, A., and Sillanpaa, M. (2018). Nanoadsorbents based on conducting polymer nanocomposites with main focus on polyaniline and its derivatives for removal of heavy metal ions/dyes: A review. *Environmental Resources*, 162:173-195.

Zhang, K., Wang, J., Wang, Y., Zhao, L. and Xu, Q. (2014). Facile high-yield synthesis of poly (aniline-co-m-sulfophenylenediamine) for cationic dye removal. *Chemical Engineering Journal*, 247:50-58.

Zhang, M., Yu, Z. and Yu, Hongchao. (2019). Adsorption of Eosin Y, methyl orange and brilliant green from aqueous solution using ferroferric oxide/polypyrrole magnetic composite. *Polymer Bulletin*, 77:1049-1066.

Zhang, W., Wang, L., Makila, E., Willfor, S. and Xu, C. (2022). Ultralight and porous cellulose nanofibers/polyethyleneimine composite aerogels with exceptional performance for selective anionic dye adsorption. *Industrial Crops & Products*, 177:114513.

Zhong, X., Lu, Z., Liang, W. and Hu, B. (2020). The magnetic covalent organic framework as a platform for highperformance extraction of Cr (VI) and bisphenol a from aqueous solution. *Journal of Hazardous Materials*, 393:122353.

Zhou, J., Lü, Q.-F. and Luo, J.-J. (2017). Efficient removal of organic dyes from aqueous solution by rapid adsorption onto polypyrrole-based composites. *Journal of Cleaner Production*, 167:739-748.